GAS PHASE RESISTANCE TO MASS TRANSFER IN A BUBBLE CAP COLUMN

by

Billy Bob Ashby

A dissertation submitted in partial fulfillment
of the requirements for the degree of
Doctor of Philosophy in The
University of Michigan
1955

Committee in charge:

Associate Professor Brymer Williams, Chairman
Associate Professor J. T. Banchero
Associate Professor S. W. Churchill
Professor D. L. Katz
Assistant Professor R. B. Morrison
Associate Professor J. L. York

To Sandy

For Acknowledgments
See Index copy

SUMMARY

Adiabatic vaporization data for six gas-liquid systems have been obtained in a rectangular, five-plate, bubble cap column with one active plate. Mass flow rates, total pressure, pressure drop, clear liquid height, froth height, temperatures, and gas compositions were recorded.

The active plate had nine 1-1/2-inch bubble caps on a 2-1/2-inch square pitch. Each cap had eighteen 1/8-inch by 3/4-inch slots, which extended to the tray floor. The plate was 7-1/2 inches wide and 13 inches long from the inlet downcomer to the outlet weir. A splash baffle was provided to smooth the flow over the outlet weir and to confine the bubbling action to the area above the bubble caps. One side of the column was sealed with glass to permit full visual observation of the bubbling action.

The operating conditions used with each system were a 1-1/2-inch weir height, a liquid rate of 8 gallons per minute, and a 3- to 4-fold range in gas flow rate. For the air-water system, data for a 2-inch weir height were also taken.

The purpose of this research was to evaluate the effects of fluid physical properties on the gas phase resistance to mass transfer in a bubble cap column. Data covering a wide range of fluid properties were obtained with the following systems: (1) Helium-water, (2) Air-water, (3) Freon 12 (dichlorodifluoromethane)-water, (4) Helium-isobutyl alcohol, (5) Nitrogen-isobutyl alcohol, and (6) Helium-methyl isobutyl ketone. These systems gave a 30-fold range in gas density, a 1-1/2-fold

range in gas viscosity, a 10-fold range in gas phase diffusivity, a 10-fold range in the gas Schmidt number, a 3-fold range in surface tension, and a 5-fold range in liquid viscosity.

The data were correlated with an average deviation of 6.7 per cent by the equation,

$$\frac{k_G a h P}{G_M} = 0.297 \left(\frac{\mu_G}{\rho_G D_V}\right)^{-0.23} \left(\frac{D_s v \rho_G}{\mu_G}\right)^{-0.33} \left(\frac{D_s \rho_G \sigma}{\mu_G^2}\right)^{0.16} \left(\frac{h_L}{D_s}\right)^{0.62} \left(\frac{\rho_L}{\rho_G}\right)^{-0.01} \left(\frac{\mu_L}{\mu_G}\right)^{-0.005}$$

where k_G is the individual gas phase mass transfer coefficient, a the area available for mass transfer per unit volume of froth, h the effective froth height on the bubble tray, P the total pressure, G_M the molar gas mass velocity, μ_G the gas viscosity, ρ_G the gas density, D_V the diffusivity of the vapor in the gas, D_s the width of the bubble cap slots, v the superficial gas velocity based on the active area of the plate, σ the surface tension, h_L the vertical distance between the bottom of the slot opening and the top of the clear liquid flowing over the weir (as calculated by the Francis weir formula), ρ_L the liquid density, and μ_L the liquid viscosity. The fluid properties were evaluated at the average bulk conditions. Since the variables are arranged in dimensionless groups, any consistent set of units may be used. The equation is applicable only to the particular bubble plate used in this work, since only the effects of fluid properties were studied, and not plate design variables. However, the effect of the Schmidt number indicated by the equation is expected to be similar for bubble plates of different design.

A significant difference between gas phase resistances to mass transfer calculated from ammonia absorption data and those obtained from humidification data was noted and qualitatively explained.

TABLE OF CONTENTS

TABLE OF CONTENTS (Continued)

LIST OF TABLES

LIST OF TABLES (Continued)

LIST OF ILLUSTRATIONS

LIST OF ILLUSTRATIONS (Continued).

INTRODUCTION

Bubble cap plates have been used for many years in the chemical and petroleum industries for various types of vapor-liquid mass transfer processes, ranging from the distillation of crude petroleum to the absorption of soluble components from natural and refinery gases. The importance and wide use of this type of equipment has resulted in a number of studies concerned with the various aspects of plate operation. Most of the research can be divided into two main categories, (1) studies of plate hydraulic characteristics and (2) mass transfer studies. The second category, of course, can not be entirely divorced from the first. Both are affected by plate design and fluid properties.

The mechanism of mass transfer on such plates is complex and little understood, and no comprehensive theory or empirical correlation has yet been developed. Most of the data have been reported in terms of column or plate efficiency; and though these terms have proved convenient for design purposes, they are difficult to relate to the fundamental variables. Much confusion and many seemingly contradictory conclusions have resulted from their use. The many variables involved and the difficulty of studying them independently have been the primary complicating factors.

Analyses of the plate efficiency have shown that it can be divided into several simpler parts, such as point efficiency, overall mass transfer coefficients, and individual phase resistances. The concept of additive resistances to interphase mass transfer has been used in such analyses. This concept permits the division of the overall resistance to mass transfer

into two parts, a liquid phase and a gas phase resistance. Since variations in the conditions on a bubble tray may affect the individual phase resistances differently, it is advantageous to study and evaluate them separately.

The present research was designed to evaluate the effects of physical properties of the fluids on the gas phase resistance to mass transfer in a pilot plant size bubble cap column. Liquid phase resistance was eliminated by restricting the study to vaporization of pure liquids into inert, insoluble gases, and by keeping the liquid temperature near the adiabatic saturation temperature of the gas. A wide range of gas and liquid properties was included by the use of six different gas-liquid systems: (1) Air-water, (2) Helium-water, (3) Freon 12-water, (4) Helium-isobutyl alcohol, (5) Nitrogen-isobutyl alcohol, and (6) Helium-methyl isobutyl ketone.

Before going into the details of the present research, a brief review of previous work on this subject will be presented.

REVIEW OF PREVIOUS WORK

The following pages attempt to show why the information obtained in the present research was needed and how this information is related to the preceding work. The common terms for expressing plate efficiency are summarized, and the connections between these terms and individual phase resistances are explained. A brief review of theories of mass transfer to turbulent fluids is made; and, finally, the data on gas phase resistances for various shapes and types of equipment are summarized.

Terms for Expressing Plate Efficiency

The results of mass transfer studies in bubble plate columns are usually reported and used in terms of some sort of column or plate efficiency. Overall column efficiency, plate efficiency, and point efficiency are the most common terms.

Overall Column Efficiency.—The simplest way at the present time to design a bubble tray column is to assume equilibrium between gas and liquid on each plate. With this assumption, plus a knowledge of vapor-liquid equilibrium data and the gas and liquid flow rates, it is possible to calculate the number of ideal, or equilibrium, stages required for a given separation. Since equilibrium between gas and liquid is not actually attained on a bubble tray, it is necessary to apply a correction factor to the number of calculated ideal plates in order to obtain the number of actual plates required for the separation. The reciprocal of this correction factor is termed the overall column efficiency and is equal to the ratio of the number of ideal plates to the number of actual plates.

$$E_o = \frac{\text{number of ideal plates}}{\text{number of actual plates}} , \qquad (1)$$

where

E_o = overall column efficiency .

Several empirical correlations of overall column efficiency have been presented (43, 10, 38). While they are of value for certain limited applications, in general, they represent an over simplification of a complicated problem.

Murphree Plate Efficiency.—The degree of approach to equilibrium on an individual plate is called the plate efficiency. It was first defined by Murphree (37) for a single bubble, but has been applied to the entire bubble plate. In terms of vapor compositions it is written as follows:

$$E_{MV} = \frac{y_o - y_1}{y_o - y_1^*} \qquad (2)$$

where

E_{MV} = Murphree vapor efficiency for plate 1,

y_o = average mole fraction of solute in vapor entering plate 1,

y_1 = average mole fraction of solute in vapor leaving plate 1,

y_1^* = mole fraction of solute in equilibrium with average liquid leaving plate 1.

Plate efficiency may be written in an analogous manner for liquid concentrations:

$$E_{ML} = \frac{x_1 - x_2}{x_1^* - x_2} \qquad (3)$$

where

E_{ML} = Murphree liquid efficiency for plate 1,

x_1 = average mole fraction of solute in liquid leaving plate 1,

x_2 = average mole fraction of solute in liquid entering plate 1 from plate 2 above,

x_1^* = mole fraction of solute in liquid in equilibrium with average vapor leaving plate 1.

Murphree plate efficiency is more convenient for theoretical purposes than the overall column efficiency, because it is a function of fewer variables. It can also be used conveniently for design purposes when plate to plate calculations are made. Much of the data in the literature are reported in this form.

However, the Murphree plate efficiency is influenced by the degree of intraphase liquid and vapor mixing occuring across the diameter of the tray, that is, by the horizontal concentration gradients between liquid inlet and liquid outlet. Therefore, to further simplify the theoretical problem, it is convenient to define a point efficiency restricted to a vertical differential section through the froth on the plate.

Point or Local Efficiency.—The point efficiency is defined in terms of vapor concentrations as follows:

$$E_{OG} = \frac{y'_o - y'_1}{y'_o - y'_1{}^*} \quad , \tag{4}$$

where

E_{OG} = point vapor efficiency.

The primes on the concentration terms indicate that the compositions are for a small vertical section through the aerated liquid, or froth, on the plate.

Turbulence on a bubble plate is generally considered sufficient to prevent any appreciable vertical concentration gradients in the liquid phase. Thus, the equilibrium composition, $y'_1{}^*$, in Equation 4 is a constant, rather than a terminal or an average value. This assumption greatly simplifies the prediction of point efficiencies.

Walter and Sherwood (64) presented an empirical equation relating point vapor efficiency to the gas solubility, the total pressure, the liquid viscosity, the slot width, and the effective liquid depth on the plate. Their equation is given below:

$$E_{OG} = 1 - e^{-s} \quad , \tag{5}$$

where s is defined by

$$s = \frac{h}{(2.50 + \frac{0.370H}{P})\mu^{0.68}{}_w{}^{0.33}} \quad ,$$

and where

h = vertical distance from middle of slots to top of liquid flowing over the weir, inches

H = Henry's law constant, ft^3-atm/lb mole,

P = total pressure, atm,

μ = liquid viscosity, centipoise, and

w = slot width, inches.

Equation (5) was based on a variety of data: (a) absorption of ammonia and carbon dioxide from air with water in a single-plate, 18-inch diameter column with seven 4-inch caps, (b) desorption of carbon dioxide from water and from aqueous solutions of glycerol in a 5-inch square column with one 3-1/2-inch cap, (c) absorption of propylene and isobutylene from inert gas at 3.14 and 4.49 atmospheres in a small 2-inch column with a segment of a

2-inch cap, using a heavy naphtha, a gas oil, and a heavy gas oil-lube oil mixture, (d) rectification of ethyl alcohol at atmospheric pressure in the 2-inch column, and (e) humidification of air at 1 to 3.72 atmospheres in the same column. The authors (64) found that the major variable was gas solubility and suggested that different efficiencies should be used for each component in the design of absorbers for natural gasoline and refinery gases.

Robinson and Gilliland (43) made a study of Equation 5 and suggested a slightly modified form for application to fractionating towers and absorbers.

Geddes (17) approached the problem of point efficiencies from a theoretical point of view, but was forced to make a number of assumptions, with regard to bubble size, shape, and uniformity, rate of bubble rise, recirculation within the bubble, liquid concentration around the bubble, and length of bubble path, in order to get a mathematical solution to the problem. He applied his equation to data on the variation of slot width and submergence, to data on the fractionation of ethyl alcohol-water mixtures, and to the data of Walter and Sherwood (64) mentioned earlier. Geddes suggested that the success of his predictions might be the result of fortuitous cancellation of the errors inherent in several of his assumptions. This suggestion is confirmed by the work of Bakowski (1), who reports that the size and shape of bubbles formed at bubble cap slots, as well as their rate of rise, are considerably different from the assumptions made by Geddes.

Point efficiencies are of little practical value, of course, unless they can be used to predict plate efficiencies. Ones ability to calculate plate efficiencies from point efficiencies is dependent on his knowledge

of the horizontal concentration gradients in the gas and liquid across the plate. Lewis (29) developed equations relating point to plate efficiencies for three types of liquid and gas flow:

Case I Vapor of uniform composition enters the plate; liquid flows across the plate without mixing.

Case II Vapor not mixed between plates; liquid not mixed flows the same direction on successive plates.

Case III Vapor not mixed between plates; liquid not mixed flows opposite directions on successive plates.

Case I represents the condition of the vapor entering the bottom plate of a column and is generally considered a good approximation of the condition of the vapor entering succeeding plates. The equation for this first case is given below:

$$E_{MV} = \frac{L_M}{mG_M}\left[\exp.\left(E_{OG}\frac{mG_M}{L_M}\right) - 1\right] , \qquad (6)$$

where

E_{MV} = Murphree vapor efficiency for plate,

E_{OG} = point vapor efficiency,

L_M = molar liquid rate, lb mole/hr, ft^2,

G_M = molar gas rate, lb mole/hr, ft^2,

m = slope of the equilibrium curve, dy/dx, and

$\exp(x)$ = e^x.

Gautreaux and O'Connell (16) have presented an equation relating point to plate efficiency when it is assumed that the degree of liquid mixing can be represented by a stepwise process. The liquid is pictured as flowing from one well-mixed pool to another across the plate, the number of pools on the plate being a measure of the degree of liquid mixing. The derivation involves the additional assumptions that vapor and liquid

loads are equal for each pool, that the vapor entering each pool is well mixed, and that the equilibrium relation can be represented by Henry's law. The equation using nomenclature corresponding to this work is given below:

$$E_{MV} = \frac{L_M}{mG_M}\left[\left(1 + \frac{mG_M}{L_M}\frac{E_{OG}}{n}\right)^n - 1\right], \qquad (7)$$

where

n = number of pools on the plate.

The authors (16) point out that the limit of Equation (7) as n approaches infinity, corresponds to Equation (6) for plug flow. It is also obvious that when n equals one, corresponding to complete liquid mixing, the plate and point efficiencies are identical.

The Relation of Efficiency to Individual Phase Resistances

It is interesting to note that the terms which are easiest to apply in practice are generally the most difficult to analyze theoretically. Thus, the trend in almost every science is to work from the general to the specific, to break large problems up into smaller, simpler parts. When each of the small pieces is understood, they can be reassembled into a more coherent whole. The two-film theory and the concept of additive resistances have contributed much to this process in the science of mass transfer. The following pages will show how this theory has made possible the subdivision of the efficiency problem into studies of individual phase resistances.

The Two-Film Theory and the Concept of Additive Resistances.—The two-film concept, first proposed by Whitman (67) in 1923, and the equation of additive film resistances presented a year later by Lewis and Whitman (30)

were based on the assumption that the rate of mass transfer from a gas to a liquid was controlled by molecular diffusion through thin gas and liquid films on each side of the interface. Though it was always suspected, and more recent work has shown, that the existence of these stagnant films cannot be taken literally, Gordon and Sherwood (24) have pointed out that the utility of the two film theory does not depend on the existence of stagnant films, but on the validity of three assumptions: (1) the rate of mass transfer within each phase is proportional to the difference in concentrations in the main body of the fluid and at the interface; (2) the phases are at equilibrium at the interface (no interfacial resistance); and (3) the holdup of diffusing solute in the region near the phase boundary is negligible compared to the total amount transferred.

If assumptions (1) and (3) are valid, the following equations may be written:

$$\begin{aligned} N_A &= k_G\, P(y - y_i) = k_L\, \rho_M (x_i - x) \\ &= K_G\, P(y - y^*) = K_L\, \rho_M (x^* - x) \quad , \end{aligned} \tag{8}$$

where

N_A = rate of mass transfer, lb mole/hr, ft^2,

k_G = individual gas phase mass transfer coefficient, lb mole/hr, ft^2, atm,

K_G = overall gas phase mass transfer coefficient, lb mole/hr, ft^2, atm,

k_L = individual liquid phase mass transfer coefficient, lb mole/hr, ft^2, lb mole/ft^3,

K_L = overall liquid phase mass transfer coefficient, lb mole/hr, ft^2, lb mole/ft^3,

P = total pressure, atm,

ρ_M = molar liquid density, lb mole/ft^3,

x = mole fraction solute in body of liquid,

x_i = mole fraction solute in liquid at interface,

x^* = mole fraction solute in liquid in equilibrium with gas of composition y,

y = mole fraction solute in body of gas,

y_i = mole fraction solute in gas at interface, and

y^* = mole fraction solute in gas at equilibrium with liquid of composition x.

If the slope of the equilibrium curve, m, is constant, and if assumption (2) is valid, x_i and y_i can be eliminated in Equation (8) to give the following relations:

$$\frac{1}{K_G} = \frac{1}{k_G} + \frac{mP}{k_L \rho_M} \tag{9}$$

and

$$\frac{1}{K_L} = \frac{\rho_M}{mP\, k_G} + \frac{1}{k_L} \tag{10}$$

where

m = slope of equilibrium curve, dy/dx.

In Equations (9) and (10), the reciprocal of the overall coefficient represents the total resistance to mass transfer between the gas and liquid. The terms on the right represent the individual gas phase and liquid phase resistances, respectively.

If the assumptions made in obtaining the above equations are valid, experiments can be devised so that the individual phase resistances can be studied independently, greatly simplifying the theoretical analysis of the problem.

The validity of the theory of additive resistances, illustrated by Equations (9) and (10), has been examined in two recent papers. Gordon

and Sherwood (24) have studied mass transfer rates of individual components from a water layer to an isobutyl alcohol layer, and vice versa, in a batch type apparatus. Both liquid layers were stirred; but the interface was smooth, and its area constant. The data covered a wide range of diffusivities and film coefficients. The equation of additve resistances held within 10 per cent over a 30-fold range of values of the overall coefficient. A discrepancy, noted in the original article (24), between individual coefficients calculated from measured overall coefficients and individual coefficients obtained by extraction tests with water and dry isobutanol, with no third solvent present, was later (49a) resolved by the use of new and more reliable data for diffusion of water in isobutanol and for diffusion of isobutanol in water.

Goodgame and Sherwood (23) tested the concept for mass transfer between gas and liquid phases. An apparatus similar to that of Gordon and Sherwood was used, and both phases were again stirred. The gas flowed continuously in and out of the device, while the liquid remained in place throughout each test. A gas phase mass transfer coefficient was determined by adiabatic vaporization of water into air, and a liquid phase coefficient was obtained by absorption of carbon dioxide from air with water. After correction of these coefficients for differences in diffusivities between systems, they were used to predict overall mass transfer coefficients for the absorption of ammonia and acetone from air with water. The resistances to mass transfer of both phases were important for these two systems. The predicted values of the overall coefficients checked the experimental values within 5 per cent.

Danckwerts (9) has proposed a new theory of absorption. In contrast to the stagnant film theory, it is suggested that in turbulent flow the

liquid surface is constantly being renewed by liquid eddies. The life of the surface is so short the absorbed gas does not penetrate deep enough into the liquid to make velocity gradients below the surface important. Instead, the surface is submerged and the absorbed gas distributed by liquid eddies. However, Gordon and Sherwood (24) point out that equations similar to Equations (8), (9), and (10) apply to the new Danckwerts theory as well as to the two-film theory, even though the two are based on entirely different models of the mass transfer process.

Interfacial Resistance.—The assumption of equilibrium at the interface has been questioned in a recent paper. Emmert and Pigford (13) studied absorption and desorption of oxygen and carbon dioxide with air and water in a wetted wall column. A theoretical equation was developed assuming equilibrium at the interface, a parabolic velocity distribution in the falling liquid film, uniform initial concentration, and no waves at the surface. Rippling of the falling film was prevented by the addition of wetting agents. The data fell 5 to 25 per cent below the mass transfer rates predicted by the equation, and the discrepancy was interpreted as an indication of an interfacial resistance.

In the tests where the wetting agent was not used and rippling occured, not only were the transfer rates two- to three-fold higher, but a significant difference in transfer rates depending on whether the solute was being absorbed or desorbed was noted (13). For oxygen, the rate of desorption was higher than the rate of adsorption; but for carbon dioxide, the rate of desorption was lower than the absorption rate. This effect of direction was also taken as evidence of interfacial resistance.

However, Warzel (65), in his studies of absorption and desorption of carbon dioxide with air and water in the bubble cap column used in the

present research, found no significant difference between absorption and desorption of carbon dioxide. Also, the work of Gordon and Sherwood (24) and of Goodgame and Sherwood (23), mentioned previously, offered no evidence of the existence of an interfacial resistance.

The theoretical analysis of Schrage (47) indicated that the interfacial resistance to mass transfer became significant only for very high mass transfer rates. In the case of vaporization of liquids in a wetted wall column at atmospheric pressure, it was estimated that the interfacial resistance probably amounted to only a few hundredths of one per cent of the total resistance.

Number of Transfer Units per Plate and Plate Efficiency.—In ordinary column calculations, mass transfer coefficients are rather inconvenient to use. It is helpful, therefore, to relate them to more general terms. Since the actual interfacial area on a given bubble tray is not known, it is common to combine the area term with the mass transfer coefficient. The resulting term, $K_G a$, is then the moles transferred per unit time per unit driving force per unit volume of froth, where a is defined as the area per unit volume of froth.

A material balance on the gas flowing through a differential horizontal element of a small vertical section through the froth on the plate (Figure 1-A) gives the following equation:

$$K_G a P \, (y'^* - y') \, dh = G_M \, dy' + y' \, dG_M \qquad (11)$$

where

a = interfacial area per unit volume of froth, ft^2/ft^3, and

d = differential operator.

If G_M changes very little in passing through the froth, as in distillation or in absorption from dilute gases, the second term on the right of Equation

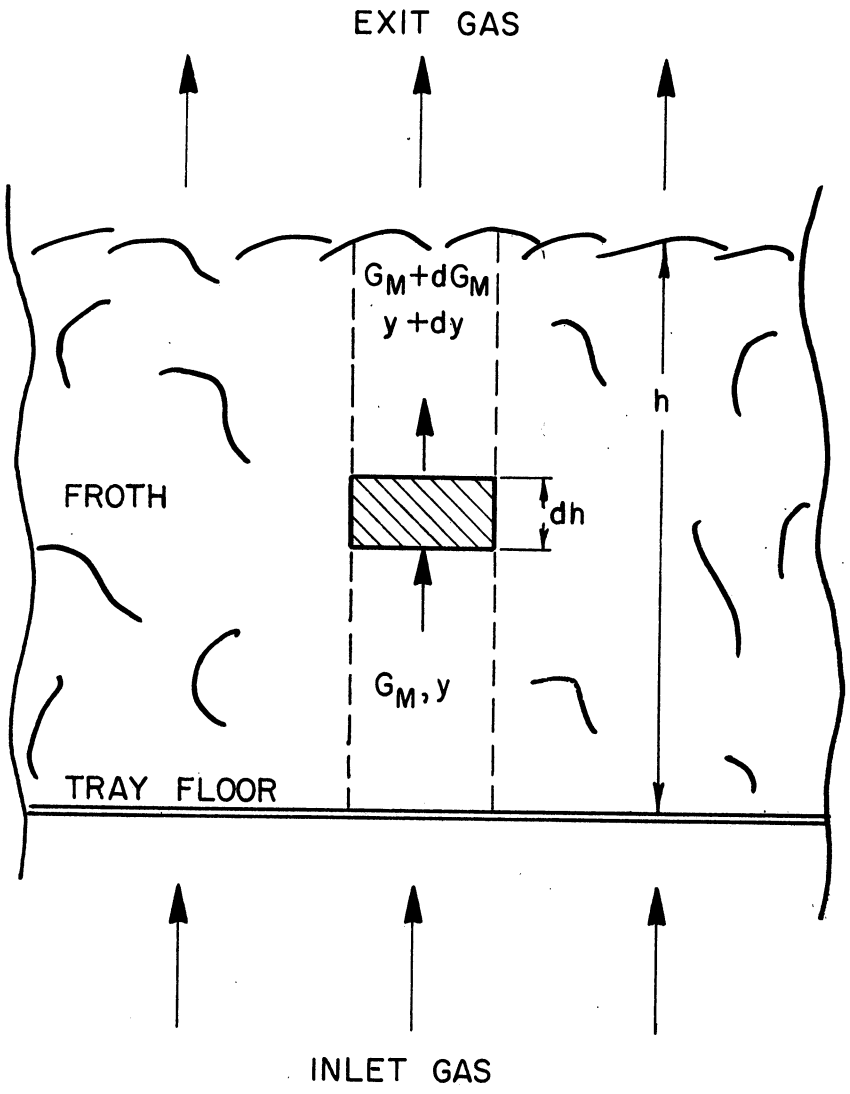

Figure 1-A. Small vertical segment through the froth on the test plate.

(11) may be considered negligible. If the liquid is well mixed vertically (y'^* is constant), the equation can be integrated from the bottom to the top of the froth to give the following equation:

$$N_{OG} = \int_{y'_o}^{y'_1} \frac{dy'}{y'^*_1 - y'} = \ln\left(\frac{y'^*_1 - y'_o}{y'^*_1 - y'_1}\right) \qquad (12)$$

where

N_{OG} = number of overall gas transfer units per plate,

$= \frac{K_G a P h}{G_M}$, and

ln = natural logarithm to the base e.

The term, N_{OG}, was defined by Chilton and Colburn (6) for use in packed column calculations. Gerster, Koffolt, and Withrow (20) extended it to bubble tray columns; and, later, the same authors (21) pointed out the relation between N_{OG} and point vapor efficiency, E_{OG}:

$$N_{OG} = -\ln(1 - E_{OG}) \qquad (13)$$

Thus, the overall mass transfer coefficient can be related to N_{OG}, which is, in turn, related to point efficiency. It has been shown that individual phase coefficients can be used to calculate the overall coefficient by use of Equation (9), and that the point efficiency can be related to plate efficiency, E_{MV}, by Equation (6) or (7) if the degree of liquid mixing can be estimated. Therefore, links have been established by Equations (9), (12), (13), (6), and (7) all the way from individual phase resistances to plate efficiencies.

Individual phase transfer units may also be defined by analogy with Equation (12):

$$N_G = \frac{k_G a P h}{G_M} , \tag{14}$$

and

$$N_L = \frac{k_L a \rho_M h}{L_M} , \tag{15}$$

where

N_G = number of individual gas transfer units per plate, and

N_L = number of individual liquid transfer units per plate.

Individual Phase Resistances in Terms of Transfer Units.—It is often convenient to define individual phase resistances in terms of transfer units. This may be done by multiplying both sides of Equation (9) by G_M/aPh and by multiplying the second term on the right by one, written as L_M/L_M. The following equation is obtained:

$$\frac{G_M}{K_G a h P} = \frac{G_M}{k_g a h P} + \frac{m G_M}{L_M} \frac{L_M}{k_L a \rho_M h} , \tag{16}$$

or

$$\frac{1}{N_{OG}} = \frac{1}{N_G} + \frac{m G_M}{L_M} \frac{1}{N_L} . \tag{17}$$

If G_M in Equation (11) changes appreciably in passing through the froth, the second term on the right of the equation should be considered. An integrated form of Equation (11) may be written as follows:

$$\frac{K_G a P h}{(G_M)_{avg.}} = \ln\left(\frac{y'_1{}^* - y'_o}{y'_1{}^* - y'_1}\right) + \int_{(G_M)_o}^{(G_M)_1} \frac{y'}{(y'_1{}^* - y')} \frac{dG_M}{G_M} \tag{18}$$

If the change in G_M is caused by absorption of a single solute from the gas, desorption of a single solute from the liquid, or evaporation of liquid vapor into the gas (the process studied in the present research), the change in G_M is a function of the change in gas concentration, y; and G_M can be eliminated from the right side of Equation (18) by substituting the following relation:

$$\frac{dG_M}{G_M} = \frac{dy}{1 - y} \quad . \tag{19}$$

Equation (18) can then be integrated analytically between the limits y'_o and y'_1. After collecting and combining terms, one obtains the following equation for N_{OG}:

$$N_{OG} = \frac{K_G a h P}{(G_M)_{avg.}} = \left(\frac{1}{1 - y'^*_1}\right) \ln\left[\left(\frac{y'^*_1 - y'_o}{y'^*_1 - y'_1}\right)\left(\frac{1 - y'_1}{1 - y'_o}\right)\right] \tag{20}$$

In the evaporation of a pure liquid into an inert gas, there is no concentration gradient in the liquid and, hence, no liquid phase resistance to mass transfer. In this case $K_G = k_G$ and $N_{OG} = N_G$. If the liquid entering the plate is near the adiabatic saturation temperature of the gas, there are no appreciable temperature gradients in the liquid; and y'^*_1 may be considered a constant throughout the froth on the entire plate. In this case the point efficiency is equal to the plate efficiency. Thus, the following equation was used to calculate N_G's from the vaporization data taken in the present research:

$$N_G = \frac{1}{1 - y_1^*} \ln\left[\left(\frac{y_1^* - y_o}{y_1^* - y_1}\right)\left(\frac{1 - y_1}{1 - y_o}\right)\right] \tag{21}$$

The preceding equations include no correction for the effect of concentration of the diffusing component on the mass transfer coefficient; that is, there has been no correction made for the effect of p_{BM} on k_G. The omission of this correction was deliberate, because its significance has not yet been definitely established.

The preceding pages have shown how the efficiency problem can be divided into studies of individual phase resistances. This is desirable, because the individual resistances may be functions of different variables, or different functions of the same variables. In the present work an attempt is made to evaluate the effects of fluid properties on the gas phase resistance to mass transfer in a bubble cap column. Hence, the following pages will review the data and correlations of similar studies made with other types of apparatus.

Theories of Mass Transfer to Fluids in Turbulent Flow

Fick's law of diffusion, which assumes the concentration gradient of the diffusing component to be the driving force, may be written as follows:

$$N_A = -D\, dc/dz \quad , \qquad (22)$$

where

N_A = mass diffusion rate, lb mole/hr, ft^2,

c = concentration of diffusing component, lb mole/ft^3,

z = coordinate in direction of diffusion, ft, and

D = diffusion coefficient, ft^2/hr.

The diffusion coefficient, D, is known to vary with concentration; and, for this reason, Randall, Longtin, and Weber (41) suggested that the free-energy gradient, rather than the concentration gradient, might be the real driving force in diffusion. However, the convenience of using concentration has

apparently outweighed its disadvantages, and concentration gradients remain in general use in diffusion correlations.

Fick's law was written for molecular diffusion within a single phase; however, mass transfer to a fluid in turbulent flow takes place by two diffusion processes, molecular and eddy diffusion. Concentration gradient is taken to be the driving force for both. In the bulk of the turbulent fluid some distance from the phase boundary the rate of molecular diffusion is usually negligible compared to eddy diffusion. However, very near the phase boundary, fluid velocity and eddy diffusion decrease to such an extent that molecular diffusion becomes important. Molecular diffusion depends only on the physical properties of the fluids; and good correlations, as well as a variety of data, are available for this process. Eddy diffusion, on the other hand, is a function of the given flow characteristics; and it has not been as extensively measured as molecular diffusivity. Sherwood and Pigford (51) give an excellent discussion of the nature of these two processes.

The processes of mass, heat, and momentum transfer have been found to be closely related; and most theoretical correlations of mass transfer data have been made by analogy with one, or both, of the other processes. Sherwood (48) and Sherwood and Pigford (52) have discussed the various analogies as applied to mass transfer: (1) the Reynolds analogy, (2) the Prandtl-Taylor modification, (3) the j-factor analogy, (4) the Murphree equation, and (5) the Von Karman analogy.

The Reynolds analogy, as applied to a fluid stream inside a pipe, assumes that the ratio of the actual rate of momentum transfer to the rate of momentum transfer necessary to bring the bulk of the stream to the wall conditions is equal to the ratio of the actual rate of mass transfer to the rate of mass transfer necessary to bring the bulk of the stream to the

wall conditions.

The Prandtl-Taylor modification of the Reynold's analogy for heat transfer introduced the concept of a laminar film adjoining the phase boundary. It was assumed that heat passed through the laminar layer by molecular conduction, and the Reynolds analogy was applied only to the turbulent core of moving fluid. Colburn (8) derived the corresponding analogy for mass transfer.

Chilton and Colburn (7) suggested a further modification of the Prandtl-Taylor concept and defined "j-factors" for heat and mass transfer as follows:

$$j_H = \frac{h}{C_p \rho v} \left(N_{Pr}\right)^{2/3} \approx 1/2\, f \quad , \tag{23}$$

and

$$j_D = \frac{k_G p_{BM}}{G_M} \left(N_{Sc}\right)^{2/3} \approx 1/2\, f \quad , \tag{24}$$

where

j_H = factor for heat transfer,

j_D = factor for mass transfer,

f = friction factor, an empirical function of the Reynold's number,

N_{Pr} = Prandtl number, $C_p \mu / k$,

N_{Sc} = Schmidt number, $\mu / \rho D$, and

p_{BM} = partial pressure of inert, non-diffusing gas.

The values of j_H and j_D were found experimentally to approximate 1/2 f only for certain streamline shapes where the impact pressure drag was small compared to the skin friction. However, j_H was found to be approximately equal to j_D for a wide variety of shapes and flow conditions.

Murphree (36) derived a theoretical relation between friction and heat transfer in pipes assuming eddy viscosity to be constant in the

turbulent core, but proportional to the cube of the distance from the wall in the region near the wall.

Von Karman (63), in a modification of the Prandtl-Taylor analogy, used experimental data on velocity gradients to calculate transfer rates near the phase boundary. The Reynolds analogy was applied to the turbulent core of fluid.

All these analogies, except the Reynolds analogy, suggest the importance of both the Reynolds number and the Schmidt number in correlating mass transfer data.

Gas Phase Resistance Data and Correlations for Various Shapes and Types of Equipment

The various theories described above have aided in the empirical correlation of mass transfer data for various shapes and types of equipment.

Plane Surfaces.—Sherwood and Pigford (53) have correlated the data of various authors on the evaporation of water and other liquids from flat surfaces into air flowing in forced convection. Most of the data are for evaporation from flat pans, whose surfaces were placed flush with the floors of small wind tunnels. The j_D defined by Equation (24) is plotted versus a length Reynolds number; a single line represents the data reasonably well. Data on evaporation of water from the wet surface of a cylinder, with its axis parallel to the direction of air flow, also fall close to this line.

Cylinders Transverse to Fluid Streams.—A plot of j_D versus Reynolds number (54) has also been successful in correlating virtually all available data on mass transfer from cylinders placed transverse to fluid streams. The data, coming from many sources, cover a wide range of fluid velocities, cylinder diameters, and fluid properties. Most of the data are for

vaporization of various solvents or volatile solids into air, but data for cast cylinders of benzoic acid and cinnamic acid dissolving in water are also included. The relatively good agreement between the air and water data lends excellent support to the two-thirds exponent on the Schmidt group, which was in the range of 2000 to 3000 for the water data.

A solid line, representative of a large collection of data on heat transfer to single cylinders placed transverse to air streams, also represents the mass transfer data quite well, indicating excellent agreement between j_D and j_H.

Single Spheres.—Sherwood and Pigford (55) report the data of Froessling on the evaporation of small drops of nitrobenzene, aniline, and water and small, solid spheres of naphthalene into air. Froessling correlated the data with the following equation:

$$\frac{k_c d}{D_V} = 2.0 \left[1 + 0.276\ N_{Re}^{1/2}\ N_{Sc}^{1/3}\right], \qquad (25)$$

where

d = diameter of drop, or sphere, ft,

D_V = diffusivity of solute in gas, ft^2/hr, and

k_c = individual gas phase mass transfer coefficient lb mole/hr, ft^2, lb mole/ ft^3.

Ranz and Marshall (42) correlate their data on evaporation of single drops of water into air with the same type of equation.

Wetted-Wall Columns.—Gilliland (22) used a 1-inch by 46-inch wetted wall column, equipped with calming sections at both ends, to obtain evaporation rates of nine different liquids into air. The data were correlated by the following equation:

$$\frac{k_c d}{D_V}\ \frac{p_{BM}}{P} = 0.023\ N_{Re}^{0.83}\ N_{Sc}^{0.44} \qquad (26)$$

Sherwood and Pigford (56) point out that the exponent of 0.44 on the Schmidt group is not well established, because the Schmidt number was only varied over a four-fold range.

Packed Columns.—Three experimental methods have been used to evaluate gas-phase resistances in packed columns, (1) vaporization of a pure liquid into an inert gas stream, (2) absorption of a gas in a liquid in which it is very soluble, and (3) absorption of a gas in a liquid with which it reacts chemically.

Sherwood and Holloway (50) report data on the absorption of ammonia from air in a tower packed to a depth of 16 to 31 inches with 1-inch rings. The absorption coefficients were 50 to 70 per cent greater when 3.5 normal sulfuric acid was used as the absorbent instead of water, and it was concluded that the liquid film offers an appreciable fraction of the total resistance, in the absorption of ammonia by water. The data of Mehta and Parekh (34) on vaporization of four liquids into air in a 3.6-inch tower, packed to a depth of 5 inches with 5/8-inch rings, were also reported (50). These data indicated that the gas film mass transfer coefficient, $k_G a$, was proportional to approximately the 0.17 power of the gas diffusivity at constant air flow rate.

Dwyer and Dodge (12) have reported data on absorption of ammonia from air with water in a one-foot diameter column packed with carbon Raschig rings. The gas film resistance was reported to represent 40 to 90 per cent of the total resistance for the various runs.

Sherwood and Pigford (57) report the extensive data of Fellinger (15) on the absorption of ammonia from air with water and point out that the $k_G a$'s obtained from ammonia absorption data are usually much lower than those obtained by vaporization of pure liquids.

Scheibel and Othmer (46) studied the absorption of four different methyl ketones from air with water in a column packed with 10-mm glass Raschig rings. On the basis of this and other data, it was decided that $k_G a$ was directly proportional to gas diffusivity at constant gas mass velocity.

Houston and Walker (27) report data on the absorption of ammonia, methanol, ethanol, and acetone from air with water in a 12-inch column packed to a height of 2 feet with 1-inch Raschig rings. Gas phase resistances were obtained from the measured overall resistances, after the liquid phase resistance had been calculated from the correlation of Sherwood and Holloway (49b). Cross plots of the data indicated $k_G a$ to be proportional to about the 2/3 power of gas diffusivity for the lower liquid rates; but at the highest liquid rate an exponent of 0 on the gas diffusivity seemed to represent the data best. Gas diffusivity was varied over only a 2-fold range.

Surosky and Dodge (62) studied the evaporation of three organic liquids and water into air at atmospheric pressure and temperature in an 8-inch tower packed with 1-inch rings. Cross plots of the data showed $k_G a$ to be proportional to the 0.15 power of gas diffusivity at constant air mass velocity. This exponent on the gas diffusivity agrees well with the one obtained from the data of Mehta and Parekh (34), mentioned previously. The authors point out great discrepancies among the results of various researchers.

Zabban and Dodge (69) report data on the absorption of acetone and methanol vapors from air with water in a 6-inch and in a 12-inch packed tower at pressures ranging from 1 to 14 atmospheres. It was found that $k_G a$ was inversely proportional to the total pressure.

Lynch and Wilke (31) studied vaporization of water into air, helium, and Freon 12 in a 1-foot-diameter column packed with 1-inch Raschig rings. These systems gave a 30-fold variation in density, a 2-fold variation in viscosity, an 8-fold variation in gas diffusivity, and a 4-1/2-fold variation in Schmidt number. The results were reported in H.T.U.'s (height of a transfer unit) as defined by the following equation:

$$H.T.U._G = \frac{G_M}{k_G a p_{BM}} \quad , \tag{27}$$

where

$H.T.U._G$ = height of a gas transfer unit, feet,

G_M = molar gas mass velocity, lb mole/hr, ft^2,

p_{BM} = mean partial pressure of inert gas in film, atm,

k_G = individual gas phase mass transfer coefficient, lb mole/hr, ft^2, atm, and

a = area available for mass transfer per unit volume of packing, ft^2/ft^3.

The $H.T.U._G$'s were plotted versus a Reynolds number and versus the "F factor" (the product of the superficial velocity in feet per second and the square root of the gas density in pounds per cubic foot). At constant Reynolds number, $H.T.U._G$ was proportional to the 0.90 power of the Schmidt number (or $k_G a$ was proportional to the 0.90 power of gas diffusivity). At constant F factor, $H.T.U._G$ was proportional to only the 0.47 power of the Schmidt number.

Shulman, et. al. (58, 59, 60) have proposed an explanation for the great discrepancies noted between $k_G a$'s obtained from data on the absorption of ammonia from air with water and the $k_G a$'s obtained from data on the vaporization of pure liquids into air. The explanation applies only to packed columns and is based on the assumption that the effective

interfacial area for ammonia absorption is proportional to operating holdup, whereas, the effective area for vaporization is proportional to total holdup (static plus operating holdup).

Bubble Plate Columns.—Studies of gas phase resistance in bubble plate columns have usually reported one of the following types of data: (1) absorption or desorption of ammonia with air and water, or (2) adiabatic humidification of air with water. Adiabatic humidification of air involves only gas phase resistance, but absorption of ammonia in water involves some liquid phase resistance. It has been assumed that this liquid phase resistance could be calculated from carbon dioxide absorption or from oxygen desorption data by merely correcting for the difference in liquid phase diffusivities, provided both sets of data were taken in the same equipment at the same operating conditions. Gas phase resistances were obtained by subtracting the calculated liquid phase resistances from the measured overall resistances. It will be shown later that this procedure for calculating the liquid phase resistance to ammonia absorption may be subject to significant error.

The data of Walter and Sherwood (64), mentioned previously under Point Efficiency, included absorption of ammonia from air with water in an 18-inch bubble cap column and humidification of air with water in a 2-inch column containing a section of a 2-inch bubble cap. Their correlation, based on these and a variety of other data, was represented by Equation (5).

Gerster, Colburn, Bonnet, and Carmody (19) and Gerster, Bonnet, and Hess (18) have reported extensive data for the vaporization of water by air on a 13-inch diameter plate equipped with 13, 1-1/2-inch bubble caps in 3 rows. Data were obtained for two skirt clearances, several different weir heights, and a range of liquid and gas flow rates. The importance of

froth height and froth density in correlating the data was pointed out.

Polich (40) studied adiabatic humidification of air with water on a 10-inch diameter plate having 4 bubble caps, each 2.39 inches in diameter, arranged on 3-1/16-inch centers. Liquid rates were varied from 1 to 50 gallons per minute and superficial gas velocities from 0.5 to 4.0 feet per second. Froth heights and froth densities were found to be useful in correlating the results. Interfacial areas, average gas velocities through the liquid, and times of contact for the gas and liquid streams were estimated from the froth height and density data.

Stone (61) reported data on the vaporization of water and aqueous solutions into air plus a few runs on the desorption of ethyl alcohol from water with air and on the absorption of ammonia from air with sulfuric acid solutions. Data on the latter two systems were meager and incomplete. A long, rectangular section of a bubble cap plate was used. The active plate area was 5 feet long in the direction of liquid flow and 13 inches wide. It contained 20 full caps and 10 half caps, which were sealed against the glass side of the column. The caps were about 4 inches in diameter and were arranged on a 6-inch triangular pattern. The plate had appreciable calming sections at each end. Stone, approaching the problem of point efficiency from a theoretical point of view, considered a bubble of initially well mixed air rising through a pool of water and applied the principles of unsteady state diffusion. His correlation, which was based on studies of both liquid film and gas film controlling systems, indicated the importance of the following variables: (1) liquid and gas diffusivity, (2) the vapor-liquid equilibrium constant, (3) liquid depth on the plate, as determined by exit weir height and liquid flow rate, (4) gas velocity, (5) average bubble radius, and (6) liquid turbulence on the

plate. It was concluded that liquid viscosity was important only as it affected the liquid phase diffusivity.

Warzel (65) obtained extensive data for the absorption and the desorption of ammonia with air and water in the same bubble cap column that was used in the present work. These data are compared with the vaporization data of the present work in the Experimental Results.

Previous data on gas film resistances in bubble plate columns have been limited largely to studies of the effects of tray design and operating variables. No comprehensive data are available to show the effects of the physical properties of the gas, such as gas density, viscosity, and diffusivity. The present work was designed to partially fill this gap in the literature.

Summary of Gas Phase Resistance Studies.—Correlations of gas phase mass transfer coefficients have been presented for a number of shapes and types of equipment. Most of them have indicated the effect of either the gas diffusivity or the Schmidt number, which contains the reciprocal of the diffusivity. The data on mass transfer to, or from, plane surfaces, cylinders transverse to fluid streams, and single spheres have been correlated by assuming k_G to be proportional to the negative 2/3 power of the Schmidt number (the positive 2/3 power of diffusivity). Gilliland's correlation of his wetted-wall column data indicated that k_G was proportional to the negative 0.56 power of the Schmidt number. The packed column data show little agreement among the various authors; and the reported exponents on the gas diffusivity, to show its effect on k_Ga, have ranged from 0.15 to 1.0 (corresponding to exponents of -0.15 to -1.0 on the Schmidt group). The effect of Schmidt number on the gas phase resistances in bubble cap columns had not been studied previous to the present work.

APPARATUS

The major elements of equipment used in the present vaporization studies were (1) a five-plate, rectangular bubble cap column, (2) a gas recirculation system, (3) a liquid recirculation system, (4) sampling and analytical equipment, and (5) auxiliary equipment.

A general view of the equipment is shown in Figure (1). The test column with glass or Plexiglas windows covering one entire side is shown in the foreground. One of two centrifugal pumps used in the liquid recirculation system can be seen behind the column. The instrument rack, which supported flow meters, manometers, control valves, and electrical equipment, extends to the left of the column. The blower, dehumidification column, mist separators, and heat exchangers, described in the following pages, are supported by steel beams above the equipment shown. Only the bottom plate of the five-plate column was active in the present tests. It had 9 bubble caps, 1-1/2-inches in diameter, arranged on a 2-1/2-inch square pitch.

This equipment was designed and constructed to be adaptable to several different types of experiments. Though only vaporization data were taken in the present research, the apparatus is suitable for absorption studies with recirculation of one, or both, the liquid and vapor streams, and would require no major piping changes.

Since gases other than air and liquids other than water were used in the present work, both the liquid and the gas had to be recirculated. A schematic flow diagram of the equipment as used in the vaporization studies

is shown in Figure (2); and a more detailed description of the major equipment items is given in the following pages.

The Test Column

The test column was constructed previous to the present work by personnel of the Chemical and Metallurgical Engineering Department and was used by Warzel (65), who has given a complete description of the column, its design, and its construction details. Figures (3), (4), (5), and (6) are reproduced from Warzel's thesis. Briefly, the back, sides, and flanged face of the column were made from a single piece of 7 gage, 3/16-inch, Incoloy sheet, approximately 10 feet long and 37 inches wide. The sheet was bent by the Central Boiler and Manufacturing Company of Detroit to form a channel, 17-1/2-inches wide and 7-1/2-inches deep, with 2-inch flanged lips to provide a facing to seal the glass windows against. The bottom, the top, the downcomers, the plate supports, and the front cross braces (all of Incoloy) were welded in permanently. The bubble plates, the inlet and outlet weirs, and the splash baffles were made removable. The entire column was set inside and tack welded to a heavy frame made of 4- x 4- x 1/2-inch steel angle, as shown in Figure (3). The frame added rigidity to the column and provided a support for the steel window frames, which can be seen in Figure (1). Figure (4) summarizes the overall column dimensions.

Bubble-Plate Design.—Dimensions of the bubble cap plate are shown in Figure (5) and summarized in Table 1. Figure (6) illustrates the construction and installation details. This small, rectangular bubble plate was designed with the hope that the fluid action on it would approximate that on a similar size section of a much larger plate. This goal was probably achieved only at low weir heights, low liquid rates, and low

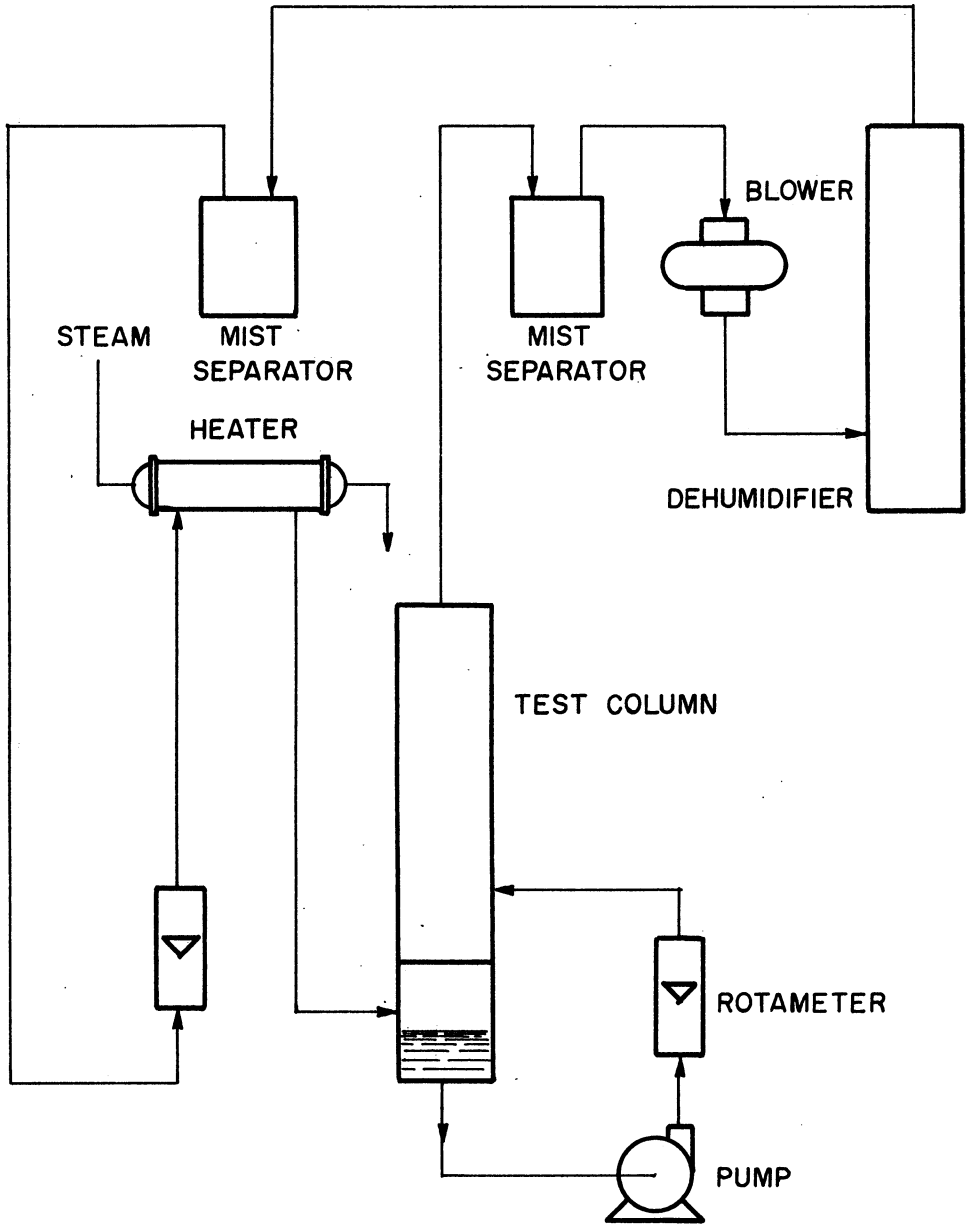

Figure 2. Schematic flow diagram of test equipment.

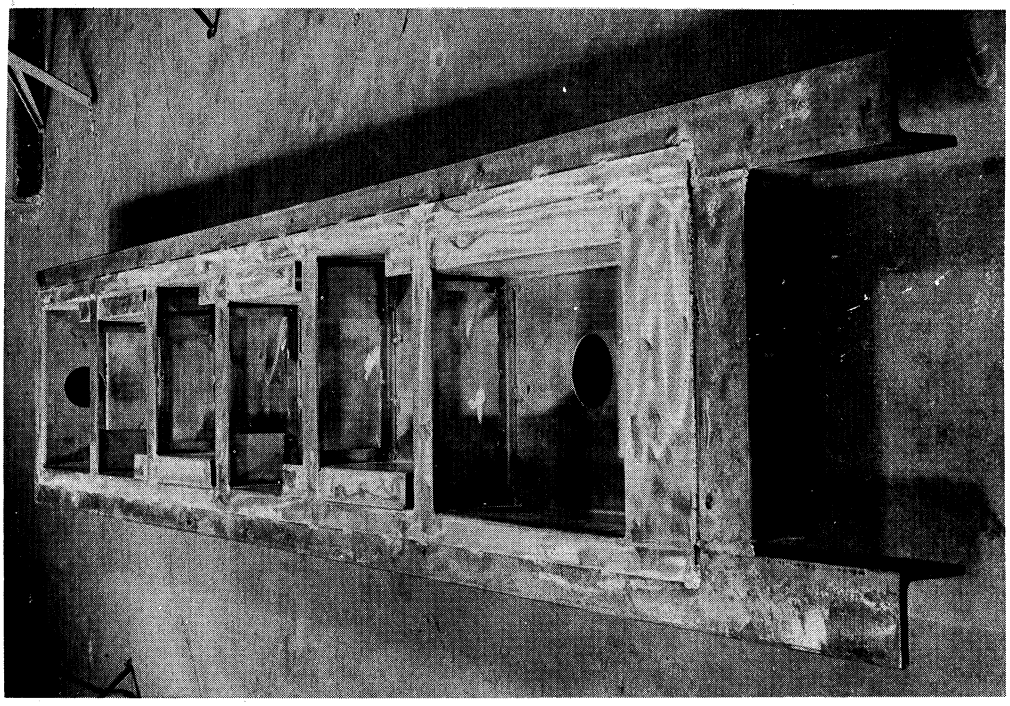

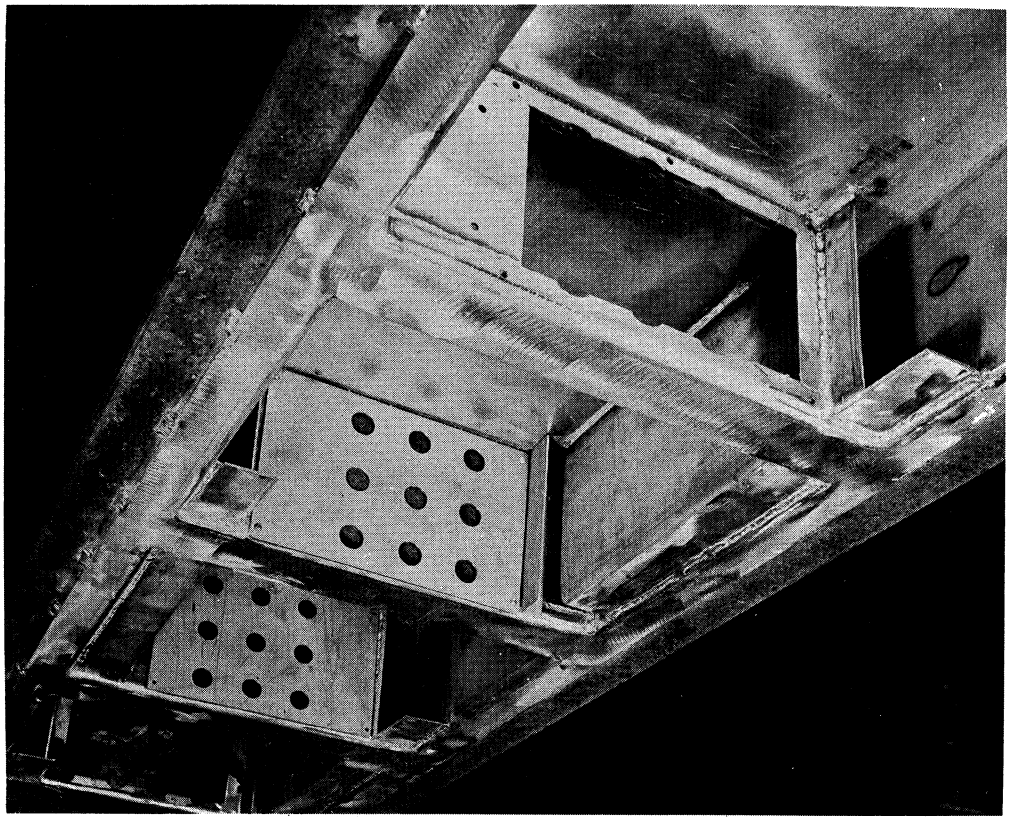

Figure 3. Test column during construction.

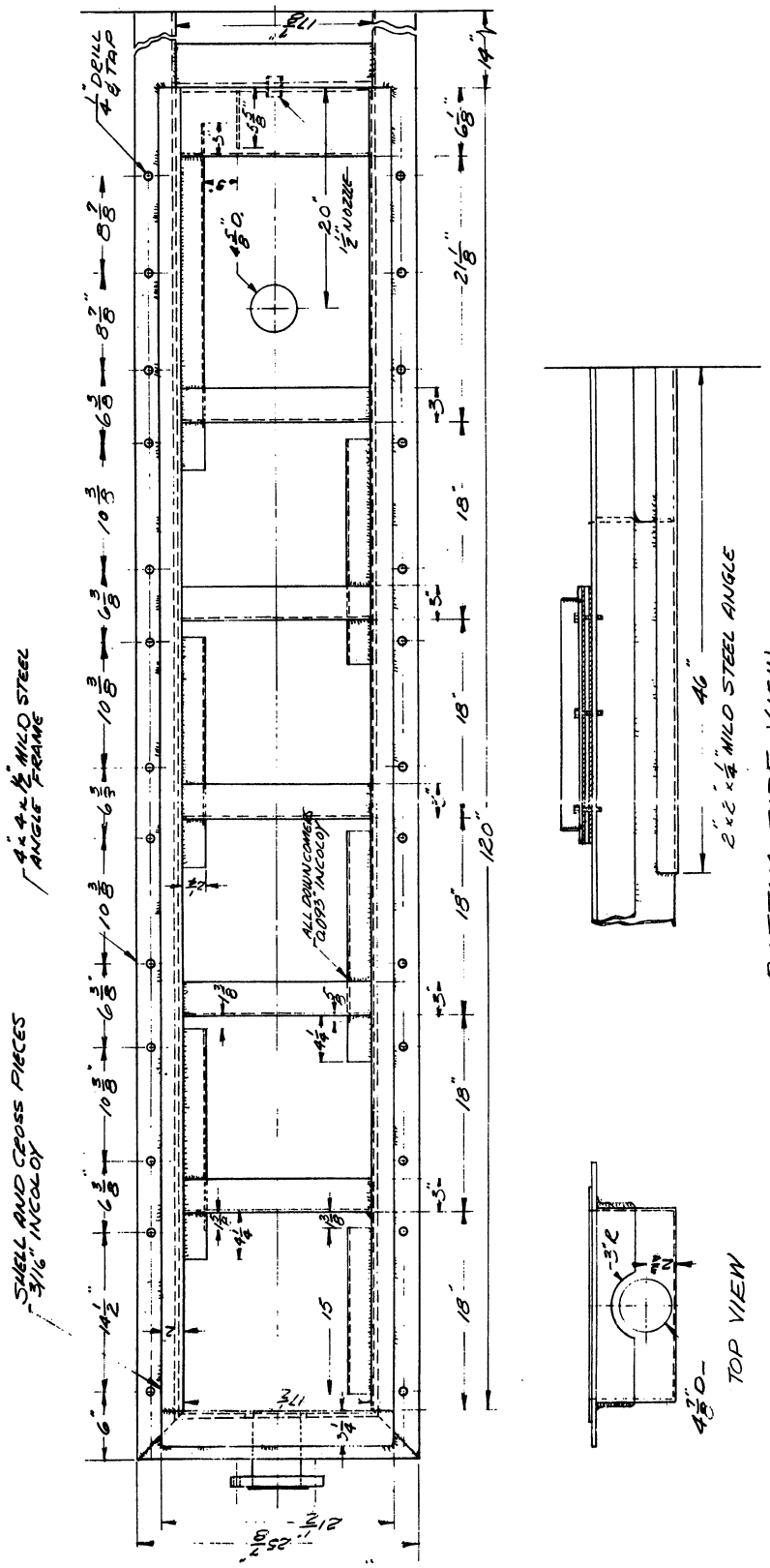

Figure 4. Tower construction.

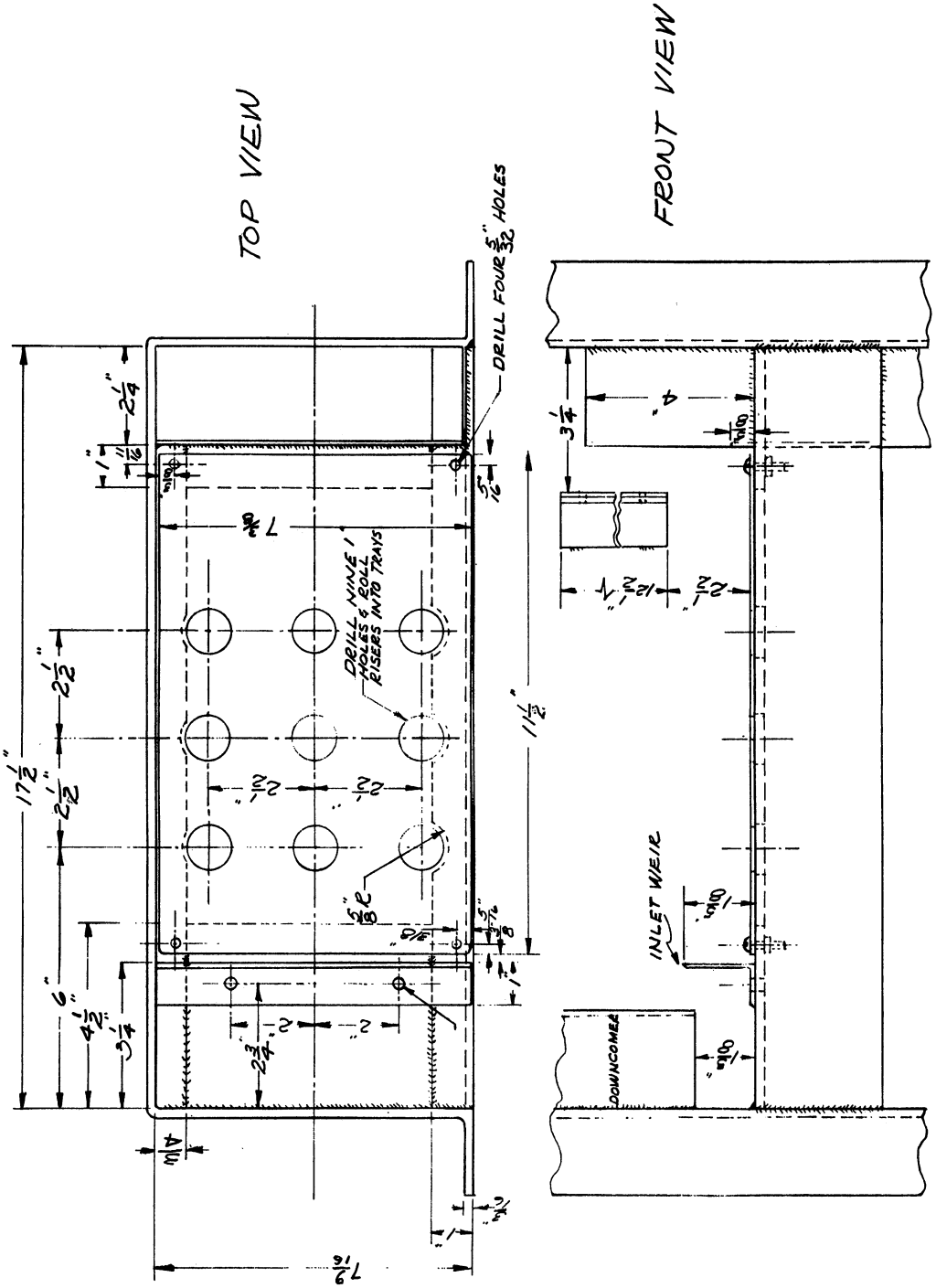

Figure 5. Plate layout.

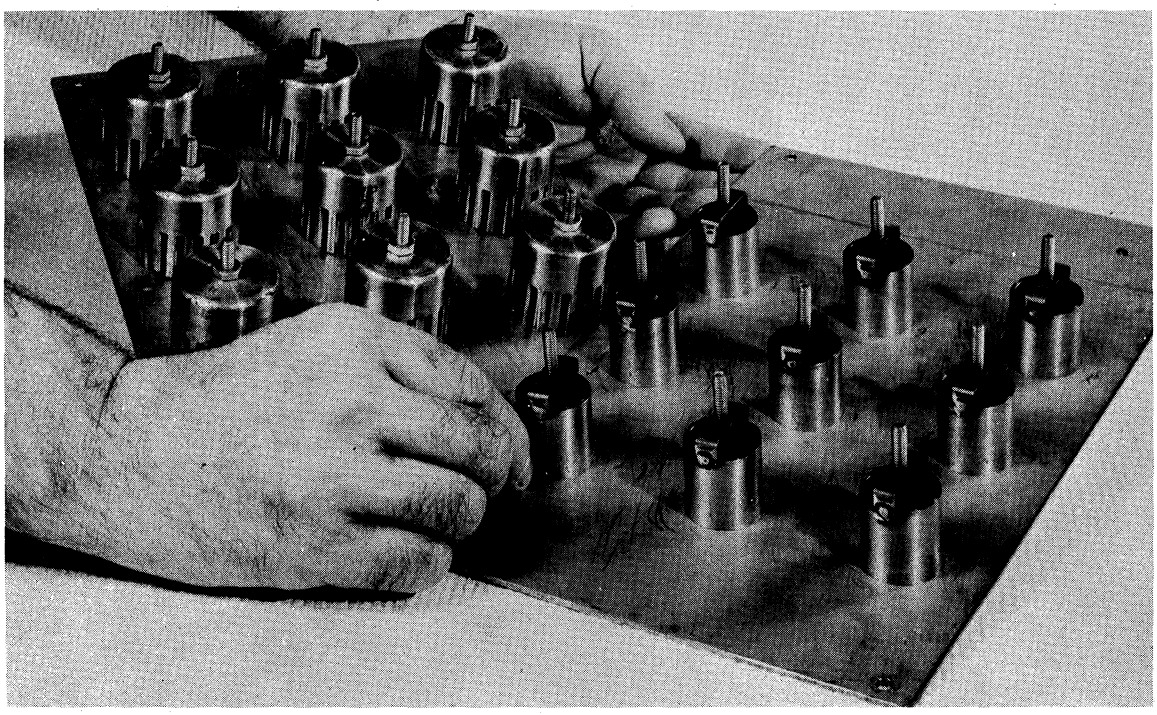

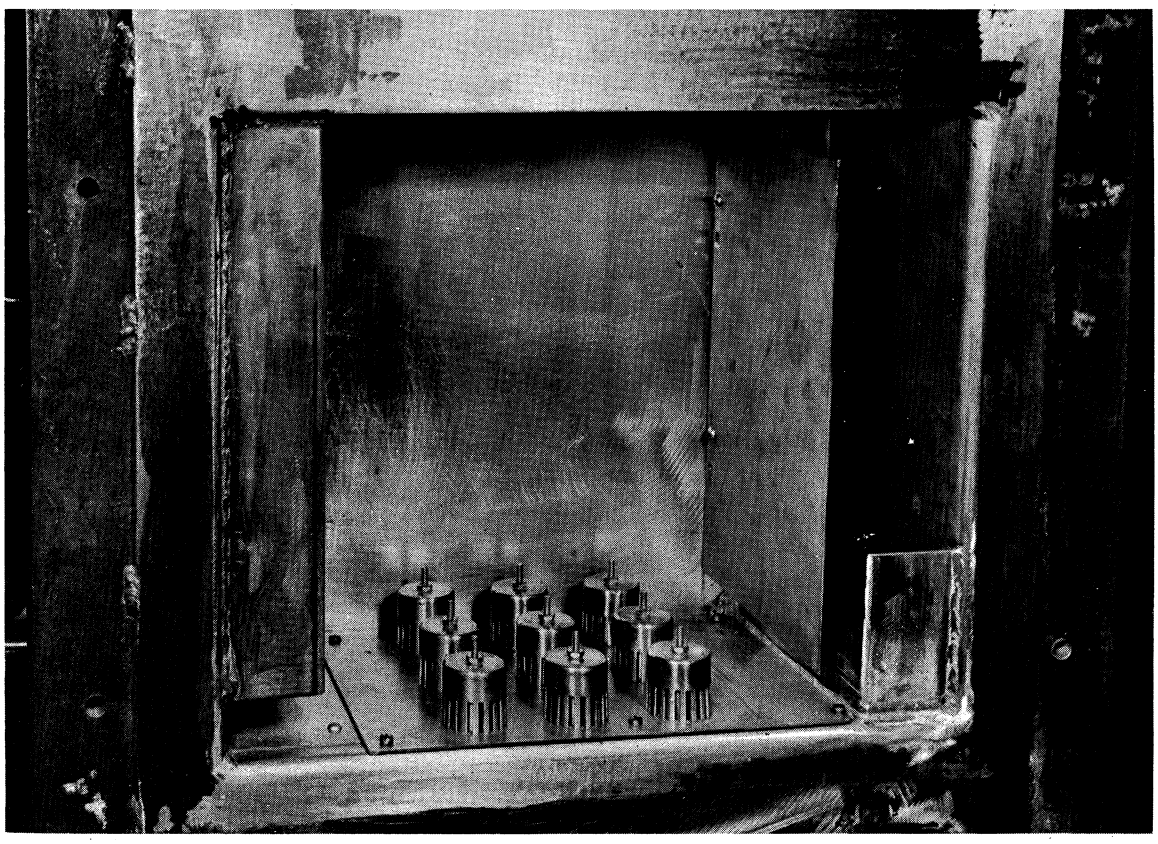

Figure 6. Removable trays and tray installation.

TABLE 1

BUBBLE TRAY DIMENSIONS

Bubble Cap	
Diameter (O.D.)	1-1/2 inch
Height	1-1/2 inch
Metal Thickness	1/16 inch
Number, per Tray	9
Slot	
Height	3/4 inch
Width	1/8 inch
Number, per Cap	18
Area, per Cap	0.0117 sq ft
Area, Fraction of Bubbling Area	0.171
Risers	
Diameter (O.D.)	1 inch
Diameter (I.D.)	7/8 inch
Height above Plate	1 inch
Area, per Cap	0.00417 sq ft
Area, Fraction of Bubbling Area	0.061
Weir (Removable)	
Length	7-3/8 inch
Height	1-1/2 and 2 inch
Splash Baffle (Removable)	
Length	12-1/2 inch
Width	7-1/2 inch
Clearance above Tray Floor	2 and 2-1/2 inch
Downcomer	
Size	7-3/8 x 2-1/8 inch
Area, Cross Sectional	0.137 sq ft
Bubbling Area (Downcomer to Splash Baffle)	
Width	7-1/2 inch
Length	11-13/16 inch
Area	0.615 sq ft
Tray Spacing	18 inch

gas rates. An increase in any one of these variables seemed to cause more pronounced end effects.

Weirs.—Removable overflow weirs were provided to permit easy adjustment of the liquid level on the plate. These weirs were slipped inside the downcomers, adjusted, leveled, and bolted to the wall of the downcomer below the tray. To avoid an extra seal against the glass face of the column, the downcomers were enclosed and made slightly less than the full column width. As a result, the outlet weirs were only 7-1/8-inches long compared to the full column width of 7-1/2-inches. This had no apparent effect on the flow patterns on the plate. Warzel (65) found that the use of an inlet weir caused undesirable anomalies in the liquid flow pattern on the plate; hence, inlet weirs were not used in his or in the present work.

Splash Baffles.—In all the present runs, a splash baffle was installed 1 inch in front of and 1/2 inch above the outlet weir. Its installation is shown in Figure (6). Warzel (65) found that plate operation without a splash baffle had two undesirable characteristics. At low liquid rates the plate discharged liquid by uneven splashing, and at high liquid rates the froth had a steep gradient toward the downcomer. The splash baffle smoothed the flow over the weir at low liquid rates, tended to level the froth at high liquid rates, and confined the bubbling action to a better defined area above the caps.

Windows.—Safety glass or Plexiglas windows, which sealed one entire side of the column, permitted full observation of the bubbling action. Continuous loops of tygon tubing were used as gaskets between the windows and the column face. Heavy steel frames, padded with sponge rubber and bolted to the 4- x 4- x 1/2-inch angle, which outlined the face of the

column, held the windows firmly against the gaskets [see Figure (1)]; and a good seal was obtained. Neither the water nor the isobutyl alcohol had any appreciable effect on the tygon gaskets, and the runs with methyl isobutyl ketone were completed before any of the gaskets dissolved enough to cause leakage.

Gas Recirculation System

The gas recirculation system consisted of a mist separator, a rotary blower, a dehumidifier, a second mist separator, a flow meter, a shell and tube type heater, and standard 3-inch connecting piping. Apparatus was also provided for adding make-up gas to the system to replace leakage and to maintain constant pressure. A schematic flow diagram of the gas recirculation system is shown in Figure (7). The solid lines indicate the path followed by the gas in the humidification tests. The dashed lines indicate auxiliary piping or alternate gas routes to be used in other types of tests.

Mist Separators.—The mist separators were 55-gallon drums with 3-inch pipe couplings brazed in their tops for pipe connections. They were designed to remove entrained droplets from the gas and prevent collection of liquid in the gas lines.

Blower.—The two-lobe, brass, rotary blower, which circulated the gas, displaced 0.18 cubic foot per revolution and had a maximum speed of 1800 revolutions per minute. It was driven by a 10-horsepower, 230-volt induction motor. An Allis-Chalmers variable speed, pulley drive, belted between the motor and blower, gave a 3-fold variation in blower speed. A 2-inch by-pass line, connected between the blower inlet and outlet, and equipped with a gate valve, gave further control of the gas flow rate.

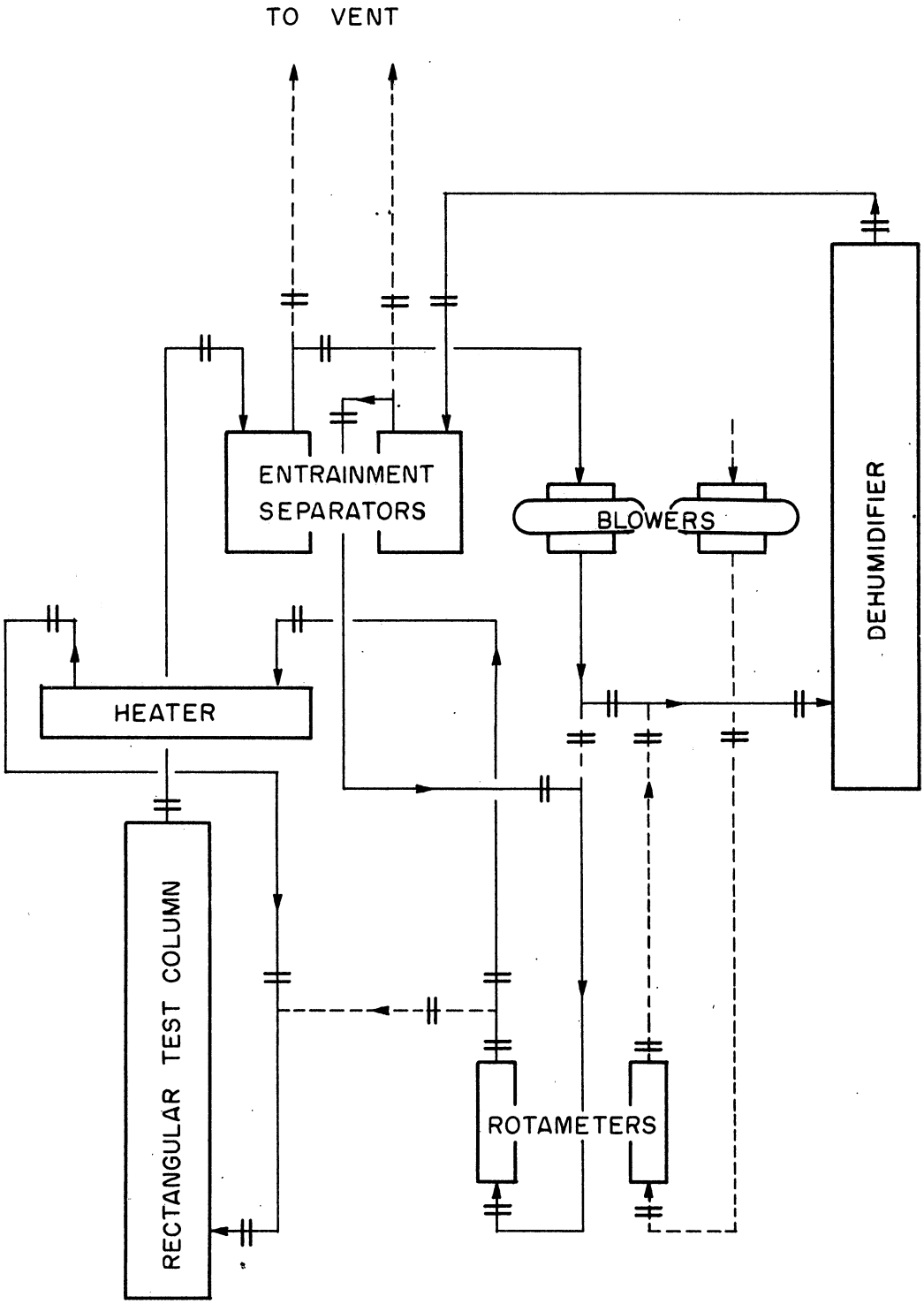

Figure 7. Flow diagram for gas recirculation system.

Dehumidifier.—The dehumidifier was a 12-inch diameter, 4-plate, sieve tray column with cold liquid circulating through it. This column was constructed by personnel of the Chemical and Metallurgical Engineering Department previous to the present work. It was designed for use as an auxiliary stripper when absorption studies were being made in the rectangular test column. For this work, however, it served well as a gas dehumidifier.

Flow Meter.—The gas flow was metered by a size 12 Fischer and Porter Flowrator (Tube No. 12-LL25, Serial No. D8-1609, Figure No. 26P-E, Chemical and Metallurgical Engineering Department No. C17-200). The precision bore tube was calibrated for 0 to 200 cubic feet per minute of 0.877 gravity gas at 14.7 psia and 60°F. Scale graduations were in increments of 2 cubic feet per minute. Warzel (65) checked the calibration of this instrument and found that the scale reading was sufficiently accurate for this work, provided, of course, suitable corrections were made for gas density.

Heater.—Before it returned to the test column, the dehumidified gas was preheated in an 8-inch diameter Ross, type "SSCF", No. 804, heat exchanger. The exchanger, constructed entirely of type 316 stainless steel, contained a 4-foot bundle of 3/8-inch tubes. The headers were designed to give four tube side passes, and the shell was baffled at 1-foot intervals. The gas flowed through the shell side of the exchanger, while steam was condensed at atmospheric pressure inside the tubes.

Piping.—The gas recirculation system was connected together with 3-inch standard galvanized pipe. Both screwed and flanged fittings were used. The flanged junctions could also be used as off-on valves by inserting or removing baffle plates between the flanges. Auxiliary piping was installed to make possible several different gas flow paths through

the equipment. The flow path could be altered by inserting or removing baffle plates between key flanges.

Flow Control.—Any particular gas flow rate within the range of the blower could be obtained by setting the blower speed, by means of the variable speed drive, slightly higher than what was required. The flow in the system could then be reduced to the desired value by opening the valve in the by-pass line.

Make-Up Gas.—A small continuous stream of gas was added to the system continuously to replace leakage and to maintain a constant, positive pressure throughout the apparatus. This make-up gas was bled from a high-pressure cylinder, through a pressure regulator designed for moderate delivery pressures, through another pressure regulator designed for very low delivery pressures, through a small rotameter, and, finally, into the main gas system at the blower inlet. Its flow rate was controlled by the pressure in the system. The rotameter was included in this line to warn the operator if the leakage rate became excessive. Some leakage around the blower shaft was apparently unavoidable.

Liquid Recirculation System

The liquid system consisted of two separate circuits; one recirculated warm liquid to the test column; and the other recirculated cold liquid to the dehumidifier. A small connecting line, equipped with a regulating valve, bled enough liquid from the dehumidifier circuit back into the test column circuit to replace the liquid evaporated there and maintain a constant liquid inventory in both. Both circuits had a centrifugal pump, a flow control valve, and a flow meter. The dehumidifier circuit also contained a shell and tube type heat exchanger in which its recirculating liquid was cooled by a stream of tap water. A small coil of

1/4-inch tubing was installed in the bottom of the test column to which either steam or cooling water could be admitted.

The pumps, control valves, and flow meters in both circuits were identical. A schematic flow diagram of the liquid recirculation system is shown in Figure (8).

Pumps.—The centrifugal pumps (Model 40, Series WS7RD-74 Durcopumps, with 7-1/2-inch open empellers) were obtained from the Duriron Company, Inc. They were made of Durimet 20, a stainless steel alloy with excellent corrosion resistance properties. The pumps were driven by 3-horsepower induction motors (1750 rpm, 220/440 volt, 60 cycles, 3-phase, totally enclosed, ball bearing, frame 225) made by General Electric.

Valves.—The flow control valves (Powell, Figure 2475, Flanged End, F and D, 150-lb, OS and Y, Bolted Bonnet, Globe Valves) were obtained from the Wm. Powell Company and were also made of Durimet 20.

Flow Meters.—Size 8, series 700, Fischer and Porter Flowraters (Serial No. W70-4024/1 used in test column circuit, with Tube No. B9-27-10/70-G and Float No. BSVT-93) measured the liquid flow rates. They were equipped with precision bore, beaded tubes and viscosity stabilized floats. The floats and all other metal parts in contact with the metered fluids were made of type 316 stainless steel. The tubes were graduated from 10 to 100 per cent of maximum capacity (32 gallons per minute of water) in increments of 1 per cent.

Piping.—Type 304 stainless steel pipe and fittings were used throughout the liquid system. Most of the pipe was standard 2-inch, schedule 5, welding type. A combination of flanged and welded joints were used to put it together. The liquid flow meters, the heat exchangers, and the two columns all had threaded female liquid fittings.

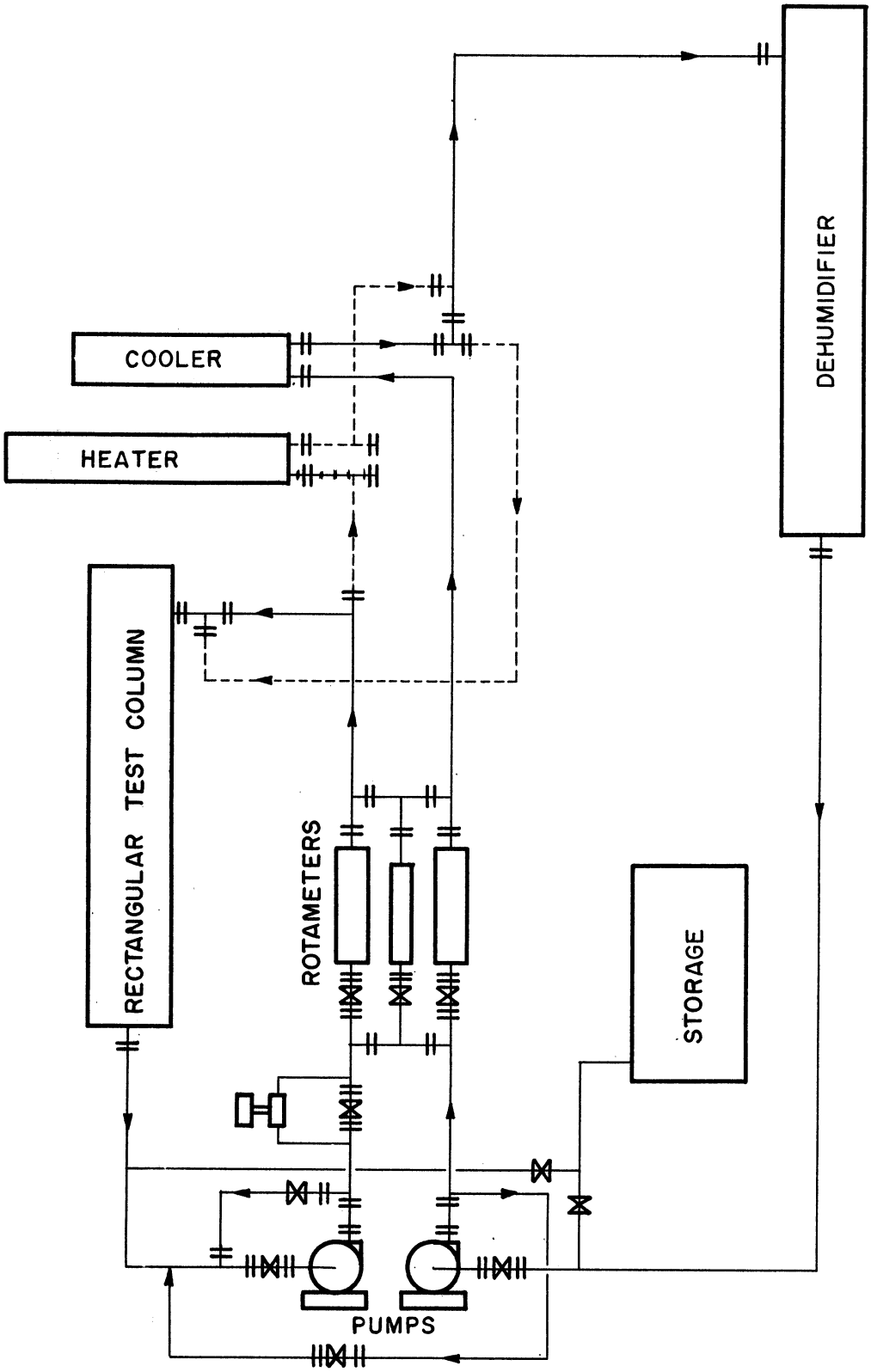

Figure 8. Flow diagram for liquid recirculation system.

These were converted to flanged connections by inserting short schedule 40 pipe nipples, with threads on one end and flanges welded to the other end.

Cooler.—The shell and tube exchanger in the dehumidifier circuit, which was used to cool the circulating liquid, was identical to the heater in the gas recirculation system, except it had a 3-foot, instead of a 4-foot, tube bundle, and its shell was baffled at 6-inch, instead of 12-inch, intervals.

Sampling and Analytical Equipment

Only gas samples were required in this work, one from above and one from below the test plate for each run. The sampling and analytical equipment consisted of sampling probes, drying tubes, wet test meters, and an analytical balance. Gravimetric type analyses were used in all cases.

Sample Probes.—Samples were withdrawn through 1/4-inch stainless steel tubes inserted through standard tubing fittings screwed into the side of the test column. The inlet sample was withdrawn from a point about three inches below the center of the test plate. Some difficulty was encountered in obtaining reliable outlet samples, due to the presence in the gas of entrained liquid droplets. Use of a "dry" bubble cap tray, 18 inches above the test plate, as an entrainment separator effectively solved this problem. The skirts of the caps on the dry tray were cut off even with the tops of the slots. Vapor samples were withdrawn from a point just below the annular space between the cap and riser of a centrally located cap, as shown in Figure (9).

The term, "dry" tray, is used here to indicate that no liquid, other than entrained droplets, was fed to this tray; and de-entrained liquid was

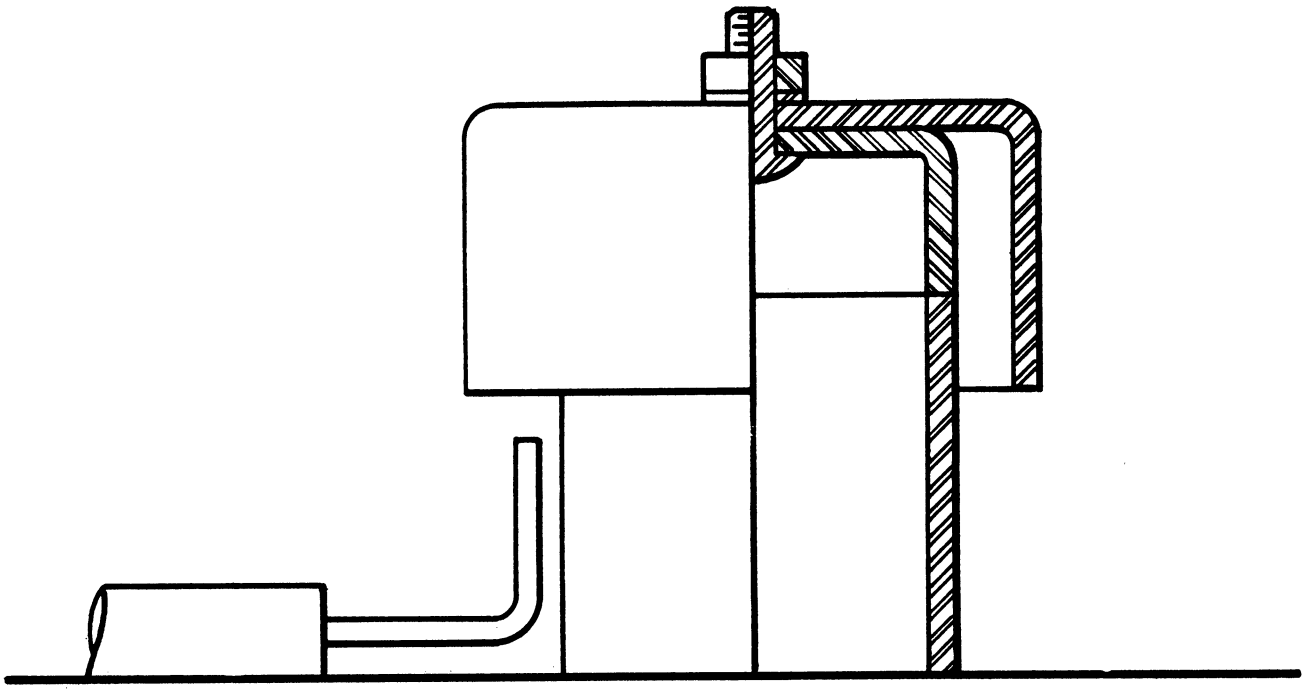

Figure 9. Position of probe for outlet gas samples.

not allowed to accumulate.

The sample lines, which were connected just outside the column to the sample probes, were wrapped with resistance wire and electrically heated to prevent condensation of vapor from the samples before they entered the drying tubes.

Drying Tubes.—These standard, glass, U-shaped tubes, equipped with stoppers and side outlets, were designed to quantitatively remove liquid vapor from the gas samples, either by absorption or by condensation of the vapors. When water vapor was to be removed, the tubes contained anhydrous calcium sulfate (Drierite). When isobutyl alcohol or methyl isobutyl ketone vapor was to be removed, the tubes were filled with 3 mm glass beads and were immersed in a constant temperature bath containing ethyl alcohol and solid carbon dioxide at -72°C. A 1-gallon, wide-mouth vacuum bottle held the bath liquid.

Sample Meters.—Calibrated wet test meters, made by the Precision Scientific Company and nominally rated at 0.1 cubic foot per revolution, were used to measure the volume of each of the gas samples.

Balance.—A Christian Becker projectomatic analytical balance and class S, stainless steel weights were used to weigh the drying tubes before and after sampling. The balance and weights were checked against standard weights having a Bureau of Standards calibration. The tolerances were found to be well within the limits of accuracy of the present work ($\pm$ 0.2 mg) with no corrections.

Auxiliary Equipment.—Equipment was also provided for measurement of temperatures and pressures at various points in the apparatus plus clear liquid heights and froth heights on the test plate.

Temperatures were measured with copper-constantan thermocouples connected to a common cold junction by an 11-point Mallory selector switch. Millivolt readings were made with a Leeds and Northrup portable precision potentiometer (Model 8662, Serial No. 773919). Successive checks indicated that the thermocouple calibrations changed slightly (as much as 0.5°C in all) from time to time, but that they all changed uniformly by the same amount. Therefore, a carefully calibrated Kimble mercury-in-glass thermometer (-1 to 51°C in increments of 0.1 C°) was installed at the outlet end of the test tray at approximately the same position as one of the thermocouples. Comparison of the thermometer reading with the thermocouple reading established a correction for all the other thermocouple readings. The thermometer used was calibrated against a similar thermometer (No. 42927) having a Bureau of Standards calibration. Suitable stem corrections were applied in all cases. A magnifying thermometer reader permitted readings within 0.01°C; and the absolute accuracy was probably within 0.05°C.

Pressures in the gas flow meter and above the test plate were measured by 30-inch, mercury-filled manometers. The pressure drop across the test plate was measured by a water-filled manometer. Pressure at the blower inlet (the lowest pressure in the entire system) was indicated by a bubbler tube immersed in water.

Clear liquid heights on the test plate were indicated by the height of the liquid meniscus in a vertical tube attached to a manometer board beside the plate. The bottom of the tube was connected to a probe in the liquid near the base of the plate, and the top was vented to the vapor space above the plate. Four such tubes were provided so that clear liquid heights could be measured at four different points on the test plate.

Froth heights were measured visually by comparison with a scale glued to the window which sealed one side of the bubbling section.

MATERIALS

Air

The air was supplied from lines in the laboratory.

Nitrogen

Anhydrous nitrogen was supplied by the Liquid Carbonics Corporation via General Stores at The University of Michigan.

Helium

The helium was supplied by the United States Department of Interior via the Liquid Carbonics Corporation and General Stores at The University of Michigan.

Freon 12

The Freon 12 (dichlorodifluoromethane) was supplied by the E. I. DuPont Company via General Stores at The University of Michigan.

Water

Distilled water was obtained from the Department of Chemical and Metallurgical Engineering.

Isobutyl Alcohol

The isobutyl alcohol was obtained from the Carbide and Carbon Chemicals Company. Though their specifications did not require the direct determination of purity, analyses of occasional samples in the past had yielded purity values in excess of 99 per cent by weight (70). The usual impurities were

water (about 0.2 per cent) and carbonyls (about 0.02 per cent as isobutyraldehyde). The ASTM distillation range was usually 106.6 to 108.6 °C. An ASTM distillation performed by the author after completion of the present experiments gave a range of 105.6 to 108.6 °C.

Methyl Isobutyl Ketone

The methyl isobutyl ketone was obtained from the Shell Chemical Corporation. Its specifications were as follows (35):

Purity.	Contains not less than 99% by weight methyl isobutyl ketone
Specific Gravity 20°/20°C. . .	0.800-0.804
Distilation Range.	Below 114.0 °C None Above 117.0 °C None

An ASTM distillation performed by the author after completion of the present experiments gave a range of 115.1 to 116.2 °C.

EXPERIMENTAL PROCEDURE

The procedure for a day of data taking normally involved the following steps: (1) selection of the operating conditions, (2) starting the equipment, (3) preparing and weighing drying tubes while the equipment came to equilibrium, (4) checking the purity of the gas in the system, (5) withdrawing samples and recording operating data, and (6) re-weighing the drying tubes to determine the weight of liquid vapor removed from each of the gas samples. Often preliminary calculations were made the same evening to check the consistency of the data.

Selection of the Operating Conditions

The volumetric liquid flow rate (8 gallons per minute), the weir height (1.5 inches), and the splash baffle height (2.0 inches) were the same for all the runs, except for a few initial air-water runs made at a 2-inch weir height. For a given system, then, the gas rate was the only real variable; and once it was selected, the operating conditions were fixed. It was necessary, however, to calculate, in advance, the adiabatic saturation temperature of the gas which would enter the bottom of the test plate, so that the liquid temperature on the plate could be held near that value during the run. The adiabatic saturation temperature can be calculated if the temperature, composition, and specific heat of the gas, the latent heat of the liquid, and the specific heat of its vapor are known. Because of heat losses, the inlet gas temperature was slightly affected by gas flow rate; the inlet gas composition was largely determined by the cooling water temperature. Both conditions could be estimated accurately enough

in advance to calculate the adiabatic saturation temperature within about 2°C.

Start Up and Column Operation

A detailed description of the start-up procedure is given in the Appendix. From 20 to 30 minutes were ordinarily required to complete this procedure. Because of the high heat capacity of the system and the low specific heat of the recirculating gas, two or three hours of steady operation were then required for the system to reach temperature equilibrium. Once equilibrium was reached, however, the system was very stable. The temperature of the liquid entering the test plate usually changed no more than 0.1 to 0.2°F during a 5 to 10 minute sampling period, and the temperature of the hot gas entering the test plate varied no more than 1°F during the same period. Periodic checks and fine adjustments of flow conditions, etc., were made while the system was coming to equilibrium, but continuous observation was not necessary. Liquid temperature on the test plate was held at the calculated adiabatic saturation temperature by the controlled flow of cooling water through a coil of tubing in the bottom of the test column.

Preparation of Drying Tubes

During the time required for the system to reach equilibrium, the drying tubes, used to remove the liquid vapor from the samples, were prepared and weighed. If water was the vapor to be removed, the tubes were filled with fresh Drierite—the indicating type, which changes color from blue to pink when it absorbs water. A small section of fiber glass was placed above the Drierite granules at each end of the drying tubes to prevent dust or fine particles from being blown out of the tubes during

sampling. The tubes were then stoppered, purged with dry air, and weighed. When the helium-water or the Freon 12-water system was being studied, the drying tubes were always purged with dry air before and after sampling so that they always contained air when weighed. This purging removed virtually all the helium or Freon 12, but did not remove a measurable amount of the chemically absorbed water. The tubes were kept sealed during the periods between sampling and weighing. Also, weighed but unused drying tubes were kept in the same box with the other drying tubes. By weighing the unused drying tubes along with the others, a correction for changes in humidity, barometric pressure, etc. was obtained. The correction normally amounted to less than 0.5 mg per tube.

If either isobutyl alcohol or methyl isobutyl ketone vapor was to be removed from the gas samples, the tubes were filled with 3 mm glass beads. A small section of fiber glass was placed in the beads near the bottom of the outlet side of the tubes to filter and prevent the escape of condensed vapor in the form of fog. Liquid condensed in the tubes the preceding day was removed by purging them at room temperature with dry nitrogen. If helium was being used in the experimental apparatus, these tubes were purged again with dry nitrogen after sampling, but before they were removed from the cold bath. The vapor pressure of isobutyl alcohol or of methyl isobutyl ketone was estimated to be less than 0.01 mm Hg at the bath temperature (-72 °C), so that a negligible amount of condensed liquid was removed by the purging.

Determination of the Purity of the Recirculating Gas

When helium or Freon 12 was being used, it was important that the system contained no more than 1 per cent of air, because of its effect on the gas density. With helium, it was desirable to reduce the air concentration

still lower, because 1 per cent of air increased the gas density about 6 per cent. Since positive displacement of the air from the system was not possible, the desired gas purity was attained by slow addition of pure helium, or Freon 12, while the gas in the system was being recirculated (a continuous dilution process). Since the approximate volume of the system was known and the gas inside was almost perfectly mixed, it was possible to calculate how much pure gas had to be added to achieve a given concentration. The following equation was used:

$$V_G = V_S \ln \left[\frac{\text{initial air concentration, \%}}{\text{final air concentration, \%}} \right] , \qquad (28)$$

where

V_G = volume of pure gas (helium or Freon 12) added to system, ft^3, and

V_S = volume of system, ft^3 .

The volume of the system was estimated to be 40 cubic feet; and, if it contained 100 per cent air to start with, about 184 cubic feet of helium had to be added to reduce the air concentration to 1 per cent. Another 92 cubic feet of helium were required to reduce the air to 0.1 per cent. A slight positive pressure was maintained throughout the system at all times to prevent any leakage of air into it. The results of the above calculations were checked by gas density measurements.

Sampling Procedure

After the system had reached equilibrium, which was indicated by constant fluid temperatures, the heated sample lines were purged with dry gas to remove any possible moisture. Then, after the various operating data had been recorded, the samples were withdrawn.

The drying tubes were connected in groups of two or three (in series) to each of the sample lines (three tubes in series for absorption of water vapor with Drierite, and two tubes in series for condensation of isobutyl alcohol or methyl isobutyl ketone vapor at -72°C). Following the drying tubes, two bubblers were connected in series to saturate the dried gas samples with water before they entered the wet test meters. Thus, a gas sample being withdrawn from the test column passed through the following equipment before escaping to the atmosphere: (1) a heated sample line, (2) a series of drying tubes, (3) two bubblers containing water, and (4) a calibrated wet test meter. The two samples for each run, one from above and one from below the test plate, were withdrawn simultaneously to minimize the error caused by slight variations in the inlet gas composition.

Analytical Procedure

A gravimetric type analysis was used in every case. The method consisted of weighing the drying tubes before and after sampling to determine the weight of liquid removed from each of the gas samples. The tubes always contained the same kind of gas for both weighings, as explained in the section on Preparation of Drying Tubes. Tubes which had been immersed in the cold bath were allowed to warm up to room temperature and dry before being weighed. Previous experiments had shown that the tubes could be immersed in the bath and dried in this manner without gaining or losing significant weight.

The efficiency of the drying tubes in removing the vapor from the samples was indicated by the relative amount of vapor absorbed, or condensed, in the first tube. For the samples containing water vapor, over

95 per cent of the vapor was absorbed in the first tube of each series and a negligible amount in the third tube. For the samples containing one of the organic vapors, over 98 per cent of the vapor was condensed in the first tube. Thus, the moles of liquid in each of the samples was determined.

The volume of inert gas in each of the samples was measured by the wet test meters; and, after the application of suitable corrections for temperature, pressure, and humidity, this measured gas volume was converted into moles of inert, dry gas. Thus, both the moles of vapor and the moles of inert gas in a sample were measured, fixing its composition.

Data Recorded

The following data were recorded for each run: date, run number, system components, operator, weir height, splash baffle height, gas rotameter reading, liquid rotameter reading, barometric pressure, pressure in gas rotameter, pressure above the test plate, pressure drop across the test plate, froth height on the test plate, clear liquid heights at four points on the test plate, liquid temperature at each end of the test plate (and for some runs in the middle of the test plate), gas temperature below the test plate, gas wet bulb temperature above the test plate, fluid temperatures in the gas and liquid rotameters, the temperature, pressure, initial and final readings of each of the wet test meters, and the tube number and initial and final weights of each of the drying tubes. Care was taken to identify the drying tubes and the wet test meter readings with the correct samples.

SOURCES OF EXPERIMENTAL ERROR

The absolute error in a series of experiments such as the ones just described is difficult, if not impossible, to determine. However, since data taken with six different systems are correlated in this work, estimates of the absolute accuracy of the data, as well as the reproducibility of the data for a given system, are important in evaluating the results and will be made.

Some idea of the reproducibility of the data can be gained from Figures 10, 11, 12, and 13 which show the point vapor efficiency E_{OG}, and the number of transfer units per plate, N_G, for each system plotted as functions of the gas F factor. These plots were made primarily to check the consistency of the data.

Errors in the present experiments may be divided into three main categories: (1) errors in the determination of the correct equilibrium composition for the gas on the test tray, (2) errors in the determination of the correct inlet and outlet compositions of the gas, and (3) miscellaneous errors.

Since the mass transfer data are correlated in terms of N_G's, as will be shown in the Experimental Results, Table 2 is presented to show the relative effects of errors of the first two categories on the calculated value of N_G.

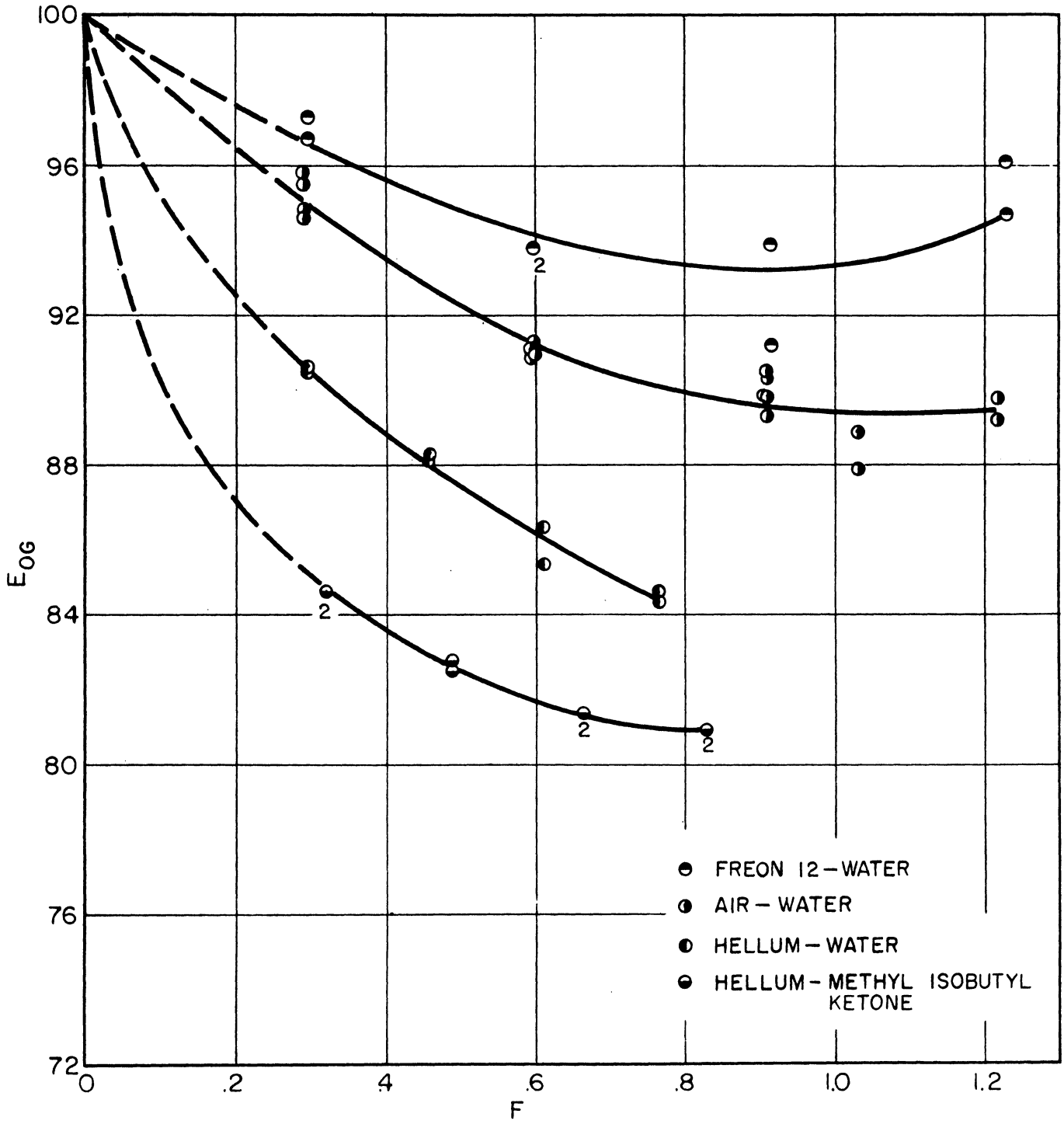

Figure 10. Effect of F factor on E_{OG}, 1-1/2-inch weir, 8 gallons per minute liquid rate.

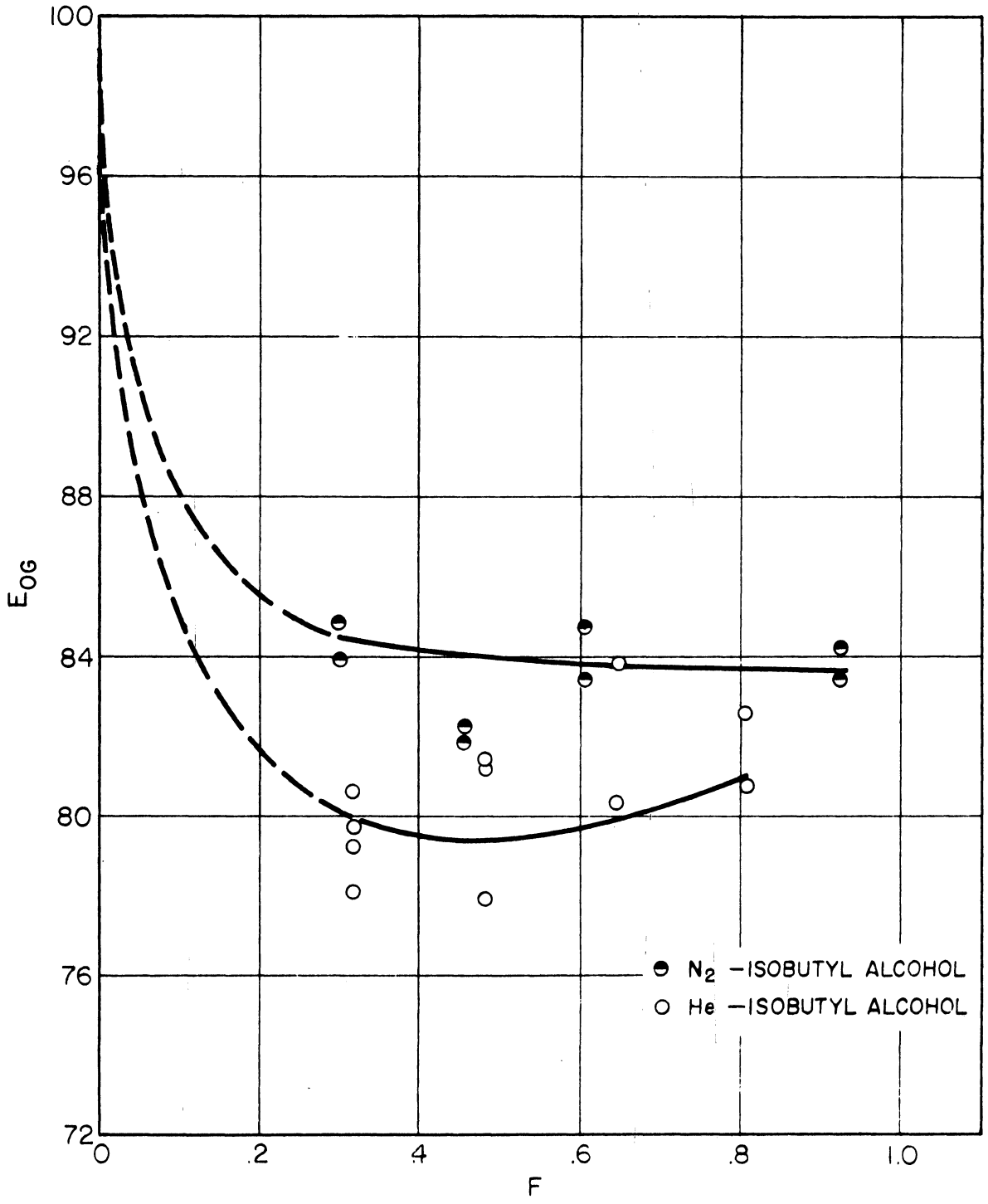

Figure 11. Effect of F factor on E_{OG}, 1-1/2-inch weir, 8 gallons per minute liquid rate.

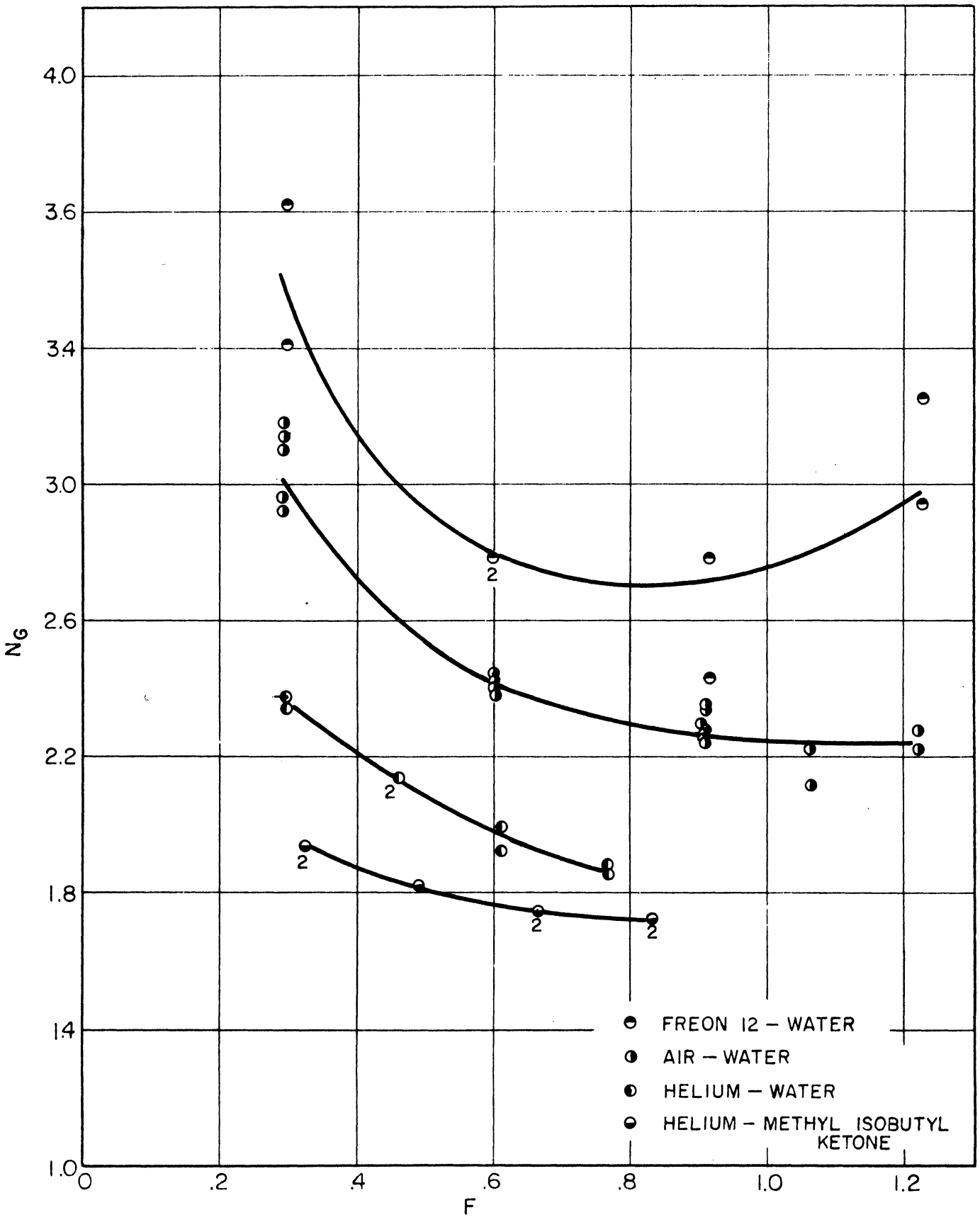

Figure 12. Effect of F factor on N_G, 1-1/2-inch weir, 8 gallons per minute liquid rate.

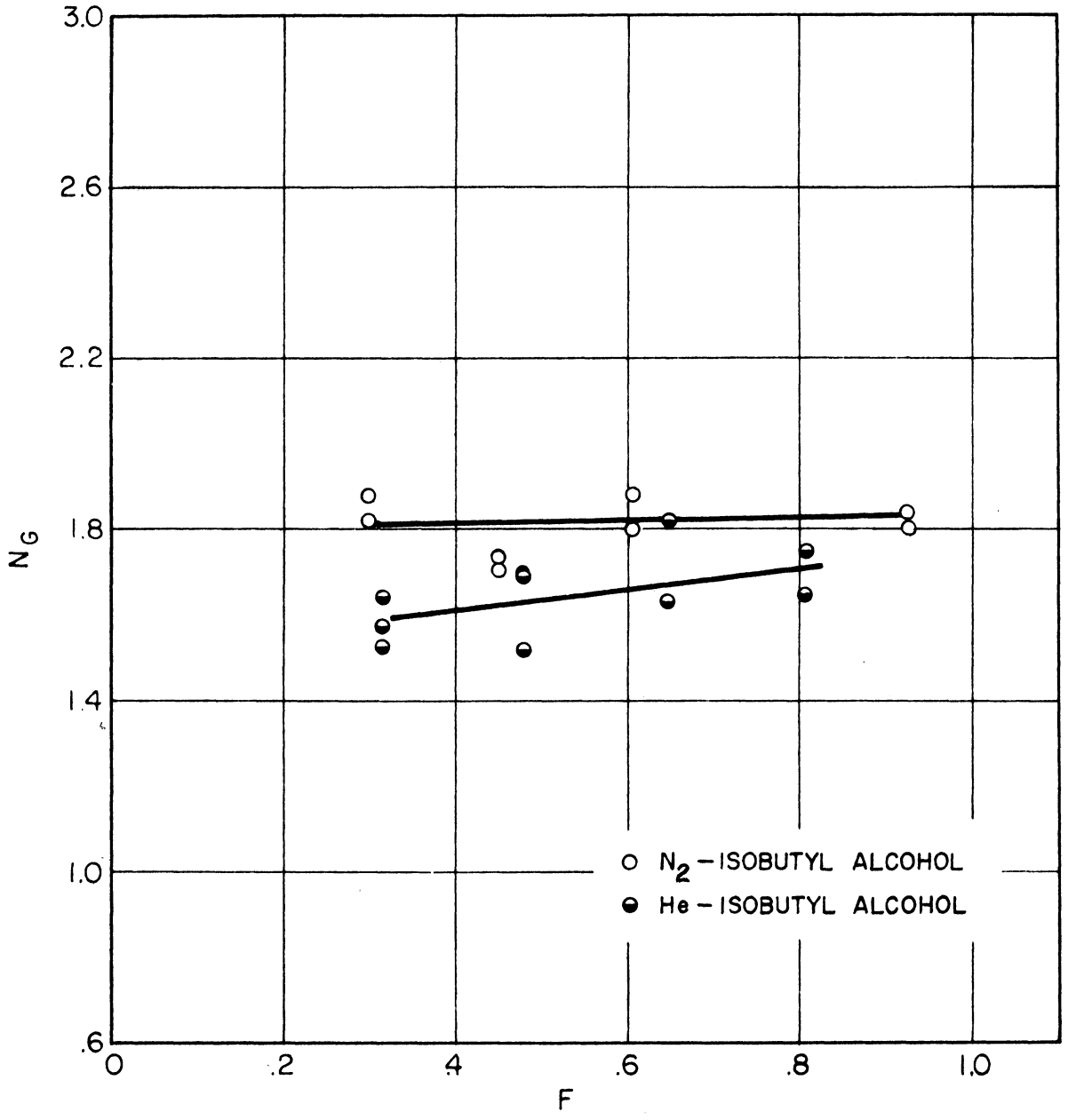

Figure 13. Effect of F factor on N_G, 1-1/2-inch weir, 8 gallons per minute liquid rate.

TABLE 2

RELATIVE ERROR IN N_G RESULTING FROM ERRORS IN y_1^*, y_1, OR y_o

	% Error in N_G Resulting From 1% Error in		
System	y_1^*	y_1	y_o
He-Water	6	6	.5
Air-Water	7.5	7.5	.5
Freon 12-Water	8	8	.5
He-Isobutyl Alc.	4.5	4.5	.5
N_2-Isobutyl Alc.	4.5	4.5	.5
He-MIBK	4.5	4.5	.5

Possible Error in the Gas Equilibrium Composition

There were five possible sources of error in the determination of the gas equilibrium composition, y_1^*:

1. Measurement of the average bulk liquid temperature on the test plate.
2. Assumption that the surface temperature of the liquid was equal to its bulk temperature.
3. Vapor pressure data.
4. Influence of impurities in the liquid on its vapor pressure.
5. Measurement of the pressure above the test plate.

Table 3 presents an estimate of the magnitude of each of these sources of error for each of the systems studied. The numbers in Table 3 correspond to the numbers given above for the various sources of error.

Item 1.—A standard mercury-in-glass thermometer, accurate to within 0.05°C, was used to measure the temperature of the liquid leaving the plate. This reading was used to correct the various thermocouple readings as explained in Auxiliary Equipment. Since the liquid temperatures at each

end of the plate differed in some cases by 0.5°C, the error in the average bulk liquid temperature was greater than the error in the thermometer reading.

TABLE 3

POSSIBLE ERROR IN THE GAS EQUILIBRIUM COMPOSITION, y_1^*

Sources of Error	Maximum Per Cent Error in y_1^* for Each System					
	Helium-Water	Air-Water	Freon 12-Water	Helium-Isobutyl Alc.	Nitrogen-Isobutyl Alc.	Helium-MIBK
1	.5	.5	.5	.5	.5	.5
2	.5	--	.5	1.0	.5	1.0
3	--	--	--	1.0	1.0	1.0
4	--	--	--	1.0	1.0	.5
5	.3	.3	.3	.3	.3	.3
Total, %	1.3	.8	1.3	3.8	3.3	3.3
Resulting Error in N_G, %	8	6	10	17	15	15

Item 2.—It was stated earlier that the liquid temperature was held near the adiabatic saturation temperature of the gas so that the surface temperature of the liquid would be the same as its bulk temperature. Actually, the temperature of the liquid surface tends toward the wet bulb temperature of the gas, instead of the adiabatic saturation temperature. The two temperatures are equal, of course, for a saturated gas, but may differ considerably when the gas is superheated. For the Freon-12-water system, the wet-bulb temperature is lower than the adiabatic saturation temperature; for the air-water system, the two temperatures are approximately equal; and, for the other four systems, the wet bulb temperature is higher than the adiabatic saturation temperature. The outlet wet bulb

temperature of the gas differed from the inlet wet bulb temperature for all the systems studied except air-water. The bulk liquid temperature on the test plate was kept somewhere between the two values, and it was assumed that internal liquid mixing was sufficient to keep the surface temperature essentially the same as the bulk liquid temperature.

Item 3.—The sources of the vapor pressure data are given in the Appendix. The water data probably have negligible error. The isobutyl alcohol data gave a smooth line when the logarithm of the vapor pressure was plotted against the reciprocal of the absolute temperature on a large sheet of accurate graph paper.

Item 4.—The water used in these tests was distilled and contained negligible impurities. Specifications for the isobutyl alcohol and the methyl isobutyl ketone were given in Materials. Some lubricant from the pump packings was dissolved in these liquids during the course of the tests. ASTM distillations of each of the liquids after completion of the tests gave a 3°C boiling range for the isobutyl alcohol and only a 1°C boiling range for the methyl isobutyl ketone.

Item 5.—The pressure above the test plate was measured with a mercury manometer with a probable error of less than 0.1 inch of mercury.

Possible Errors in the Inlet and Outlet Gas Compositions

The sources of error in the determination of the inlet and outlet gas compositions are listed below, and the estimated magnitudes of these errors are presented in Tables 4 and 5, respectively.

1. Weighing of the drying tubes.
2. Correction for change in weight due to atmospheric changes in the balance room.

TABLE 4

POSSIBLE ERROR IN GAS INLET COMPOSITION, y_o

Sources of Error	Maximum Per Cent Error in y_o for Each System					
	Helium-Water	Air-Water	Freon 12-Water	Helium-Isobutyl Alc.	Nitrogen-Isobutyl Alc.	Helium-MIBK
1	.6	.6	.6	.3	.3	.3
2	.3	.3	.3	--	--	--
3	.2	.2	.2	.2	.2	.2
4	.5	.5	.5	.5	.5	.5
Total, %	1.6	1.6	1.6	1.0	1.0	1.0
Error in N_G, %	.8	.8	.8	.5	.5	.5

TABLE 5

POSSIBLE ERROR IN GAS OUTLET COMPOSITION, y_1

Sources of Error	Maximum Per Cent Error in y_1 for Each System					
	Helium-Water	Air-Water	Freon 12-Water	Helium-Isobutyl Alc.	Nitrogen-Isobutyl Alc.	Helium-MIBK
1	.3	.3	.3	.2	.2	.1
2	.2	.2	.2	--	--	--
3	.2	.2	.2	.2	.2	.2
4	.5	.5	.5	.5	.5	.5
Total, %	1.2	1.2	1.2	.9	.9	.8
Error in N_G, %	7	9	9	4	4	4

3. Failure of the drying tubes to completely remove all vapor from the gas samples.

4. Inaccuracy of the wet test meters.

The items mentioned above have all been discussed in the sections, Experimental Apparatus and Experimental Procedure.

Sampling errors would result if small entrained droplets of liquid managed to get into the outlet gas sample probe, shown in Figure 9. This type of error was more likely to occur at high gas rates, when the amount of entrainment was relatively large. However, the probe was observed carefully during the runs; and it is believed by the author that no entrained droplets entered the sample probe. The consistency and reproducibility of the data are the best proofs in support of this statement.

Miscellaneous Errors

Miscellaneous sources of error are found in the measurement of the liquid and gas flow rates and in variations in the inlet gas composition. The fluid flow rates were not critical in determining the N_G's. The calibrations of the flow meters (given in the Appendix) were considered sufficiently accurate to cause negligible error. The flow rates of the gas and liquid were steady and required only occasional adjustment. However, there was some instability in the gas rate at the lowest values.

As a rule, the inlet gas composition was nearly constant. However, in the runs with isobutyl alcohol, the liquid circulating through the dehumidifier could not be cooled sufficiently to keep it below room temperature; and condensation of liquid occurred in the gas line between the dehumidifier and the preheater. This caused some variation in the inlet gas composition and may be the explanation for the relatively poor reproducibility of the helium-isobutyl alcohol and the nitrogen-isobutyl alcohol data.

Summary of Possible Error

It has been shown that if all the possible errors existed and were additive for a given run, a considerable error in N_G (20-30%) would result. The possibility of such large errors exists primarily, because the outlet gas closely approaches the equilibrium condition. This fact is illustrated by the extreme sensitivity of N_G to the equilibrium concentration and to the outlet gas concentration.

EXPERIMENTAL RESULTS

Tables 6, 7, 8, 9, 10, 11, and 12, given in the Appendix, summarize the experimental data. In the following sections the various data are discussed and presented graphically, either in the original or in a correlated form.

Hydraulic Characteristics of the Test Plate

Pressure drop, clear liquid height, and froth height were measured for each of the mass transfer runs. These data are tabulated separately in Table 13 of the Appendix. Though they do not include a wide range of the operating variables, except the gas rate, they are still of interest, because they do include a wide range of fluid physical properties. Warzel (65) had already made a thorough study of the effect of operating and design variables on the hydraulic characteristics of this column for the air-water system. His data and conclusions influenced the choice of operating conditions used in the present work.

Pressure Drop.—The pressure drop through the test plate is plotted as a function of gas rate for all six gas-liquid systems in Figure (14). The upper solid line represents the three gas-water systems; the lower solid line represents the gas-organic liquid systems. The dashed line represents the lower solid line when corrected for liquid density as shown on the figure. This correction shows that if the pressure drop were measured in inches of a liquid having the same density as the liquid on the tray, all the points in Figure (14) would fall approximately on the same smooth curve. The F factor is shown to be a significant variable

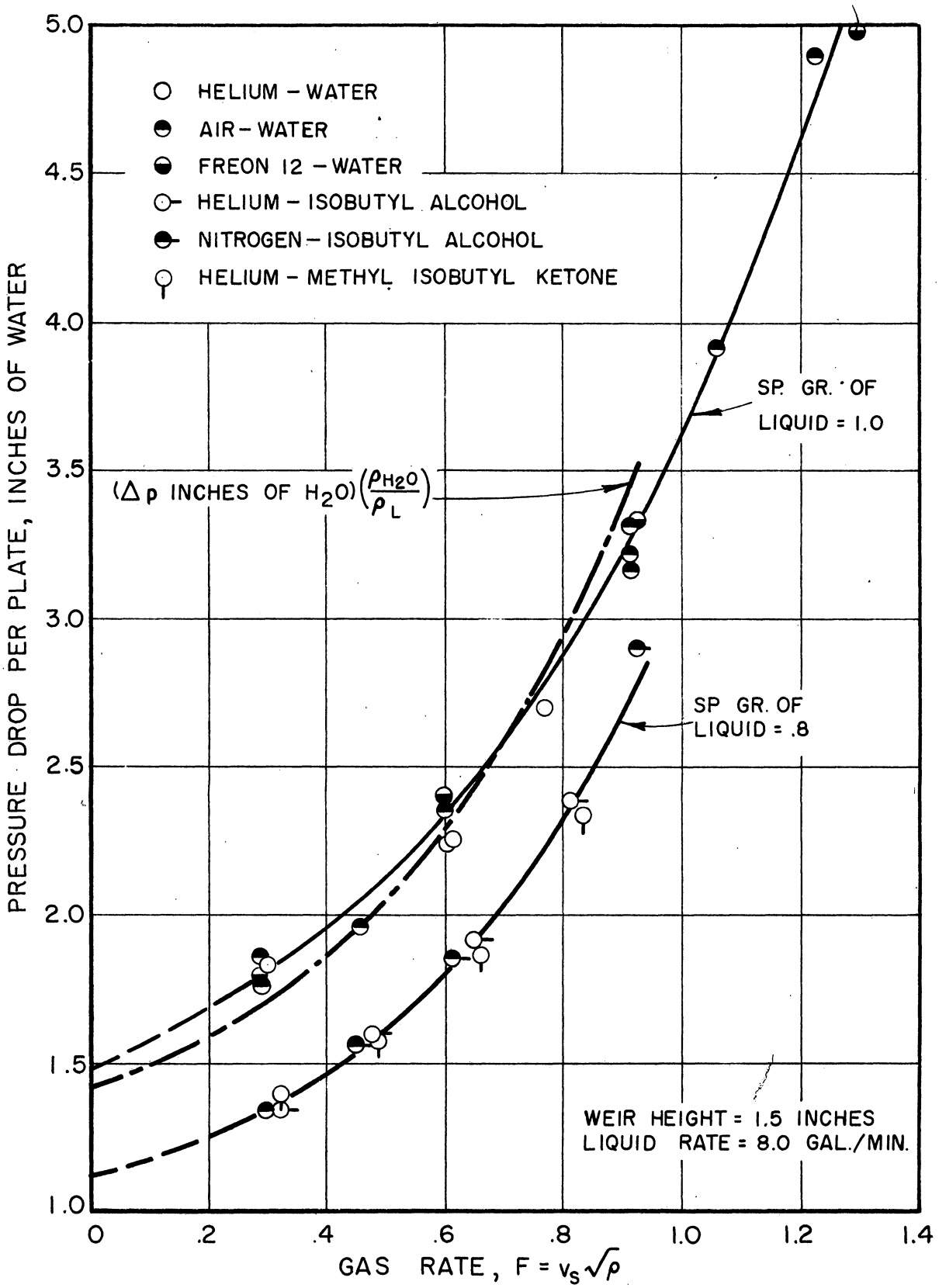

Figure 14. Pressure drop across the test plate.

in the prediction of pressure drop through bubble cap trays, since it adequately correlates these data, which have a 30-fold range in gas density.

Clear Liquid Height.—Figure (15) shows the points on the test plate where the clear liquid heights were measured, and Figure (16) shows how the clear liquid heights varied with gas rate at Points B and D. The curves of Figure (16) are extrapolated to zero gas flow, where the clear liquid heights on the tray are level with the top of the clear liquid flowing over the weir. Clear liquid heights at point B (between two rows of caps) decrease with increasing gas rate due to increased aeration at this point; however, the clear liquid heights at point D, downstream from the bubble caps and just in front of the splash baffle, are virtually constant over the entire range of operating conditions covered in these tests.

Froth Height.—The froth heights are plotted as a function of F factor in Figure (17). The froth height in these tests was defined as the height of the transition point between the liquid continuous and the gas continuous phases. That is, as long as the gas was contained by bubbles which were surrounded by liquid, it was considered to be in the froth. But when the bubbles broke into spray and the gas became the continuous phase, it was considered to be above the froth. The spray of liquid droplets, then, was not considered part of the froth. At low gas rates, this definition gave reasonably reproducible results (within 0.5 inch), and the froth height was almost constant across the active bubbling area of the plate. However, at high gas rates the transition point from one continuous phase to the other was not clear; and the amount of liquid spray in the gas was so great that it seemed that it should not be neglected. Furthermore, the froth height was far from constant across the active plate area. Instead, it rose to a peak in the middle. Thus, at

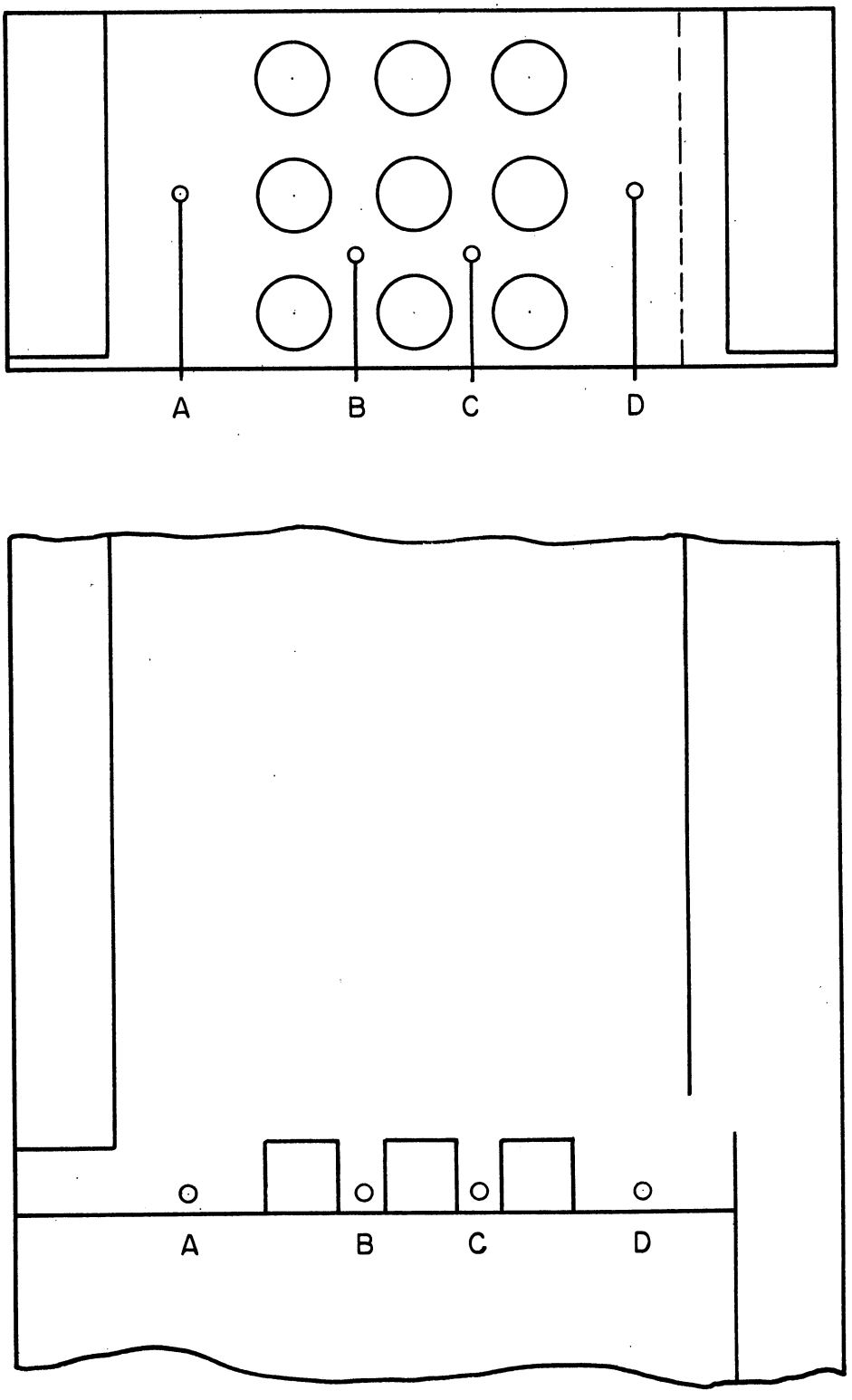

Figure 15. Points on test tray at which clear liquid heights were measured.

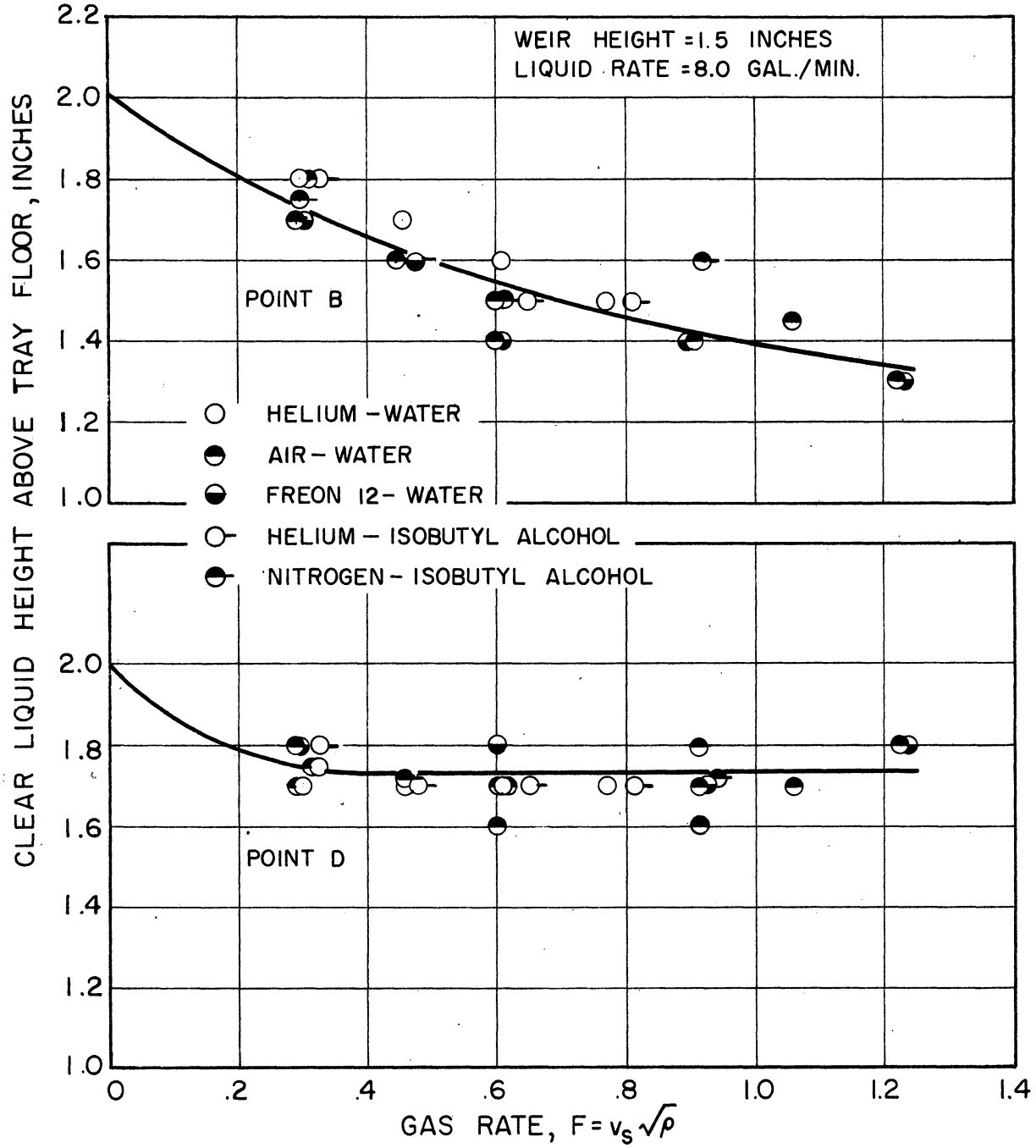
WEIR HEIGHT = 1.5 INCHES
LIQUID RATE = 8.0 GAL./MIN.
POINT B
POINT D
HELIUM – WATER
AIR – WATER
FREON 12 – WATER
HELIUM – ISOBUTYL ALCOHOL
NITROGEN – ISOBUTYL ALCOHOL
CLEAR LIQUID HEIGHT ABOVE TRAY FLOOR, INCHES
GAS RATE, F = $v_s\sqrt{\rho}$
2.2
2.0
1.8
1.6
1.4
1.2
1.0
0
.2
.4
.6
.8
1.0
1.2
1.4

tray floor.

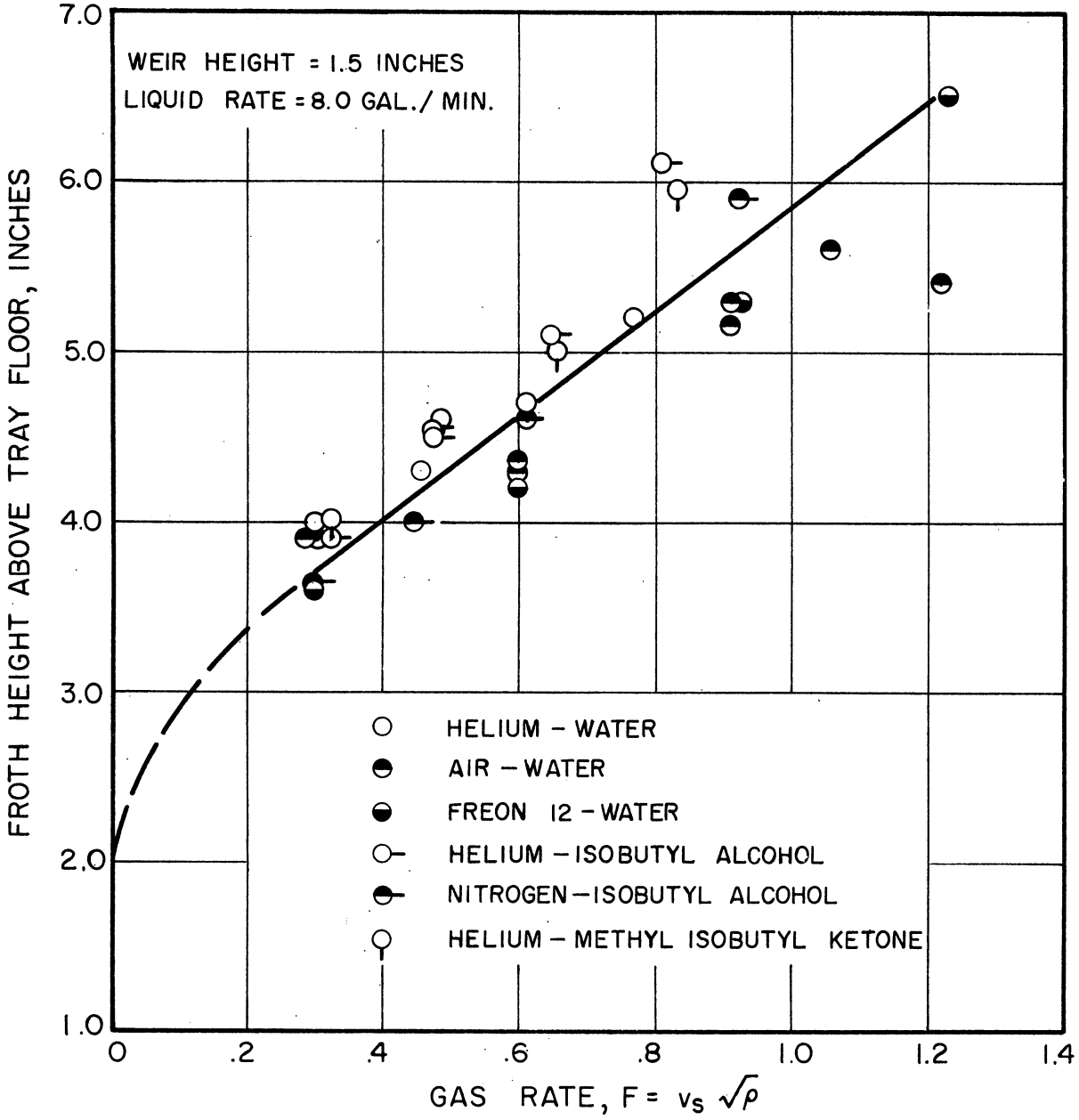

Figure 17. Froth heights above the tray floor.

high gas rates, the observed froth heights were subject to personal interpretation and not very reproducible. For this reason the observed froth height was not utilized as a fundamental variable in the correlation of the mass transfer data obtained in these tests. A discussion of the variables that were chosen for this correlation follows in the next section.

Correlation of the Humidification Data

It was decided that the correlation should be written in a generalized form in order to include all the variables which might have affected the results of this series of experiments.

Selection of Variables.—Before any correlation could be attempted it was necessary to decide just what the important variables were. The mass transfer coefficient and the total area available for mass transfer were considered the dependent variables. Then, based on analogies with mass transfer correlations for other types of apparatus, on visual observations of the bubble tray hydraulics, on the data itself, and on intuition, the following variables were selected as the ones which probably have some effect on the gas phase mass transfer coefficient, k_c or k_G, the interfacial area per unit volume of froth, a, and/or the froth height, h: (1) gas density, (2) gas viscosity, (3) diffusivity of the vapor in the gas, (4) surface tension, (5) liquid viscosity, (6) liquid density, (7) width of the bubble cap slots, (8) superficial velocity of the gas, based on the active bubbling area, and (9) an equivalent clear liquid height, arbitrarily defined as the vertical distance from the bottom of the slot opening to the top of the liquid flowing over the weir, as calculated from the Francis weir formula. Since the mass transfer coefficient, k_c, and the interfacial area, a, cannot be measured independently in a bubble cap column, it was necessary to combine them. The froth height,

h, can be estimated visually, and this was done for all the runs. However, as mentioned earlier, estimation of the froth height was not a precise measurement and became rather arbitrary at high gas flow rates. At the same time, most of the variables that determine $k_c a$ might also be expected to affect froth height. For these reasons, it was decided that all three dependent variables, k_c, a, and h, should be combined and correlated as a unit.

Development of the Correlation.—After selection of the variables, the problem of combining them in the correct functional form was taken up. Since little is known about the true mechanism of mass transfer in any system as complicated as the turbulent mass of bubbles, liquid, and spray found on a bubble cap tray, a rigorous mathematical approach was not possible. In addition, the technique of evaluating the effect of each variable independently by experiments in which all the other variables are held constant was not feasible in this case, because it was virtually impossible to change one variable without simultaneously changing others; this was especially true of the physical properties of the fluids, which were the primary variables under study. Finally, the number of independent variables involved was discouragingly large.

In order to reduce the number of independent variables and, at the same time, put them in a more convenient form, the method of dimensional analysis was employed. By analogy with other correlations of mass and heat transfer data, the dimensionless group, $k_c D_S ah/D_V$, was selected as the dependent variable and was set equal to some function of the nine independent variables. The standard procedure outlined by Bridgman (2) or by Duncan (11) on the use of dimensional analysis was followed, and the nine independent variables were arranged in a set of six dimensionless

groups. In this case, several different sets of dimensionless groups were obtainable; and any one of these sets might have been used.

Once a set was selected, the groups in that set were thought of as independent, dimensionless variables, and the equation relating them to the dependent variable was written as follows:

$$\frac{k_c D_s a h}{D_V} = f\left[\left(\frac{\mu}{\rho D}\right)_G, \left(\frac{D_s v \rho}{\mu}\right)_G, \left(\frac{D_s \rho_G \sigma}{\mu_G^2}\right), \left(\frac{h_L}{D_s}\right), \left(\frac{\rho_L}{\rho_G}\right), \left(\frac{\mu_L}{\mu_G}\right)\right] \quad (29)$$

It can be seen from Equation (29) that the set chosen included a Reynolds number for the gas, a Schmidt number for the gas, and four other groups. This was all the aid that could be obtained from dimensional analysis; the functional relationships among the new set of dimensionless variables remained to be determined.

If it is assumed that the effect of each of the dimensionless variables can be represented by a power series, and that each of the power series can be approximated over the range involved by a single term, Equation (29) can be written in the following form:

$$\frac{k_c D_s a h}{D_V} = C_o \left(\frac{\mu}{\rho D}\right)_G^{C_1'} \left(\frac{D_s v \rho}{\mu}\right)_G^{C_2'} \left(\frac{D_s \rho_G \sigma}{\mu_G^2}\right)^{C_3} \left(\frac{h_L}{D_s}\right)^{C_4} \left(\frac{\rho_L}{\rho_G}\right)^{C_5} \left(\frac{\mu_L}{\mu_G}\right)^{C_6} \quad (30)$$

This equation can just as well be written in another form:

$$N_G = \frac{k_G a h P}{G_M} = C_o \left(\frac{\mu}{\rho D}\right)_G^{C_1} \left(\frac{D_s v \rho}{\mu}\right)_G^{C_2} \left(\frac{D_s \rho_G \sigma}{\mu_G^2}\right)^{C_3} \left(\frac{h_L}{D_s}\right)^{C_4} \left(\frac{\rho_L}{\rho_G}\right)^{C_5} \left(\frac{\mu_L}{\mu_G}\right)^{C_6} \quad (31)$$

where

$$C_1 = C_1' = 1, \text{ and}$$
$$C_2 = C_2' = 1.$$

The dependent variable appearing in Equation (31) is used in the rest of this work for two reasons: (1) it is relatively constant, and (2) it has already been used extensively in mass transfer correlations for bubble plate columns.

Evaluation of the Constants in the Correlation Equation.—The constants in Equation (31) were determined by the method of least squares. All the data were used. Before the method was applied, Equation (31) was put in a more convenient linear form by taking the logarithm of both sides and defining a new set of variables as the logarithms of the respective dimensionless groups. This technique gives better results for most engineering purposes because it tends to give a minimum percentage deviation between the calculated and experimental N_G's rather than a minimum absolute deviation.

The results of the analysis are given in the following equation:

$$N_G = 0.297\left(\frac{\mu_G}{\rho_G D_V}\right)^{-0.23}\left(\frac{D_s v \rho_G}{\mu_G}\right)^{-0.33}\left(\frac{D_s \rho_G \sigma}{\mu_G^2}\right)^{0.16}\left(\frac{h_L}{D_s}\right)^{0.62}\left(\frac{\rho_L}{\rho_G}\right)^{-0.01}\left(\frac{\mu_L}{\mu_G}\right)^{-0.005} \quad (32)$$

Comparison of the Correlation with the Data.—Equation (32) was then used to recalculate the N_G's for each of the experimental runs so that the experimental and the calculated values could be compared. This comparison is presented graphically in Figure 18. The average absolute deviation of the calculated values from the experimental values is less than 7 per cent. This is considered good agreement, because it is within the estimated accuracy of the data. Therefore, further refinements of the correlation, do not appear to be justified.

The validity and constancy of the exponents on the first three groups on the right hand side of Equation (32) are demonstrated graphically in

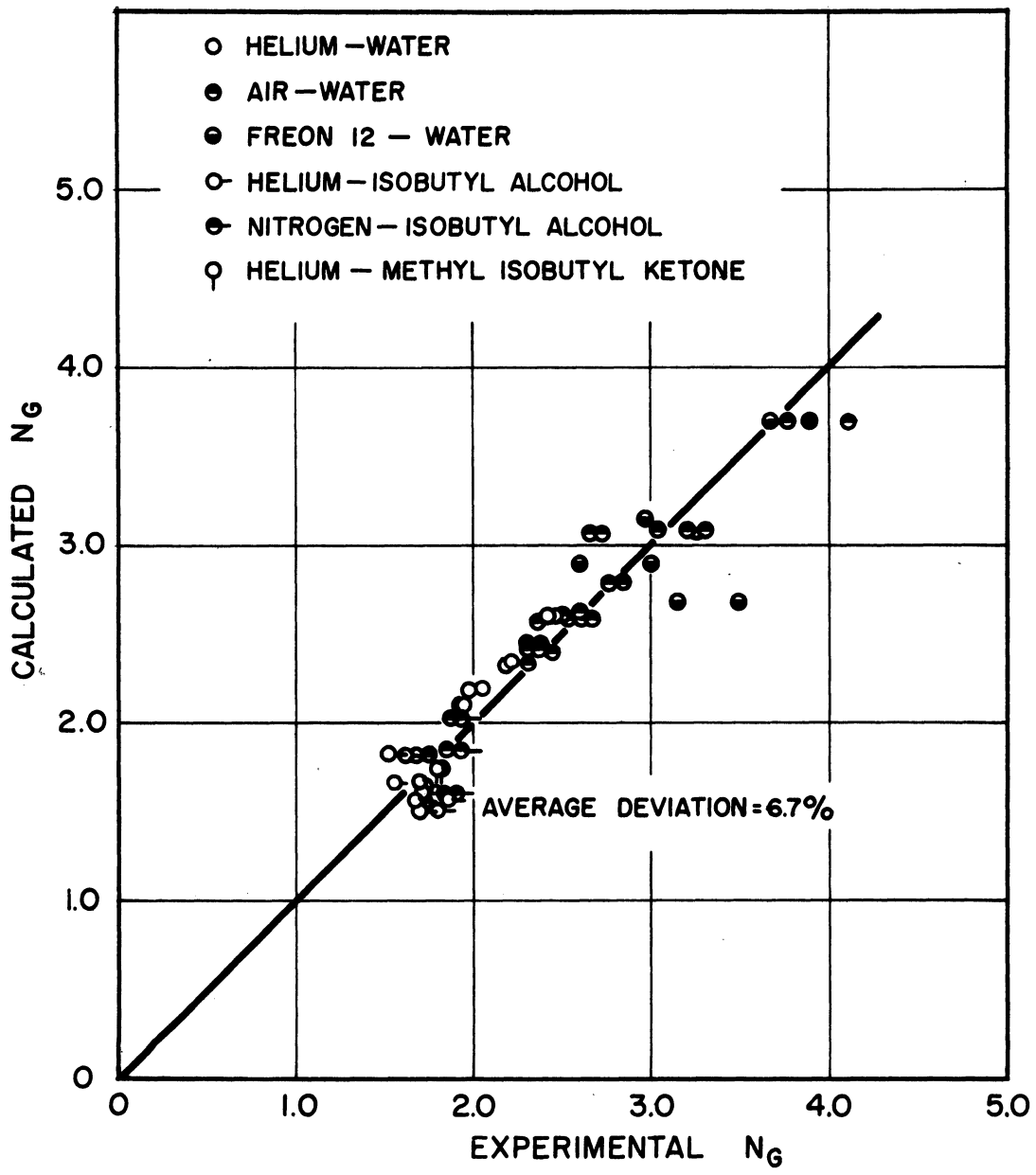

Figure 18. Comparison of the experimental humidification data with the correlation.

Figures (19), (20), and (21), respectively. Each of the six points appearing in Figures (19) and (21) represents an arithmetic average of the ordinates calculated for all the runs made on that particular system. For instance, in Figure (19), the point for the helium-water system represents an arithmetic average of the ordinates calculated for all eight of the helium-water runs, each with virtually the same abscissa, or Schmidt number. The slopes of the lines drawn through the points in these two figures confirm the values of the exponents already determined by the method of least squares.

Each of the points on Figure (20) represents the arithmetic average of the ordinates calculated for two or three runs made under identical conditions for the same system. Thus, each of the helium-water points represents the arithmetic average of the ordinates of two runs with the same Reynolds number. Again, the slope of the line drawn through the points confirms the results obtained by the method of least squares.

Discussion of the Correlation.—Although Equation (32) satisfactorily correlates this particular series of data, and is in convenient form for extension, the limitations of the data on which it is based should be kept firmly in mind. For instance, all the data were taken from a single column with a single tray and cap design. All the data except that for one series of air-water runs were taken at the same weir height, and all the runs were made at a single liquid rate. The primary variables studied were the fluid properties, especially the properties of the gas. The ranges covered by each of the variables included in the correlation are listed below:

Variable	Range
N_G	1.5-3.7

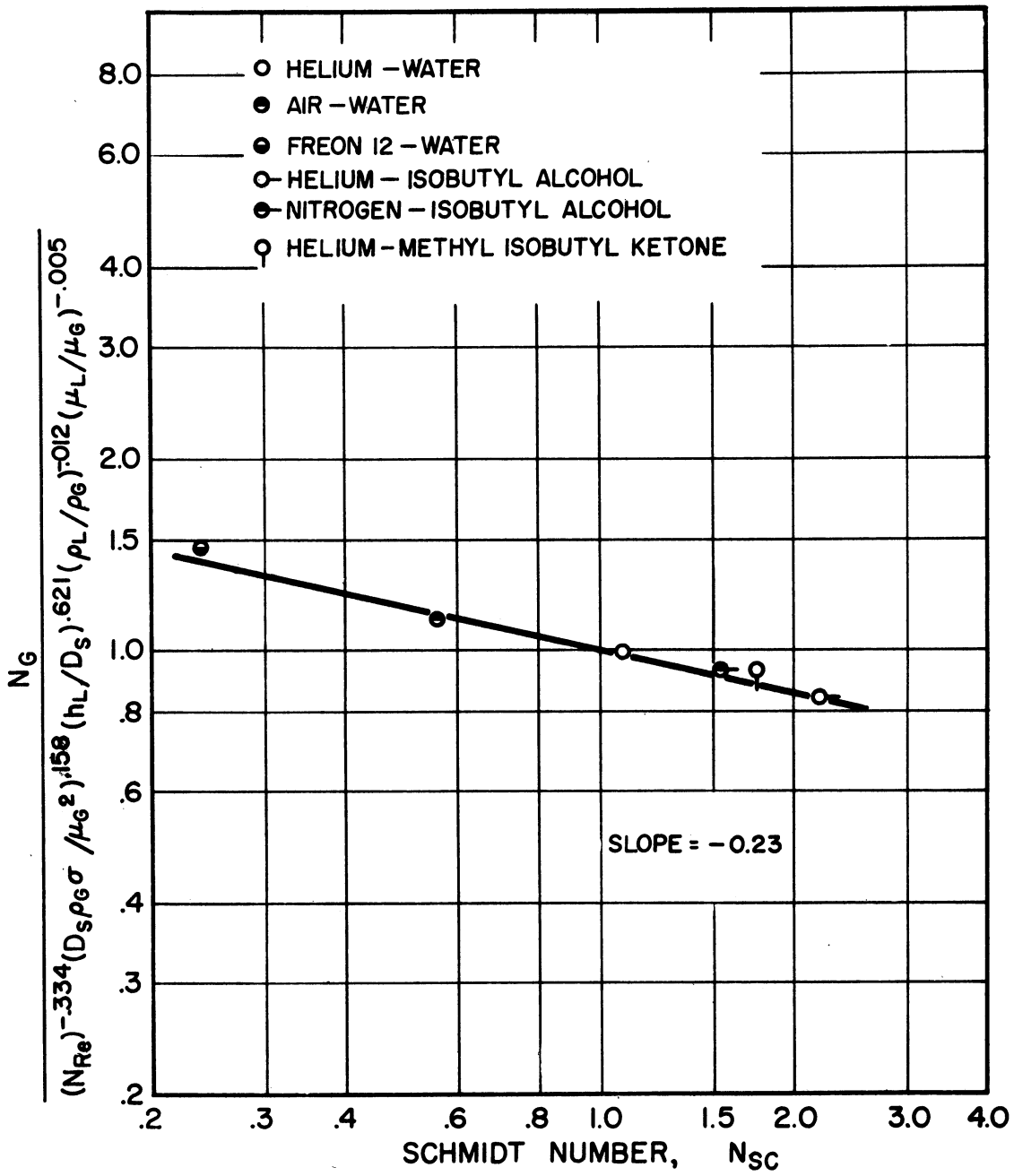

Figure 19. Effect of Schmidt number on N_G.

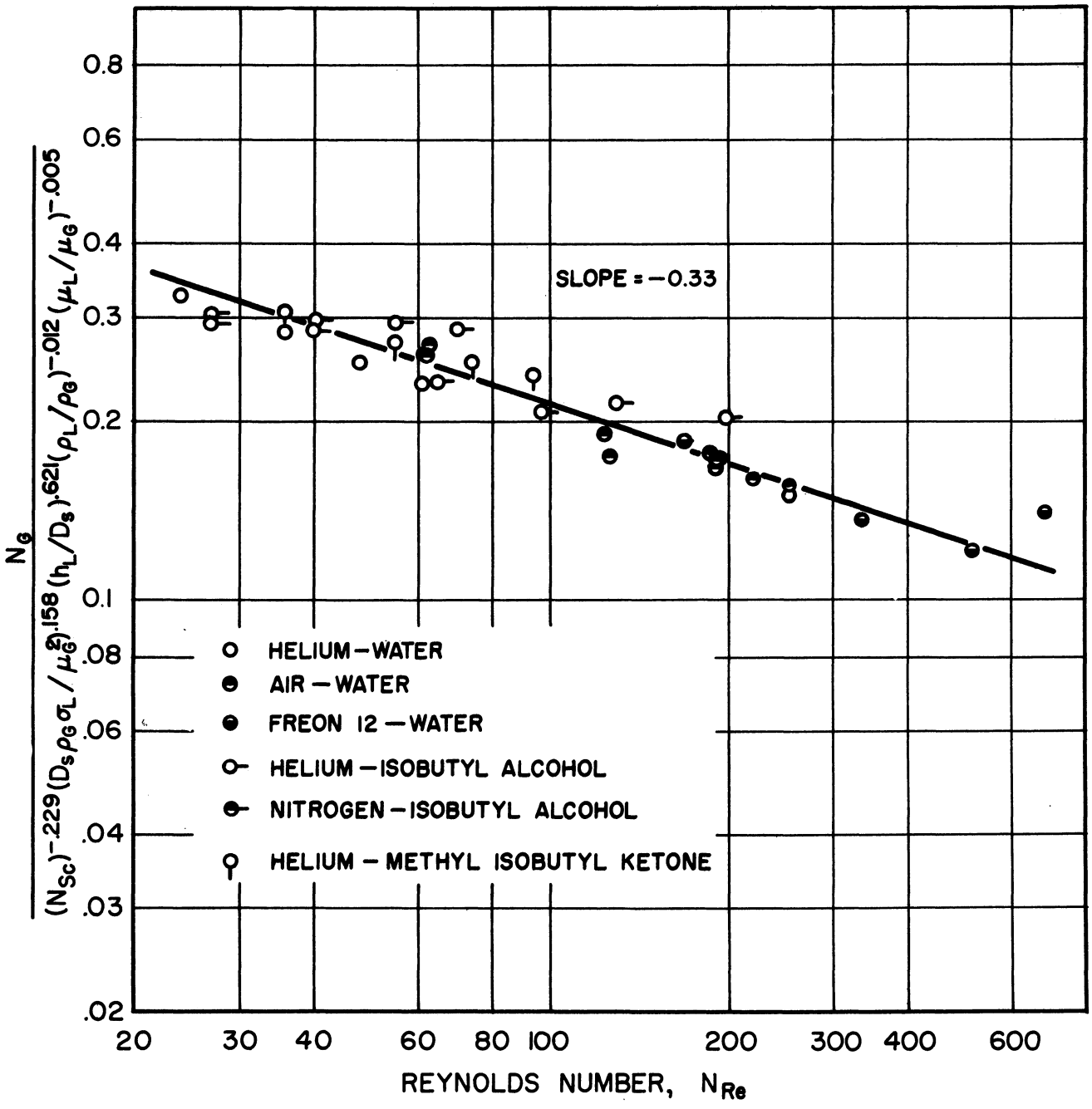

Figure 20. Effect of Reynolds number on N_G.

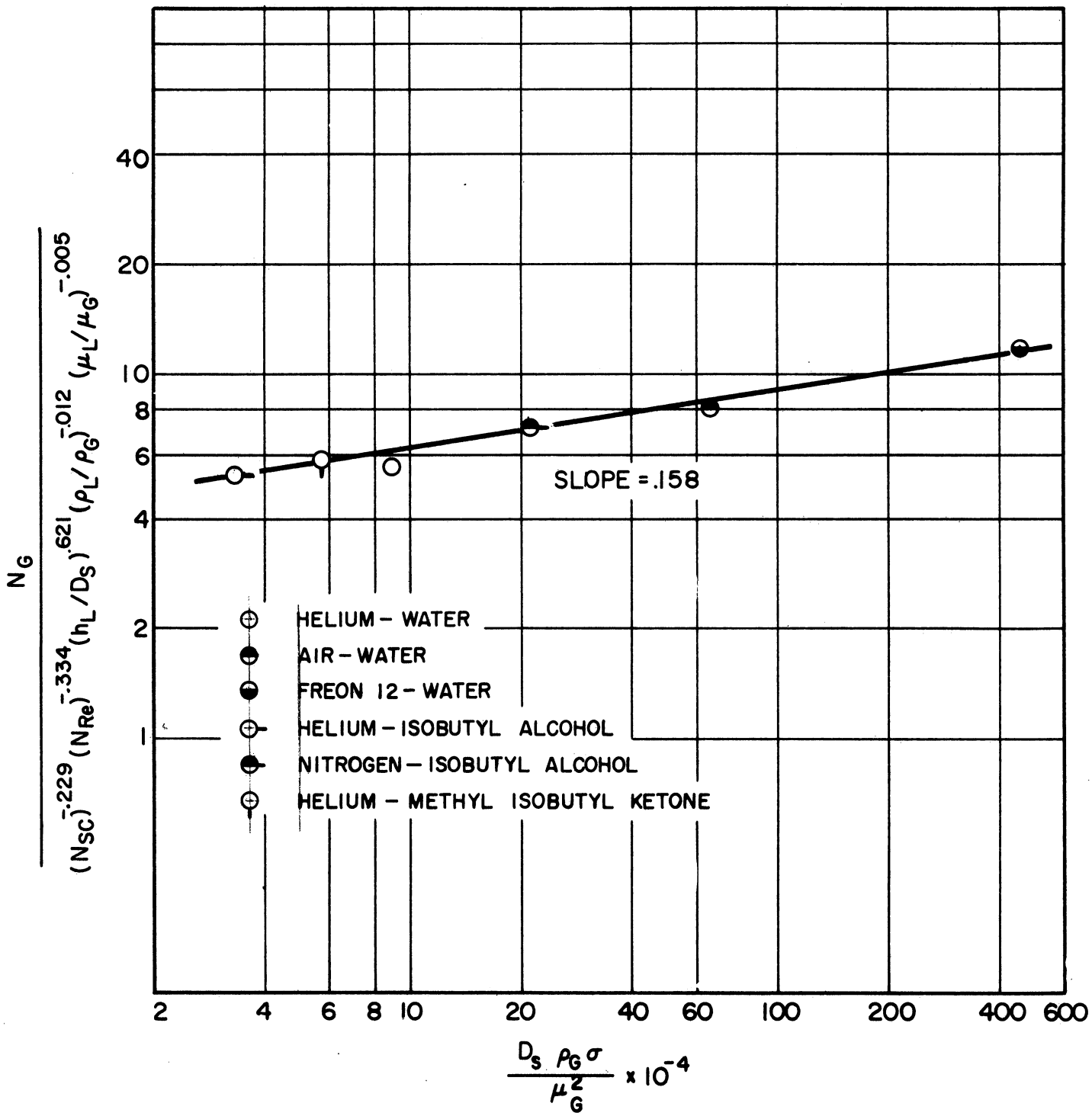

Figure 21. Effect of $D_S\rho_G\sigma/\mu_G{}^2$ on N_G.

Variable	Range
$\frac{\mu_G}{\rho_G D_V}$	0.24-2.2
$\frac{D_s v \rho_G}{\mu_G}$	25-680
$\frac{D_s \rho_G \sigma}{\mu_G^2}$	3.2×10^4-4.6×10^6
h_L/D_s	13.-20.
$\frac{\rho_L}{\rho_G}$	230-6480
$\frac{\mu_L}{\mu_G}$	27-126
D_s	not changed

From the information listed above, it can be seen that the Schmidt number was given the most complete coverage. The exponent on this group should be reasonably reliable, even when applied at other operating conditions and with other bubble cap and tray designs, especially since each of the individual components of this group covered a considerable range. The Reynolds number and the group which includes the surface tension also covered a considerable range; but each of these groups contains the slot width, which was not changed for this series of data. Thus, the exponents on these two groups are tentative until the equation can be applied to data taken with caps of different design and different slot width. The group, h_L/D_s, is apparently very significant in determining the value of N_G. However, in the present series of data, h_L covers less than a two-fold

range; and D_s does not change at all. Obviously, the exponent on this group must be considered tentative until the equation can be tested with other data. The exponents on the last two groups indicate that variations in liquid density or in liquid viscosity have a negligible effect on N_G. However, this conclusion can be taken as valid only for the range of values covered in the data.

The negligible effect of changes in liquid viscosity is in agreement with the work of Stone (61), whose data included adiabatic humidification of air with water and with acqueous sucrose solutions. He concluded that the only effect of liquid viscosity on point efficiency was in its effect on the diffusivity of the solute in the liquid phase.

Since the present work was designed solely to determine the effects of fluid properties on the gas phase resistance to mass transfer, only one plate design was used; and conclusions regarding the effects of h_L, D_s, and other plate design variables cannot be drawn.

Comparison of the Humidification Data with Ammonia Absorption and Desorption Data

Warzel (65) has obtained extensive absorption and desorption data for the ammonia-air-water and for the carbon dioxide-air-water systems. The apparatus used by Warzel was the same as that used in the humidification studies just described; that is, the column, the tray, and the bubble caps were identical for the two series of data. Since the mass transfer rates in the carbon dioxide-air-water system are controlled almost exclusively by the liquid phase resistance, liquid phase resistances for this system were obtained over the entire range of operating conditions. The N_L's from the carbon dioxide-air-water data were then used to calculate N_L's for the ammonia-air-water system according to the following equation:

$$(N_L)_{NH_3} = (N_L)_{CO_2} \left[\frac{(\mu/\rho D_L)_{CO_2}}{(\mu/\rho D_L)_{NH_3}}\right]^{1/2} \qquad (33)$$

This equation was applied only at corresponding operating conditions. The number of overall gas phase transfer units, N_{OG}, for the ammonia-air-water system was determined for each run directly from the data. Therefore, since N_L and N_{OG} were known for each run, N_G could be obtained from the following equation:

$$\frac{1}{N_G} = \frac{1}{N_{OG}} - \frac{1}{N_L}\frac{mG_M}{L_M}\frac{(1-x)_f}{(1-y)_f} \qquad (34)$$

The N_G's obtained by Warzel from the ammonia-air-water data were compared with corresponding values calculated from Equation (32), which represents the humidification data. A significant discrepancy was noted; all the ammonia-air-water N_G's fell considerably below the values predicted by Equation (32), as shown in Figure (22). The data shown in the figure are tabulated in Table 15 in the Appendix.

Both the ammonia-air-water data and the adiabatic humidification data show good internal consistency and are considered reliable; and, since both series were run in the same equipment, some fundamental difference between ammonia absorption and humidification in a bubble tray column seems to be evident.

This discrepancy has not yet been completely resolved. There may be several contributing factors. One possible explanation is that a significant error is introduced when it is assumed that the liquid phase resistance for the ammonia-air-water system can be calculated from the liquid phase resistance of the carbon dioxide-air-water system by use of Equation (33). This statement is based on the following reasoning.

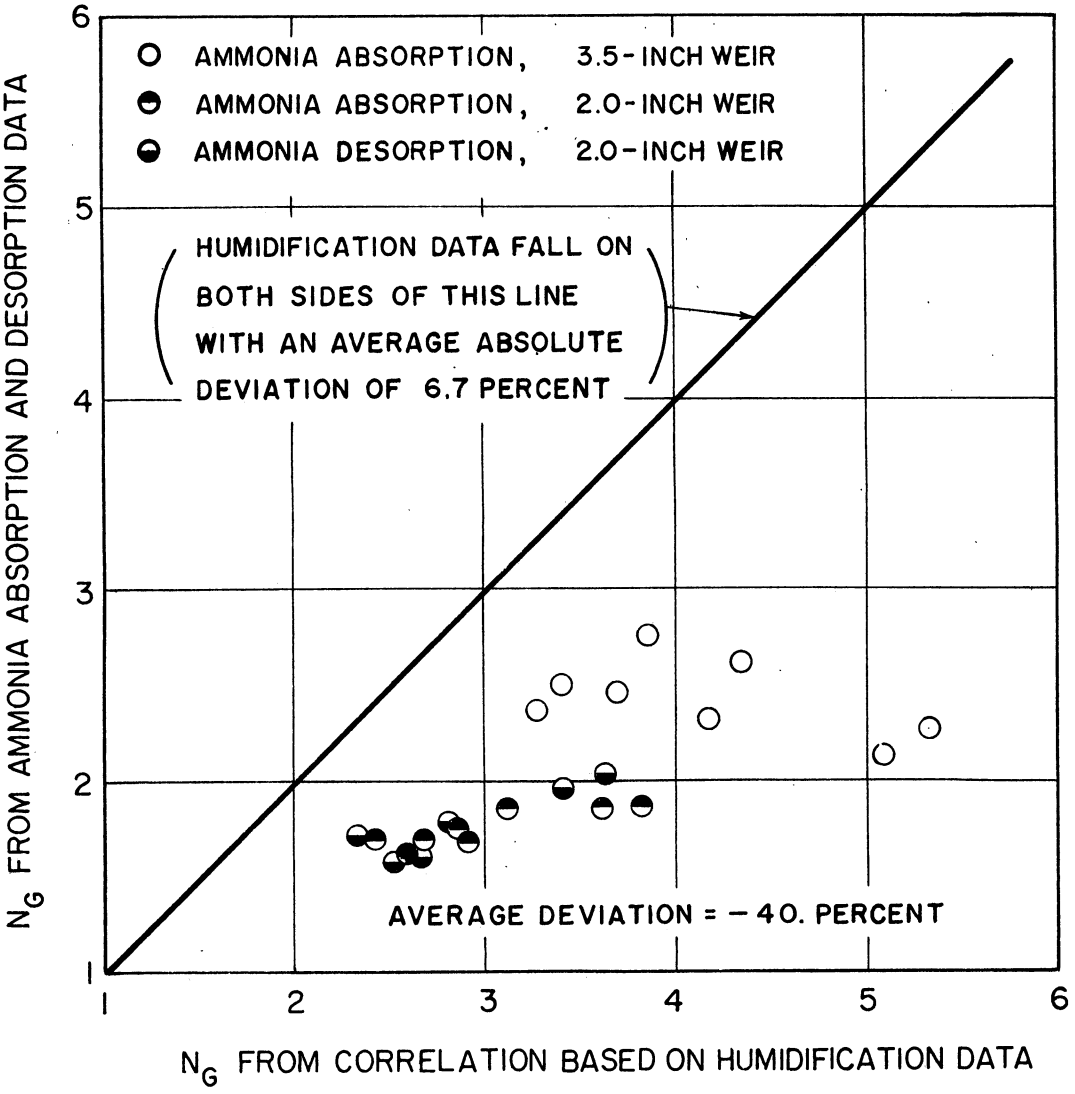

Figure 22. Comparison of humidification data with ammonia-air-water data.

The column used in all these tests had a completely transparent front, and it was possible to observe the action taking place at nearly every point in the column (except in the downcomers, which were enclosed). It was like being able to see the cross section of an ordinary column split down the middle parallel to the direction of liquid flow. About the only thing that obstructed vision was the swirling mass of bubbles on the trays, ranging in size from about 1 mm to perhaps 1 inch. The very large bubbles which rose quickly and transported the bulk of the gas through the froth could never be seen distinctly because of the presence of a great many smaller bubbles and because of the high velocity and non-uniformity of the larger bubbles. It seemed apparent, though, that these bubbles were greatly distorted by the turbulence of the system and that they occasionally broke up into smaller bubbles or coalesced into still larger ones. The smaller bubbles remained in the froth longer, and many of them were swept from the top of the froth back down to the tray floor by swirling liquid eddies.

The relative importance of these small bubbles in the overall mass transfer process has not been quantitatively determined, but it seems reasonable to assume that they might be more important in one system than in another. For instance, in the absorption of carbon dioxide from air with water, the overall vapor efficiency is very low, ranging from two to six per cent (65). However, the gas contained in the smaller bubbles (because of their smaller diameter and longer residence time) might approach equilibrium with the liquid much more closely. If it were assumed that the gas in these small bubbles had a vapor efficiency of 90 per cent compared to the average vapor efficiency of say 3 per cent and that the volume of gas contained in these bubbles amounted to as little as 1 or 2 per cent of the total gas flowing through the froth, then these small

bubbles might account for as much as 30 to 60 per cent of the total carbon dioxide transferred from the gas to the liquid. On the other hand, in the absorption of ammonia from air with water, the vapor efficiencies are very high, ranging from 75 to 95 percent. Thus, even if the gas in the smaller bubbles did reach equilibrium with the liquid, it could not contribute significantly to the total mass transfer of ammonia to the liquid, because of its relatively small volume.

In a sense, then, there is a larger effective area for carbon dioxide absorption on a bubble plate than for ammonia absorption, due to the presence in the liquid of large numbers of small entrained bubbles. If liquid phase resistances determined from carbon dioxide absorption data are used to calculate liquid phase resistances for ammonia absorption, this difference in effective interfacial areas must be taken into account, or potentially large errors will result. Failure to take this difference into account makes the calculated liquid phase resistance for the ammonia absorption too low, and, thus, makes the apparent gas phase resistance too high (corresponding to low values for N_G). This argument explains qualitatively why N_G's calculated from ammonia absorption data are lower than the N_G's obtained from humidification data in bubble cap columns.

The above reasoning is similar in principle to the theory recently proposed by Shulman, *et al.* (58, 59, 60) which seems to explain the differences observed when gas phase mass transfer rates are measured by absorption and vaporization methods in packed towers.

CONCLUSIONS

The following conclusions may be drawn with regard to gas phase mass transfer in the bubble cap column used in the present work:

1. Gas density, gas viscosity, and gas phase diffusivity are important variables in the determination of the gas phase resistance to mass transfer, and may be combined in the form of the Schmidt number for use in the prediction of gas phase resistances.

2. For the range of conditions included in this study, the liquid density and liquid viscosity were not important variables in the determination of the number of individual gas phase transfer units.

3. The number of individual gas phase transfer units per plate decreases with Schmidt number and Reynolds number and increases with clear liquid height and $D_s\rho_G\sigma/\mu_G^2$.

4. The equation given below, which was obtained by the method of dimensional analysis, has been found to correlate the mass transfer data for a wide range of fluid physical properties:

$$N_G = 0.297 \left(\frac{\mu_G}{\rho_G D_V}\right)^{-0.23} \left(\frac{D_s v \rho_G}{\mu_G}\right)^{-0.33} \left(\frac{D_s \rho_G \sigma}{\mu_G^2}\right)^{0.16} \left(\frac{h_L}{D_s}\right)^{0.62} \left(\frac{\rho_L}{\rho_G}\right)^{-0.01} \left(\frac{\mu_L}{\mu_G}\right)^{-0.005}$$

5. Data on ammonia absorption in water cannot be used to predict the gas phase resistance to mass transfer in a bubble cap column by the conventional methods, because of the inadequacy of present theories in describing the relative importance of various size bubbles in different systems.

If dimensionless groups two and three on the right hand side of Equation (32) are combined and if the groups with the very low exponent [groups five and six on the right side of Equation (32)] are eliminated, it can be seen that the data are represented adequately by a much simpler equation as given below:

$$N_G = 0.253 \left(\frac{\mu_G}{\rho_G D_V}\right)^{-0.23} \left(\frac{\sigma}{D_S v^2 \rho_G}\right)^{0.16} \left(\frac{h_L}{D_S}\right)^{0.62}$$

The combination of groups two and three reduces the exponent on the Reynolds number to -0.01, so small that the effect of variation of the Reynolds number can be assumed negligible, as well as the variations in (ρ_L/ρ_G) and $\mu_L/\mu_G)$. However, omission of these low-exponent groups makes necessary the slight modification of the constant coefficient in the correlation equation.

The new dimensionless group, formed by the combination of groups two and three and appearing for the first time in the above equation, is the Weber number. It may be described as the ratio of the surface forces to the inertial forces in a gas liquid system. Thus, it takes into account the fluid dynamic characteristics of the bubble plate. The Schmidt number, which remains as a fundamental variable in the above equation, has been termed the ratio of molecular momentum transfer to molecular mass transfer. Both the Schmidt number and the Weber number were varied over a wide range in the present tests, and the exponents are considered reliable.

The above equation indicates that one of the most significant variables which affect N_G is the group (h_L/D_S). However, D_S was not changed in these tests and h_L was varied only over a two-fold range, so that the exponent of 0.62 has not been reliably established.

APPENDICES

APPENDIX A

TABLES OF ORIGINAL AND CALCULATED DATA

TABLE 6

HUMIDIFICATION OF HELIUM WITH WATER

1-1/2-in. weir; 2-in. baffle height; liquid rate = 8.0 gallons per minute

Run Number	115	116	117	118	119	120	121	122
Barometric Pressure, In. Hg Abs.	29.08	29.08	29.08	29.08	29.16	29.16	29.16	29.16
Liquid on Test Plate								
1. Temperature Entering, °F	89.7	89.7	91.1	91.2	87.3	87.5	85.6	85.7
2. Temperature Leaving, °F	90.1	90.2	91.5	91.5	87.7	87.8	85.8	86.0
3. Average Temperature, °F	90.0	90.0	91.4	91.3	87.5	87.7	85.7	85.9
4. [1]Froth Height, in.	4.7	4.7	5.2	5.2	4.3	4.3	4.0	4.0
[1]Clear Liquid Height, in.								
5. Position A	2.3	2.3	2.3	2.3	2.25	2.25	2.25	2.25
6. Position B	1.6	1.6	1.55	1.55	1.7	1.7	1.8	1.8
7. Position C	1.7	1.7	1.65	1.65	1.75	1.75	1.8	1.8
8. Position D	1.7	1.7	1.75	1.7	1.7	1.7	1.75	1.75
Gas Flowing Through Test Plate (Below Test Plate)								
9. Lb mole per minute x 10^2	51.3	51.3	64.1	64.1	38.8	38.8	25.6	25.6
10. Temperature, °F	177.	178.	180.	180.	172.	172.	165.	165.
(Above Test Plate)								
11. Lb mole per minute x 10^2	52.5	52.5	65.6	65.6	39.6	39.6	26.0	26.0
12. [2]Temperature, °F	102.	103.	105.	105.	97.	98.	93.	94.
13. Pressure, in. Hg abs.	30.68	30.68	30.70	30.70	30.66	30.66	30.64	30.64
(Average Conditions)								
14. Lb mole per minute x 10^2	51.9	51.9	64.9	64.9	39.2	39.2	25.8	25.8
15. Temperature, °F	140.	140.	142.	142.	135.	135.	129.	129.
16. [3]Superficial Velocity, ft per sec	5.99	5.99	7.50	7.50	4.49	4.49	2.92	2.92
17. "F" factor	.612	.612	.767	.767	.460	.460	.300	.300
Composition, Mole Fraction x 10^2								
18. y_o	2.182	2.164	2.263	2.269	2.084	2.062	2.066	2.084
19. y_1	4.275	4.260	4.418	4.411	4.019	4.032	3.845	3.875
20. y_1*	4.607	4.620	4.809	4.809	4.276	4.295	4.034	4.060
21. Pressure Drop, in. H_2O	2.26	2.26	2.70	2.70	1.96	1.96	1.83	1.83
Equilibrium Conditions on Test Tray								
22. Temperature, °F	90.0	90.0	91.4	91.3	87.5	87.7	85.7	85.9
23. Vapor Pressure of Liquid, mm Hg	35.9	36.0	37.5	37.5	33.3	33.4	31.4	31.6
24. Pressure Above Plate, mm Hg abs.	779.	779.	780.	780.	779.	779.	778.	778.
25. Murphrey Vapor Efficiency, %	86.3	85.3	84.6	84.3	88.3	88.2	90.4	90.6
26. Number of Gas Transfer Units per Plate, $N_G = N_{OG}$	1.99	1.92	1.88	1.85	2.14	2.14	2.34	2.37

[1]Measured from tray floor.
[2]Calculated assuming a linear relation between the temperature and composition of the gas.
[3]Based on active area between inlet downcomer and splash baffle (.615 ft^2).

TABLE 7

HUMIDIFICATION OF AIR WITH WATER

1-1/2-in. weir; 2-in. baffle height; liquid rate = 8.0 gallons per minute

Run Number	64	65	66	67	68	69	70	71	72
Barometric Pressure, In. Hg Abs.	28.68	28.68	28.68	28.68	28.68	28.98	28.98	28.98	28.98
Liquid on Test Plate									
1. Temperature Entering, °F	89.8	90.0	88.0	87.7	87.5	90.9	90.9	92.1	92.1
2. Temperature Leaving, °F	90.0	90.2	88.0	87.8	87.6	91.1	91.2	92.3	92.4
3. Average Temperature, °F	89.9	90.1	88.0	87.8	87.6	91.1	91.2	92.3	92.3
4. [1]Froth Height, in.	4.4	4.3	3.9	3.9	3.9	5.2	5.1	5.4?	5.4?
[1]Clear Liquid Height, in.									
5. Position A	1.8	1.8	1.75	1.75	1.75	1.9	1.9	1.95	1.95
6. Position B	1.4	1.4	1.7	1.7	1.7	1.4	1.4	1.3	1.3
7. Position C	1.7	1.7	1.85	1.85	1.85	1.45	1.45	1.45	1.45
8. Position D	1.75	1.75	1.85	1.85	1.85	1.8	1.8	1.8	1.8
Gas Flowing Through Test Plate (Below Test Plate)									
9. Lb mole per minute x 10^2	19.9	19.9	9.9	9.9	9.9	30.4	30.4	40.5	40.5
10. Temperature, °F	166.	167.	154.	154.	154.	175.	175.	178.	178.
(Above Test Plate)									
11. Lb mole per minute x 10^2	20.4	20.4	10.1	10.1	10.1	31.2	31.2	41.6	41.6
12. [2]Temperature, °F	97.	97.	91.	91.	91.	101.	100.	101.	101.
13. Pressure, in. Hg abs.	30.89	30.92	31.11	31.10	31.10	31.33	31.33	30.87	30.87
(Average Conditions)									
14. Lb mole per minute x 10^2	20.2	20.2	10.0	10.0	10.0	30.8	30.8	41.0	41.0
15. Temperature, °F	131.	133.	123.	122.	123.	138.	138.	140.	140.
16. [3]Superficial Velocity, ft per sec	2.27	2.28	1.11	1.11	1.11	3.46	3.46	4.70	4.70
17. "F" factor	.596	.597	.294	.294	.294	.909	.909	1.223	1.223
Composition, Mole Fraction x 10^2									
18. y_o	1.982	1.971	2.135	2.156	2.119	1.942	1.938	2.057	2.038
19. y_1	4.337	4.362	4.180	4.166	4.114	4.400	4.401	4.619	4.641
20. y_1*	4.576	4.596	4.277	4.253	4.228	4.680	4.695	4.930	4.937
21. Pressure Drop, in. H_2O	2.36	2.36	1.86	1.86	1.86	3.31	3.31	4.89	4.89
Equilibrium Conditions on Test Tray									
22. Temperature, °F	89.9	90.1	88.0	87.8	87.6	91.1	91.2	92.3	92.3
23. Vapor Pressure of Liquid, mm Hg	35.9	36.1	33.8	33.6	33.4	37.2	37.4	38.7	38.7
24. Pressure Above Plate, mm Hg abs.	785.	785.	790.	790.	790.	796.	796.	784.	784.
25. Murphrey Vapor Efficiency, %	90.8	91.1	95.5	95.8	94.6	89.8	89.3	89.2	89.8
26. Number of Gas Transfer Units per Plate, $N_G = N_{OG}$	2.38	2.42	3.10	3.18	2.92	2.28	2.24	2.22	2.28

[1]Measured from tray floor.
[2]Calculated assuming a linear relation between the temperature and composition of the gas.
[3]Based on active area between inlet downcomer and splash baffle (.615 ft^2).

TABLE 7 (Continued)

HUMIDIFICATION OF AIR WITH WATER

1-1/2-in. weir; 2-in. baffle height; liquid rate = 8.0 gallons per minute

Run Number	123	124	125	126	127	128	129	130	131
Barometric Pressure, In. Hg Abs.	28.96	28.96	28.96	28.96	28.88	28.88	28.88	28.88	28.88
Liquid on Test Plate									
1. Temperature Entering, °F	91.3	91.4	92.6	92.2	91.8	89.8	90.1	87.7	87.6
2. Temperature Leaving, °F	91.7	91.8	92.9	92.6	92.1	90.1	90.3	87.9	87.7
3. Average Temperature, °F	91.5	91.6	92.7	92.4	91.9	90.0	90.2	87.8	87.6
4. [1]Froth Height, in.	5.3	5.3	5.6	5.6	5.2	4.3	4.3	3.9	3.9
[1]Clear Liquid Height, in.									
5. Position A	2.2	2.2	2.25	2.2	2.2	2.2	2.2	2.25	2.25
6. Position B	1.45	1.45	1.5	1.45	1.45	1.5	1.5	1.8	1.8
7. Position C	1.45	1.45	1.35	1.35	1.45	1.65	1.65	1.8	1.8
8. Position D	1.65	1.7	1.7	1.65	1.7	1.65	1.65	1.75	1.75
Gas Flowing Through Test Plate (Below Test Plate)									
9. Lb mole per minute x 10^2	29.9	30.0	35.1	35.1	29.8	20.0	20.0	9.8	9.8
10. Temperature, °F	177.	177.	179.	178.	176.	171.	171.	158.	158.
(Above Test Plate)									
11. Lb mole per minute x 10^2	30.7	30.7	36.1	36.1	30.6	20.3	20.3	10.0	10.0
12. [2]Temperature, °F	100.	100.	102.	103.	100.	97.	97.	91.	91.
13. Pressure, in. Hg abs.	30.59	30.76	30.73	30.59	30.38	30.38	30.38	30.36	30.38
(Average Conditions)									
14. Lb mole per minute x 10^2	30.3	30.4	35.6	35.6	30.2	20.1	20.1	9.9	9.9
15. Temperature, °F	138.	138.	141.	141.	138.	134.	134.	125.	124.
16. [3]Superficial Velocity, ft per sec	3.49	3.48	4.10	4.12	3.50	2.32	2.32	1.12	1.12
17. "F" factor	.906	.906	1.064	1.067	.904	.601	.601	.293	.293
Composition, Mole Fraction x 10^2									
18. y_o	2.132	2.129	2.213	2.162	2.206	2.136	2.146	2.203	2.186
19. y_1	4.588	4.576	4.704	4.650	4.672	4.444	4.461	4.245	4.235
20. y_1*	4.846	4.838	5.014	4.994	4.950	4.665	4.691	4.357	4.328
21. Pressure Drop, in. H_2O	3.22	3.23	3.92	3.90	3.17	2.24	2.24	1.76	1.76
Equilibrium Conditions on Test Tray									
22. Temperature, °F	91.5	91.6	92.7	92.4	91.9	90.0	90.2	87.8	87.6
23. Vapor Pressure of Liquid, mm Hg	37.7	37.8	39.1	38.8	38.2	36.0	36.2	33.6	33.4
24. Pressure Above Plate, mm Hg	777.	781.	781.	777.	772.	772.	772.	771.	772.
25. Murphrey Vapor Efficiency, %	90.5	90.3	88.9	87.9	89.9	91.3	91.0	94.8	95.7
26. Number of Gas Transfer Units per Plate, $N_G = N_{OG}$	2.35	2.34	2.22	2.11	2.29	2.44	2.40	2.96	3.14

[1]Measured from tray floor.
[2]Calculated assuming a linear relation between the temperature and composition of the gas.
[3]Based on active area between inlet downcomer and splash baffle (.615 ft^2).

TABLE 8

HUMIDIFICATION OF AIR WITH WATER

2-in. weir; 2-1/2-in. baffle height; liquid rate = 8.0 gallons per minute

Run Number	53	54	55	56	57	58	59	60	61	62	63
Barometric Pressure, In. Hg Abs.	29.06	29.06	29.06	29.02	29.02	29.02	28.97	28.97	28.97	28.97	28.97
Liquid on Test Plate											
1. Temperature Entering, °F	89.9	89.9	89.9	91.3	91.4	91.3	92.1	92.0	92.3	88.3	88.0
2. Temperature Leaving, °F	90.1	90.1	90.0	91.6	91.7	91.6	92.3	92.3	92.6	88.5	88.1
3. Average Temperature, °F	90.0	90.0	90.0	91.5	91.6	91.5	92.2	92.2	92.5	88.4	88.1
4. [1]Froth Height, in.	5.3	5.4	5.2	7.2	7.2	7.3	6.1	6.2	7.4	4.6	4.6
[1]Clear Liquid Height, in.											
5. Position A	2.25	2.25	2.25	2.4	2.4	2.4	2.3	2.35	2.5	2.1	2.1
6. Position B	1.9	1.95	1.9	1.7	1.7	1.7	1.9	1.9	1.8	2.05	2.05
7. Position C	2.1	2.1	2.1	1.9	1.9	1.9	1.9	1.9	2.0	2.2	2.2
8. Position D	2.15	2.15	2.15	2.1	2.1	2.1	2.2	2.2	2.1	2.15	2.15
Gas Flowing Through Test Plate (Below Test Plate)											
9. Lb mole per minute x 10^2	20.1	20.1	20.1	40.5	40.5	40.5	30.4	30.4	40.4	10.0	10.0
10. Temperature, °F	166.	166.	166.	177.	178.	179.	176.	177.	180	154.	155.
(Above Test Plate)											
11. Lb mole per minute x 10^2	20.7	20.7	20.7	41.7	41.7	41.7	31.3	31.3	41.5	10.3	10.3
12. [2]Temperature, °F	95.	95.	96.	98.	98.	100.	98.	98.	100.	90.	90.
13. Pressure, in. Hg abs.	31.35	31.34	31.35	30.94	30.85	30.85	31.66	31.64	30.76	31.83	31.78
(Average Conditions)											
14. Lb mole per minute x 10^2	20.4	20.4	20.4	41.1	41.1	41.1	30.8	30.8	40.9	10.2	10.2
15. Temperature, °F	130.	130.	131.	138.	138.	139.	137.	137.	140.	122.	122.
16. [3]Superficial Velocity, ft per sec	2.26	2.26	2.26	4.68	4.63	4.70	3.43	3.49	4.60	1.10	1.10
17. "F" factor	.598	.598	.599	1.222	1.215	1.224	.906	.921	.908	.294	.294
Composition, Mole Fraction x 10^2											
18. y_o	1.689	1.661	1.652	1.928	1.912	1.894	1.944	1.919	2.040	1.963	1.953
19. y_1	4.309	4.307	4.294	4.573	4.585	4.549	4.605	4.591	4.734	4.190	4.141
20. y_1*	4.512	4.516	4.512	4.792	4.820	4.849	4.791	4.794	4.979	4.233	4.200
21. Pressure Drop, in. H_2O	2.71	2.69	2.68	5.40	5.35	5.55	3.67	3.67	5.25	2.20	2.20
Equilibrium Conditions on Test Tray											
22. Temperature, °F	90.0	90.0	90.0	91.5	91.6	91.5	92.2	92.2	92.5	88.4	88.1
23. Vapor Pressure of Liquid, mm Hg	35.9	35.9	35.9	37.7	37.8	37.7	38.5	38.5	38.9	34.2	33.9
24. Pressure Above Plate, mm Hg abs.	796.	796.	796.	786.	784.	784.	804.	804.	781.	809.	807.
25. Murphrey Vapor Efficiency, %	92.8	92.7	92.4	92.4	91.9	90.8	93.5	92.9	91.7	98.1	97.4
26. Number of Gas Transfer Units per Plate, $N_{OG} = N_G$	2.63	2.62	2.57	2.57	2.52	2.38	2.73	2.65	2.48	4.01	3.64

[1]Measured from tray floor.

[2]Calculated assuming a linear relation between the temperature and composition of the gas.

[3]Based on active area between inlet downcomer and splash baffle (.615 ft^2).

TABLE 9

HUMIDIFICATION OF FREON-12 WITH WATER

1-1/2-in. weir; 2-in. baffle height; liquid rate = 8.0 gallons per minute

Run Number	87	88	89	90	91	92	93	94
Barometric Pressure, In. Hg Abs.	28.94	28.94	28.94	28.94	28.90	28.90	28.90	28.90
Liquid on Test Plate								
1. Temperature Entering, °F	113.7	113.7	113.4	113.5	112.3	112.2	111.3	111.4
2. Temperature Leaving, °F	113.6	113.5	113.3	113.4	112.2	112.1	111.2	111.3
3. Average Temperature, °F	113.7	113.6	113.4	113.5	112.3	112.2	111.3	111.2
4. [1]Froth Height, in.	4.2	4.2	3.6	3.6	5.3	5.3	6.5	6.5
[1]Clear Liquid Height, in.								
5. Position A	1.85	1.85	1.7	1.7	1.9	1.9	2.1	2.1
6. Position B	1.4	1.4	1.7	1.7	1.4	1.4	1.3	1.3
7. Position C	1.75	1.75	1.85	1.85	1.45	1.45	1.5	1.5
8. Position D	1.8	1.8	1.85	1.85	1.75	1.75	1.85	1.85
Gas Flowing Through Test Plate (Below Test Plate)								
9. Lb mole per minute x 10^2	9.8	9.8	4.9	4.9	14.8	14.8	19.6	19.6
10. Temperature, °F	179.	179.	171.	171.	182.	182.	182.	183.
(Above Test Plate)								
11. Lb mole per minute x 10^2	10.4	10.4	5.2	5.2	15.7	15.7	20.9	20.9
12. [2]Temperature, °F	118.	118.	115.	115.	118.	116.	115.	114.
13. Pressure, in. Hg abs.	31.24	31.24	31.32	31.32	31.25	31.25	30.57	30.57
(Average Conditions)								
14. Lb mole per minute x 10^2	10.1	10.1	5.0	5.0	15.2	15.2	20.3	20.3
15. Temperature, °F	148.	148.	143.	143.	150	149.	149.	148.
16. [3]Superficial Velocity, ft per sec	1.15	1.15	.57	.57	1.75	1.75	2.38	2.38
17. "F" factor	.600	.600	.300	.300	.917	.917	1.231	1.231
Composition, Mole Fraction x 10^2								
18. y_o	2.420	2.445	2.541	2.595	2.544	8.510	2.577	2.544
19. y_1	8.777	8.769	8.882	8.949	8.278	8.422	8.442	8.516
20. y_1*	9.199	9.187	9.100	9.125	8.831	8.806	8.770	8.757
21. Pressure Drop, in. H_2O	2.40	2.40	1.78	1.78	3.33	3.33	4.98	4.98
Equilibrium Conditions on Test Tray								
22. Temperature, °F	113.7	113.6	113.4	113.5	112.3	112.2	111.3	111.2
23. Vapor Pressure of Liquid, mm Hg	73.0	72.9	72.4	72.6	70.1	69.9	68.1	68.0
24. Pressure Above Plate, mm Hg	794.	794.	796.	796.	794.	794.	777.	777.
25. Murphrey Vapor Efficiency, %	93.8	93.8	96.7	97.3	91.2	93.9	94.7	96.1
26. Number of Gas Transfer Units per Plate, $N_G = N_{OG}$	2.78	2.78	3.40	3.62	2.43	2.79	2.94	3.25

[1]Measured from tray floor.
[2]Calculated assuming a linear relation between the temperature and composition of the gas.
[3]Based on active area between inlet downcomer and splash baffle (.615 ft^2).

TABLE 10

HUMIDIFICATION OF HELIUM WITH ISOBUTYL ALCOHOL

1-1/2-in. weir; 2-1/2-in. baffle height; liquid rate = 8.0 gallons per minute

Run Number	147	148	149	150	151	152	153	154	155	156	157
Barometric Pressure, In. Hg Abs.	28.85	28.85	28.85	28.82	28.82	28.82	28.82	28.98	28.98	28.98	28.98
Liquid on Test Plate											
1. Temperature Entering, °F	101.7	100.4	100.0	103.5	103.7	104.8	104.6	100.9	100.8	99.0	98.5
2. Temperature Leaving, °F	102.1	100.7	100.3	104.1	104.1	105.2	105.1	101.3	101.1	99.3	98.8
3. Average Temperature, °F	101.9	100.6	100.2	103.8	104.0	105.1	105.0	101.2	101.0	99.1	98.6
4. [1]Froth Height, in.	4.5	3.9	3.9	5.0	5.2	6.0	6.2	4.6	4.5	3.9	3.9
[1]Clear Liquid Height, in.											
5. Position A	2.15	2.1	2.15	2.2	2.2	2.2	2.2	2.2	2.2	2.15	2.15
6. Position B	1.6	1.8	1.8	1.5	1.5	1.55	1.55	1.6	1.6	1.8	1.8
7. Position C	1.75	1.8	1.8	1.65	1.6	1.55	1.6	1.8	1.75	1.8	1.8
8. Position D	1.7	1.75	1.8	1.75	1.7	1.7	1.75	1.75	1.7	1.8	1.8
Gas Flowing Through Test Plate (Below Test Plate)											
9. Lb mole per minute x 10^2	35.0	23.2	23.3	46.0	46.5	57.7	57.7	35.2	35.4	23.6	23.6
10. Temperature, °F	177.	170.	170.	182.	182.	185.	185.	177.	177.	170.	170.
(Above Test Plate)											
11. Lb mole per minute x 10^2	35.7	23.7	23.8	47.0	47.5	58.9	58.9	35.9	36.1	24.1	24.1
12. [2]Temperature, °F	116.	115.	114.	117.	119.	121.	119.	115.	118.	113.	114.
13. Pressure, in. Hg abs.	30.18	29.90	29.90	29.92	29.93	30.27	30.27	30.22	30.10	30.03	30.00
(Average Conditions)											
14. Lb mole per minute x 10^2	35.3	23.4	23.5	46.5	46.7	58.3	58.3	35.5	35.7	23.8	23.8
15. Temperature, °F	147.	143.	142.	150.	150.	153.	152.	146.	147.	142.	142.
16. [3]Superficial Velocity, ft per sec	4.20	2.78	2.79	5.60	5.61	6.95	6.95	4.20	4.25	2.82	2.82
17. "F" factor	.481	.316	.316	.650	.645	.806	.804	.480	.480	.317	.317
Composition, Mole Fraction x 10^2											
18. y_o	1.587	1.561	1.478	1.759	1.735	1.790	1.790	1.465	1.387	1.325	1.350
19. y_1	3.389	3.236	3.206	3.724	3.659	3.746	3.778	3.294	3.189	3.068	3.013
20. y_1*	3.809	3.706	3.647	4.105	4.130	4.214	4.201	3.713	3.701	3.487	3.451
21. Pressure Drop, in. H_2O	1.60	1.34	1.36	1.93	1.92	2.39	2.39	1.60	1.60	1.34	1.34
Equilibrium Conditions on Test Tray											
22. Temperature, °F	101.9	100.6	100.2	103.8	104.0	105.1	105.0	101.2	101.0	99.1	98.6
23. Vapor Pressure of Liquid, mm Hg	29.2	28.1	27.7	31.2	31.4	32.4	32.3	28.5	28.3	26.6	26.3
24. Pressure Above Plate, mm Hg	767.	760.	760.	760.	760.	769.	769.	768.	765.	763.	762.
25. Murphrey Vapor Efficiency, %	81.1	78.1	79.7	83.8	80.3	80.7	82.5	81.4	77.9	80.6	79.2
26. Number of Gas Transfer Units per Plate, $N_G = N_{OG}$	1.66	1.52	1.59	1.82	1.63	1.64	1.74	1.68	1.51	1.64	1.57

[1]Measured from tray floor.
[2]Calculated assuming a linear relation between the temperature and composition of the gas.
[3]Based on active area between inlet downcomer and splash baffle (.615 ft^2).

TABLE 11

HUMIDIFICATION OF NITROGEN WITH ISOBUTYL ALCOHOL

1-1/2-in. weir; 2-in. baffle height; liquid rate = 8.0 gallons per minute

Run Number	134	135	136	137	138	139	140	141
Barometric Pressure, In. Hg Abs.	28.82	28.82	28.82	28.82	28.65	28.65	28.65	28.65
Liquid on Test Plate								
1. Temperature Entering, °F	104.2	104.4	102.2	102.1	101.8	101.7	105.8	105.7
2. Temperature Leaving, °F	104.6	104.8	102.6	102.2	102.1	102.0	106.3	106.1
3. Average Temperature, °F	104.4	104.6	102.4	102.2	102.0	101.9	106.0	105.9
4. [1]Froth Height, in.	4.6	4.6	3.7	3.6	4.0	4.0	5.8	6.0
[1]Clear Liquid Height, in.								
5. Position A	2.2	2.2	2.1	2.05	2.1	2.1	2.2	2.15
6. Position B	1.5	1.5	1.8	1.75	1.65	1.65	1.6	1.6
7. Position C	1.65	1.65	1.8	1.75	1.75	1.75	1.45	1.55
8. Position D	1.75	1.75	1.8	1.75	1.7	1.7	1.75	1.7
Gas Flowing Through Test Plate (Below Test Plate)								
9. Lb mole per minute x 10^2	19.6	19.6	9.8	9.8	14.7	14.7	29.6	29.6
10. Temperature, °F (Above Test Plate)	174.	174.	164.	163.	167.	168.	181.	181.
11. Lb mole per minute x 10^2	20.1	20.1	10.0	10.0	15.0	15.0	30.2	30.2
12. [2]Temperature, °F	115.	116.	111.	112.	114.	114.	119.	118.
13. Pressure, in. Hg abs. (Average Conditions)	30.22	30.22	30.22	30.32	29.93	29.93	30.20	30.20
14. Lb mole per minute x 10^2	19.8	19.8	9.9	9.9	14.8	14.8	29.9	29.9
15. Temperature, °F	144.	145.	137.	137.	141.	141.	150.	150.
16. [3]Superficial Velocity, ft per sec	2.34	2.34	1.15	1.15	1.76	1.76	3.58	3.58
17. "F" factor	.606	.606	.300	.300	.453	.453	.924	.924
Composition, Mole Fraction x 10^2								
18. y_o	1.509	1.518	1.441	1.420	1.442	1.445	1.630	1.656
19. y_1	3.723	3.718	3.502	3.447	3.426	3.426	3.891	3.905
20. y_1*	4.123	4.156	3.873	3.837	3.867	3.854	4.341	4.328
21. Pressure Drop, in. H_2O	1.85	1.85	1.34	1.34	1.57	1.57	2.91	2.90
Equilibrium Conditions on Test Tray								
22. Temperature, °F	104.4	104.6	102.4	102.2	102.0	101.9	106.0	105.9
23. Vapor Pressure of Liquid, mm Hg	31.7	31.9	29.8	29.6	29.4	29.3	33.3	33.2
24. Pressure Above Plate, mm Hg	768.	768.	768.	770.	760.	760.	767.	767.
25. Murphrey Vapor Efficiency, %	84.7	83.4	84.8	83.9	81.8	82.2	83.4	84.2
26. Number of Gas Transfer Units per Plate, $N_G = N_{OG}$	1.88	1.80	1.88	1.82	1.70	1.73	1.80	1.84

[1]Measured from tray floor.
[2]Calculated assuming a linear relation between the temperature and composition of the gas.
[3]Based on active area between inlet downcomer and splash baffle (.615 ft^2).

TABLE 12

HUMIDIFICATION OF HELIUM WITH METHYL ISOBUTYL KETONE

1-1/2-in. weir; 2-in. baffle height; liquid rate = 8.0 gallons per minute

Run Number	158	159	160	161	162	163	164	165
Barometric Pressure, In. Hg Abs.	28.93	28.93	28.93	28.93	28.90	28.90	28.90	28.90
Liquid on Test Plate								
1. Temperature Entering, °F	98.4	98.6	96.8	96.5	99.5	100.0	101.1	101.0
2. Temperature Leaving, °F	98.9	99.1	97.1	96.9	100.3	100.6	101.7	101.9
3. Average Temperature, °F	98.7	98.9	97.0	96.7	100.0	100.4	101.5	101.6
4. [1]Froth Height, in.	4.6	4.6	4.0	4.0	5.0	5.0	5.9	6.0
[1]Clear Liquid Height, in.								
5. Position A								
6. Position B								
7. Position C								
8. Position D								
Gas Flowing Through Test Plate (Below Test Plate)								
9. Lb mole per minute x 10^2	32.0	32.0	21.4	21.4	43.0	43.0	53.3	53.3
10. Temperature, °F	175.	176.	169.	169.	179.	180.	182.	182.
(Above Test Plate)								
11. Lb mole per minute x 10^2	32.8	32.8	21.9	21.9	44.1	44.1	54.6	54.6
12. [2]Temperature, °F	110.	110.	106.	106.	113.	114.	115.	115.
13. Pressure, in. Hg abs.	29.87	29.88	29.95	29.95	30.05	30.05	30.16	30.13
(Average Conditions)								
14. Lb mole per minute x 10^2	32.4	32.4	21.6	21.6	43.5	43.5	53.9	53.9
15. Temperature, °F	142.	143.	137.	137.	146.	147.	148.	148.
16. [3]Superficial Velocity, ft per sec	3.85	3.85	2.55	2.55	5.20	5.20	6.42	6.42
17. "F" factor	.491	.491	.324	.324	.665	.665	.830	.830
Composition, Mole Fraction x 10^2								
18. y_o	2.073	2.097	2.015	2.013	2.103	2.105	2.257	2.257
19. y_1	4.456	4.486	4.291	4.267	4.548	4.591	4.719	4.732
20. y_1*	4.962	4.987	4.706	4.679	5.109	5.163	5.300	5.318
21. Pressure Drop, in. H_2O	1.57	1.57	1.40	1.40	1.86	1.86	2.34	2.32
Equilibrium Conditions on Test Tray								
22. Temperature, °F	98.7	98.9	97.0	96.7	100.0	100.4	101.5	101.6
23. Vapor Pressure of Liquid, mm Hg	37.7	37.9	35.8	35.6	39.0	39.4	40.6	40.7
24. Pressure Above Plate, mm Hg	759.	759.	761.	761.	763.	763.	766.	765.
25. Murphrey Vapor Efficiency, %	82.5	82.7	84.6	84.6	81.3	81.3	80.9	80.9
26. Number of Gas Transfer Units per Plate, $N_G = N_{OG}$	1.74	1.75	1.87	1.87	1.68	1.68	1.65	1.65

[1]Measured from tray floor.

[2]Calculated assuming a linear relation between the temperature and composition of the gas.

[3]Based on active area between inlet downcomer and splash baffle (.615 ft^2).

TABLE 13

PRESSURE DROP, FROTH HEIGHT, AND CLEAR LIQUID HEIGHT
FOR THE MASS TRANSFER RUNS
1.5-IN. WEIR, 2-IN. BAFFLE HEIGHT, 8 GAL/MIN

[1]Run No.	[2]"F" factor	[3]Pressure Drop, in.H2O	[4]Froth Height, in.	[4,5]Clear Liquid Height, in., at Positions A	B	C	D
115	.61	2.26	4.7	2.3	1.6	1.7	1.7
116	.61	2.26	4.7	2.3	1.6	1.7	1.7
117	.77	2.70	5.2	2.3	1.5	1.6	1.7
118	.77	2.70	5.2	2.3	1.5	1.6	1.7
119	.46	1.96	4.3	2.2	1.7	1.7	1.7
120	.46	1.96	4.3	2.2	1.7	1.7	1.7
121	.30	1.83	4.0	2.2	1.8	1.8	1.7
122	.30	1.83	4.0	2.2	1.8	1.8	1.7
64	.60	2.36	4.4	1.8	1.4	1.7	1.7
65	.60	2.36	4.3	1.8	1.4	1.7	1.7
66	.29	1.86	3.9	1.7	1.7	1.8	1.8
67	.29	1.86	3.9	1.7	1.7	1.8	1.8
68	.29	1.86	3.9	1.7	1.7	1.8	1.8
69	.91	3.31	5.2	1.9	1.4	1.4	1.8
70	.91	3.31	5.1	1.9	1.4	1.4	1.8
71	1.22	4.89	5.4	1.9	1.3	1.4	1.8
72	1.22	4.89	5.4	1.9	1.3	1.4	1.8
123	.91	3.22	5.3	2.2	1.4	1.4	1.6
124	.91	3.23	5.3	2.2	1.4	1.4	1.7
125	1.06	3.92	5.6	2.2	1.5	1.3	1.7
126	1.06	3.90	5.6	2.2	1.4	1.3	1.7
127	.91	3.17	5.2	2.2	1.4	1.4	1.7
128	.60	2.24	4.3	2.2	1.5	1.6	1.6
129	.60	2.24	4.3	2.2	1.5	1.6	1.6
130	.29	1.76	3.9	2.2	1.8	1.8	1.7
131	.29	1.76	3.9	2.2	1.8	1.8	1.7
87	.60	2.40	4.2	1.8	1.4	1.7	1.8
88	.60	2.40	4.2	1.8	1.4	1.7	1.8
89	.30	1.78	3.6	1.7	1.7	1.8	1.8
90	.30	1.78	3.6	1.7	1.7	1.8	1.8
91	.92	3.33	5.3	1.9	1.4	1.4	1.7
92	.92	3.33	5.3	1.9	1.4	1.4	1.7
93	1.23	4.98	6.5	2.1	1.3	1.5	1.8
94	1.23	4.98	6.5	2.1	1.3	1.5	1.8

TABLE 13 (Continued)

[1]Run No.	[2]"F" factor	[3]Pressure Drop, in.H2O	[4]Froth Height, in.	[4,5]Clear Liquid Height, in., at Positions A	B	C	D
147	.48	1.60	4.5	2.1	1.6	1.7	1.7
148	.32	1.34	3.9	2.1	1.8	1.8	1.7
149	.32	1.36	3.9	2.1	1.8	1.8	1.8
150	.65	1.93	5.0	2.2	1.5	1.6	1.7
151	.65	1.92	5.2	2.2	1.5	1.6	1.7
152	.81	2.39	6.0	2.2	1.5	1.5	1.7
153	.81	2.39	6.2	2.2	1.5	1.6	1.7
154	.48	1.60	4.6	2.2	1.6	1.8	1.7
155	.48	1.60	4.5	2.2	1.6	1.7	1.7
156	.32	1.34	3.9	2.1	1.8	1.8	1.8
157	.32	1.34	3.9	2.1	1.8	1.8	1.8
134	.61	1.85	4.6	2.2	1.5	1.6	1.7
135	.61	1.85	4.6	2.2	1.5	1.6	1.7
136	.30	1.34	3.7	2.1	1.8	1.8	1.8
137	.30	1.34	3.6	2.0	1.7	1.7	1.7
138	.45	1.57	4.0	2.1	1.6	1.6	1.7
139	.45	1.57	4.0	2.1	1.6	1.6	1.7
140	.92	2.91	5.8	2.2	1.6	1.4	1.7
141	.92	2.90	6.0	2.1	1.6	1.5	1.7
158	.491	1.57	4.6				
159	.491	1.57	4.6				
160	.324	1.40	4.0				
161	.324	1.40	4.0				
162	.665	1.86	5.0				
163	.665	1.86	5.0				
164	.830	2.34	5.9				
165	.830	2.32	6.0				

Clear Liquid Heights Not Measured for This System

[1]Helium-Water (115-122); Air-Water (64-72, 123-131); Freon-12-Water (87-94); Helium-Isobutyl Alcohol (147-157); Nitrogen-Isobutyl Alcohol (134-141); Helium-Methyl Isobutyl Ketone (158-165).

[2]See Nomenclature.

[3]Pressure drop across test plate.

[4]Measured from tray floor.

[5]See Figure (15) for locations on test plate.

TABLE 14

CALCULATED DATA FOR ADIABATIC HUMIDIFICATION TESTS[3]

[1]Run No.	$\frac{\mu_G}{\rho_G D_V}$	$\frac{D_s \, v \, \rho_G}{\mu_G}$	$\frac{D_s \rho_G \sigma}{\mu_G^2} \times 10^{-4}$	$\frac{h_L}{D_s}$	$\frac{\rho_L}{\rho_G}$	$\frac{\mu_L}{\mu_G}$	N_G Calculated	N_G Experimental	[2]Absolute Per Cent Deviation	[4]Ordinate of Figure 19	[5]Ordinate of Figure 20	[6]Ordinate of Figure 21
115	1.09	48.	8.74	14.1	6480.	38.2	2.20	2.06	6.8	.917	.256	5.63
116	1.09	48.	8.74	14.1	6480.	38.2	2.20	1.99	10.6	.885	.247	5.43
117	1.09	61.	8.74	14.8	6480.	37.8	2.11	1.95	8.4	.905	.234	5.55
118	1.09	61.	8.74	14.8	6480.	37.8	2.11	1.92	9.6	.895	.232	5.49
119	1.09	36.	8.84	13.5	6450.	39.0	2.35	2.22	6.0	.922	.284	5.68
120	1.09	36.	8.84	13.5	6450.	39.0	2.35	2.21	6.6	.917	.282	5.65
121	1.09	24.	9.01	12.6	6390.	39.8	2.60	2.42	7.4	.910	.322	5.62
122	1.09	24.	9.01	12.6	6390.	39.8	2.60	2.45	6.2	.920	.326	5.69
Averages			8.83							.909		5.59
53	.56	126.	66.4	18.1	887.	39.2	3.07	2.73	12.6	1.015	.177	7.35
54	.56	126.	66.4	18.1	887.	39.2	3.07	2.70	13.8	1.004	.175	7.27
55	.56	126.	66.4	18.1	887.	39.2	3.07	2.67	15.2	.992	.173	7.19
56	.56	253.	64.4	20.1	909.	38.6	2.58	2.67	3.6	1.183	.163	8.54
57	.56	253.	65.0	20.1	901.	38.6	2.58	2.61	1.1	1.156	.159	8.34
58	.56	253.	64.0	20.1	914.	38.6	2.57	2.38	8.2	1.053	.146	7.61
59	.56	192.	66.1	19.3	887.	38.1	2.79	2.84	1.6	1.166	.176	8.41
60	.56	192.	66.0	19.3	888.	38.1	2.78	2.76	.8	1.138	.171	8.21
61	.56	252.	66.0	20.1	888.	38.1	2.61	2.59	.9	1.138	.156	8.19
62	.56	63.	68.5	16.6	860.	39.8	3.69	4.12	10.6	1.278	.281	9.30
63	.56	63.	68.3	16.6	862.	39.8	3.69	3.78	2.4	1.169	.257	8.52
Averages			66.1							1.117		8.08
64	.56	124.	65.4	14.1	901.	39.2	2.62	2.47	6.1	1.07	.188	7.78
65	.56	124.	65.2	14.1	902.	39.2	2.62	2.51	4.5	1.09	.191	7.90
66	.56	62.	66.8	12.6	881.	39.8	3.09	3.21	3.8	1.18	.262	8.61
67	.56	62.	66.8	12.6	881.	39.8	3.09	3.30	6.5	1.21	.269	8.85
68	.56	62.	66.8	12.6	881.	39.8	3.09	3.03	2.1	1.11	.247	8.11
69	.56	190.	65.6	15.4	899.	38.8	2.42	2.37	2.2	1.12	.170	8.08
70	.56	190.	65.6	15.4	899.	38.8	2.42	2.32	4.1	1.10	.167	7.93
71	.56	253.	64.0	16.1	914.	38.1	2.45	2.31	6.0	1.08	.149	7.76
72	.56	253.	64.0	16.1	914.	38.1	2.45	2.37	3.3	1.10	.152	7.96
123	.56	187.	63.6	15.4	921.	38.6	2.40	2.44	1.6	1.15	.177	8.35
124	.56	187.	63.9	15.4	916.	38.6	2.41	2.43	.8	1.15	.176	8.29
125	.56	219.	63.7	16.0	920.	38.1	2.34	2.31	1.4	1.12	.163	8.11
126	.56	219.	63.4	16.0	924.	38.1	2.34	2.19	6.5	1.07	.157	7.71
127	.56	186.	63.3	15.4	925.	38.3	2.40	2.38	.8	1.13	.173	8.14
128	.56	124.	64.0	14.1	920.	39.2	2.61	2.53	3.1	1.10	.194	7.98
129	.56	124.	64.0	14.1	920.	39.2	2.61	2.50	4.4	1.09	.191	7.88
130	.56	61.	65.0	12.6	906.	40.3	3.08	3.07	.3	2.13	.253	8.23
131	.56	61.	65.1	12.6	904.	40.3	3.08	3.26	5.4	1.19	.268	8.72
Averages			64.8							1.12		8.13

TABLE 14 (Continued)

[1]Run No.	$\frac{\mu_G}{\rho_G D_V}$	$\frac{D_S v \rho_G}{\mu_G}$	$\frac{D_S \rho_G \sigma}{\mu_G^2} \times 10^{-4}$	$\frac{h_L}{D_S}$	$\frac{\rho_L}{\rho_G}$	$\frac{\mu_L}{\mu_G}$	N_G Calculated	N_G Experimental	[2]Absolute Per Cent Deviation	[4]Ordinate of Figure 19	[5]Ordinate of Figure 20	[6]Ordinate of Figure 21
87	.24	336.	457.	14.1	225.	40.7	3.15	2.98	5.6	1.32	.136	10.63
88	.24	336.	457.	14.1	225.	40.7	3.15	2.99	5.4	1.31	.136	10.64
89	.24	169.	462.	12.6	222.	41.0	3.70	3.67	.8	1.37	.179	11.15
90	.24	169.	462.	12.6	222.	41.0	3.70	3.90	5.1	1.45	.190	11.84
91	.24	514.	457.	15.4	225.	41.6	2.89	2.60	11.1	1.24	.112	10.10
92	.24	514.	457.	15.4	225.	41.6	2.89	3.00	3.6	1.43	.129	11.64
93	.24	683.	448.	16.1	230.	42.2	2.68	3.15	15.1	1.62	.133	13.17
94	.24	683.	448.	16.1	230.	42.2	2.68	3.49	23.3	1.83	.147	14.59
Averages			456.							1.45		11.72
147	2.20	41.	3.31	13.6	3750.	113.	1.67	1.71	2.6	.857	.298	5.30
148	2.20	27.	3.29	12.7	3790.	117.	1.83	1.56	17.3	.707	.285	4.40
149	2.20	27.	3.26	12.7	3820.	117.	1.83	1.63	11.8	.741	.299	4.60
150	2.20	55.	3.38	14.4	3650.	111.	1.57	1.87	16.1	1.000	.311	6.17
151	2.20	55.	3.33	14.4	3710.	111.	1.57	1.68	6.2	.894	.279	5.59
152	2.20	70.	3.37	15.1	3650.	109.	1.51	1.70	11.1	.948	.273	5.82
153	2.20	70.	3.37	15.1	3650.	109.	1.51	1.80	16.0	1.003	.289	6.16
154	2.20	40.	3.30	13.6	3780.	115.	1.67	1.72	3.4	.861	.300	5.34
155	2.20	40.	3.23	13.6	3850.	115.	1.66	1.55	7.2	.774	.272	4.80
156	2.20	27.	3.22	12.7	3870.	119.	1.82	1.68	8.0	.765	.310	4.76
157	2.20	27.	3.21	12.7	3880.	119.	1.82	1.61	13.0	.730	.296	4.51
Averages			3.30							.844		5.22
134	1.54	130.	21.0	14.3	731.	123.	1.85	1.94	4.7	.951	.220	7.24
135	1.54	130.	21.0	14.3	731.	123.	1.85	1.85	.3	.910	.210	6.92
136	1.54	65.	21.4	12.7	722.	126.	2.03	1.94	4.9	.863	.237	6.60
137	1.54	65.	21.4	12.7	722.	126.	2.03	1.88	8.2	.837	.229	6.40
138	1.54	97.	20.9	13.6	737.	126.	1.84	1.75	4.9	.861	.207	6.58
139	1.54	97.	20.9	13.6	737.	126.	1.84	1.78	3.5	.872	.209	6.66
140	1.54	197.	20.7	15.7	739.	120.	1.60	1.85	13.9	1.056	.199	8.00
141	1.54	197.	20.7	15.7	739.	120.	1.60	1.90	16.2	1.084	.204	8.22
Averages			21.0							.929		7.08
158	1.76	55.	5.69	13.6	3010.	27.9	1.74	1.81	3.7	.910	.272	5.84
159	1.76	55.	5.69	13.6	3010.	27.9	1.74	1.82	4.3	.916	.274	5.87
160	1.76	36.	5.63	12.7	3050.	28.1	1.91	1.94	1.5	.885	.307	5.70
161	1.76	36.	5.63	12.7	3050.	28.1	1.91	1.94	1.4	.884	.306	5.69
162	1.76	74.	5.68	14.4	3010.	27.4	1.64	1.74	6.1	.936	.253	5.99
163	1.76	74.	5.68	14.4	3010.	27.4	1.64	1.74	6.1	.936	.252	5.98
164	1.76	94.	5.79	15.1	2940.	27.2	1.57	1.72	8.7	.968	.240	6.17
165	1.76	94.	5.79	15.1	2940.	27.2	1.57	1.72	8.6	.966	.240	6.16
Averages			5.70							.925		5.93

[1]Helium-Water (115-122); Air-Water, 2-in. weir (53-63); Air-Water, 1.5-in. weir (64-72, 123-131); Freon-12-Water (87-94); Helium-Isobutyl Alcohol (147-157); Nitrogen-Iosbutyl Alcohol (134-141); Helium-Methyl Isobutyl Ketone (158-165).

[2]Abs. per cent deviation = $\left| \frac{\text{Calc. } N_G - \text{Exp. } N_G}{\text{Exp. } N_G} \right| \times 100$

The overall average absolute deviation was 6.6 per cent.
The maximum deviation was 23.3 per cent.

[3]See Nomenclature for definitions of symbols.

[4]See Figure (19).

[5]See Figure (20).

[6]See Figure (21).

TABLE 15

COMPARISON OF N_G'S OBTAINED FROM AMMONIA ABSORPTION AND DESORPTION DATA[1]

WITH THE CORRELATION OF THE ADIABATIC HUMIDIFICATION DATA OF THE PRESENT WORK

[2]Run No.	[3]Weir Height, in.	[4]Liquid Flow Rate, gal/min	$\frac{\mu_G}{\rho_G D_V}$	$\frac{D_s v \rho_G}{\mu_G}$	$\frac{D_s \rho_G \sigma}{\mu_G^2} \times 10^{-4}$	$\frac{h_L}{D_s}$	$\frac{\rho_L}{\rho_G}$	$\frac{\mu_L}{\mu_G}$	N_G Calculated	N_G Experimental	[5]Per Cent Deviation
A-2	3.5	4.58	.613	59.	81.0	26.9	860.	47.5	5.09	2.13	-58
A-9	3.5	4.58	.613	119.	81.0	28.2	860.	47.5	4.18	2.34	-44
A-11	3.5	4.58	.613	190.	81.0	30.0	860.	47.5	3.70	2.47	-33
A-13	3.5	4.58	.613	288.	81.0	30.9	860.	47.5	3.27	2.39	-27
A-3	3.5	9.16	.613	60.	81.0	28.6	860.	47.5	5.33	2.28	-57
A-8	3.5	9.16	.613	118.	81.0	29.9	860.	47.5	4.35	2.64	-39
A-10	3.5	9.16	.613	183.	81.0	31.4	860.	47.5	3.86	2.76	-29
A-12	3.5	9.16	.613	279.	81.0	32.6	860.	47.5	3.41	2.51	-26
Average											-39
A-32	2.0	4.58	.613	60.	80.9	14.9	862.	47.5	3.62	1.86	-49
A-29	2.0	4.58	.613	124.	80.9	16.4	862.	47.5	2.92	1.70	-42
A-19	2.0	4.58	.613	188.	80.9	17.8	862.	47.5	2.69	1.69	-37
A-21	2.0	4.58	.613	281.	80.9	18.9	862.	47.5	2.43	1.71	-30
A-31	2.0	9.16	.613	58.	80.9	16.6	862.	47.5	3.82	1.87	-51
A-28	2.0	9.16	.613	123.	80.9	18.1	862.	47.5	3.12	1.86	-40
A-18	2.0	9.16	.613	182.	80.9	19.4	862.	47.5	2.86	1.76	-39
A-20	2.0	9.16	.613	275.	80.9	20.6	862.	47.5	2.60	1.64	-37
Average											-40
AD-39	2.0	4.58	.616	64.	76.9	15.0	857.	46.2	3.41	1.96	-43
AD-40	2.0	4.58	.616	193.	78.6	17.9	838.	46.2	2.66	1.61	-39
AD-45	2.0	4.58	.616	293.	81.0	18.9	818.	46.2	2.34	1.72	-36
AD-38	2.0	9.16	.616	64.	76.9	16.7	859.	46.2	3.64	2.05	-44
AD-37	2.0	9.16	.616	194.	79.1	19.6	834.	46.2	2.83	1.78	-37
AD-44	2.0	9.16	.616	296.	81.9	20.6	804.	46.2	2.53	1.58	-37
Average											-39

[1]Data of Warzel (65), who used the same column and the same bubble cap plate that were used in the present work.

[2]"A" denotes ammonia absorption from air with water. "AD" denotes ammonia desorption from water with air.

[3]Most of the humidification tests were made with a 1.5-in. weir. However, one group of air-water humidification runs was made with a 2-in. weir, and this group seemed to correlate as well as the runs using the 1.5-in. weir.

[4]The liquid flow rate for all the adiabatic humidification runs was 8.0 gal/min.

[5]Per cent deviation of ammonia data from correlation $= \left[\frac{(N_G)_{NH_3} - (N_G)_{\text{correlation}}}{(N_G)_{\text{correlation}}}\right] \times 100.$

APPENDIX B

PHYSICAL PROPERTIES OF THE FLUIDS

1. Gas Density

The average molecular weight of the gas was calculated from the measured compositions. The average temperature and pressure were measured. With these data, the average density of the gas was calculated according to the ideal gas laws.

2. Gas Viscosity

Experimental data for the pure gases and vapors were obtained from Reference (26), pp. 1736-40. The calculated data were obtained by the method of Bromley and Wilke (3).

TABLE 16

GAS VISCOSITY

Gas or Vapor	Type of Data	Viscosity at 1 atm in Micropoises	
		40°C	60°C
Helium	Exp.	203	211
Air	Exp.	191	200
Nitrogen	Exp.	182	190
Freon 12	Calc.	135	143
Water	Exp.	105	111
Ammonia	Exp.	105	111
Isobutyl Alc.	Exp.	118	125
MIBK	Calc.	60	64

The effects of vapor concentration on the viscosities of the pure inert gases were calculated by the method of Bromley and Wilke (3). The results are plotted in Figure 23.

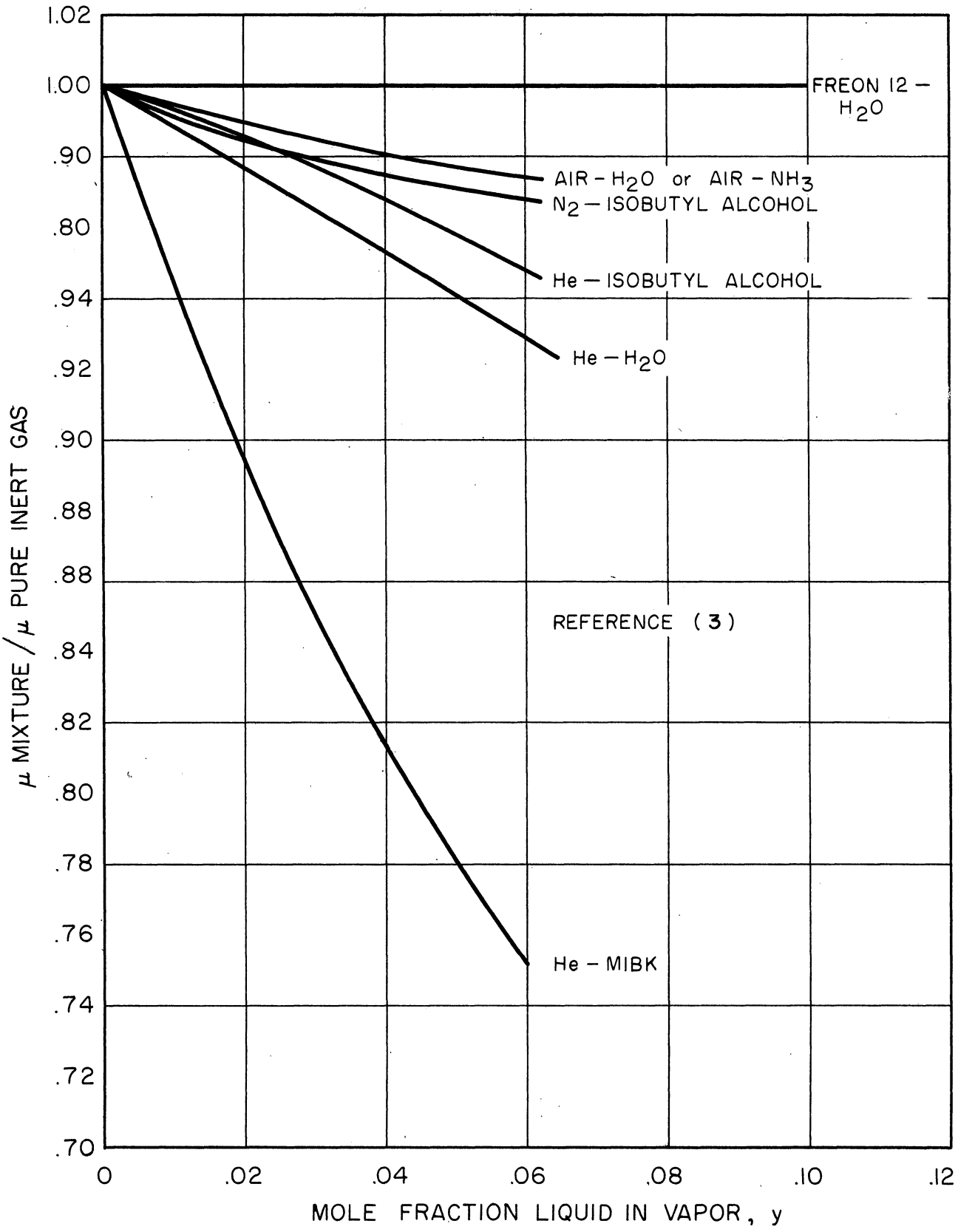

Figure 23. Effect of composition on the viscosity of gas mixtures.

3. Gas Phase Diffusivity

The experimental data were taken from Reference (68). These data were extended over the required temperature range with the modified Hirshfelder, Bird, and Spoty equation suggested by Wilke and Lee (68). The same equation was used to calculate diffusivities for the systems for which no experimental data were available.

TABLE 17

GAS PHASE DIFFUSIVITY

System	Type of Data	Gas Phase Diffusivity at 1 atm, ft^2/hr	
		25°C	60°C
He-H_2O	Exp.	3.52	4.25
Air-H_2O	Exp.	1.01	1.24
Freon 12-H_2O	Exp.	.407	.51
Air-NH_3	Exp.	.98	1.21
He-Isobutyl Alc.	Calc.	1.41	1.71
N_2-Isobutyl Alc.	Calc.	.35	.43
He-MIBK	Calc.	1.20	1.46

The effect of composition on the diffusivity was small enough that an average value of composition for each system could be used. The above values have been corrected for this small effect of composition.

4. Surface Tension

The surface tensions of water and of isobutyl alcohol were obtained from Reference (26), pp. 1723-1726. The surface tension of methyl isobutyl ketone was obtained from Reference (35). It was assumed that the surface tension between a gas and a given liquid was approximately

the same for all the gases used in these tests. The data were extended over the required temperature range by comparison with surface tension vs. temperature data for similar liquids.

TABLE 18

SURFACE TENSION

Liquid	Surface Tension, dynes/cm	
	20°C	40°C
Water	72.8	69.7
Isobutyl Alc.	23.0	21.3
MIBK	22.7	21.0

5. Liquid Viscosity

TABLE 19

LIQUID VISCOSITY

Liquid	Reference	Viscosity in Centipoises at		
		20°C	30°C	40°C
Water	(26), p. 1729	1.005	0.801	0.656
Isobutyl Alc.	(26), p. 1733 (33), p. 409	3.98	3.02	2.30
MIBK	(35), p. 66	0.585	0.522	0.47

6. Liquid Density

TABLE 20

LIQUID DENSITY

Liquid	Reference	Density, gm/cc at 30°C	40°C
Water	(26), p. 1695	.995	.992
Isobutyl Alc.	(26), p. 875	.794	.785
MIBK	(35), p. 66	.791	.782

7. Vapor Pressure

The vapor pressure data for water and isobutyl alcohol are found in standard reference books and are not reproduced here. For water, Reference 26, pp. 1825-31 was used. For isobutyl alcohol, Reference 39, p. 154 was used.

The data for methyl isobutyl ketone, obtained from Reference 35, p. 67, were represented by the following equation:

$$\log_{10} p \text{ (mm Hg)} = 23.66786 - \frac{2790.4}{T} - 5.2566 \log_{10} T$$

where

p = vapor pressure, mm Hg, and

T = t°C + 273.15.

APPENDIX C

SAMPLE CALCULATIONS

The calculations for Run No. 64 (air-water system) are given below. The calculations for all the other runs were similar to the ones shown.

1. Gas Equilibrium Composition, y_1^*

Pressure above test plate = 784.6 mm Hg

Avg liquid temperature on test plate = 89.9°F

Vapor pressure of liquid = 35.9 mm Hg

$$y_1^* = \frac{35.9}{784.6} = .04576$$

2. Gas Outlet Composition, y_1

Measured sample volume (wet test meter rdg) = 0.4996 ft^3

Meter correction factor = 0.996

Corrected sample volume = (0.996)(0.4996) = 0.4981 ft^3

The lb moles of dry, inert gas per cubic foot of gas metered were calculated assuming that the gas was saturated with water vapor at the temperature and pressure of the meter and assuming the ideal gas laws. In this case, the meter temperature was 75.6°F; the meter pressure was 28.68 in. Hg; and the lb-mole of air per cubic foot of gas metered was 2.375×10^{-3}.

Amount of air in sample = $(0.4981)(2.375 \times 10^{-3})$

= 1.183×10^{-3} lb mole

Weight of water absorbed in the drying tubes = 0.4385 gms.

= 5.365×10^{-5} lb mole

Total moles of gas originally in sample = 118.3×10^{-5} moles air

+ 5.4×10^{-5} moles water

123.7×10^{-5} moles sample

$$y_1 = \frac{5.365 \times 10^{-5}}{123.7 \times 10^{-5}} = .04337$$

3. Gas Inlet Composition, y_o

The method used to determine the gas inlet composition was identical to that used to determine the outlet composition, shown above.

$$y_o = .01982$$

4. Point Vapor Efficiency

The point and plate efficiencies were assumed to be identical for these runs ($E_{OG} = E_{MV}$).

Therefore, $E_{OG} = \frac{y_1 - y_o}{y_1^* - y_o}$ from Equation (2).

$$E_{OG} = \frac{.04337 - .01982}{.04576 - .01982} = 0.908 \text{ or } 90.8\%$$

5. Number of Individual Gas Transfer Units per Plate, N_G

$$N_G = \frac{1}{1 - y_1^*} \left[\ln \frac{(y_1^* - y_o)(1 - y_1)}{(y_1^* - y_1)(1 - y_o)} \right] \text{ according to Eq. (21).}$$

$$N_G = \frac{1}{1 - .04576} \left[\ln \frac{(.04576 - .01982)(1 - .04337)}{(.04576 - .04337)(1 - .01982)} \right] = 2.47$$

6. Gas Flow Rate

The gas rotameter calibration was applied to gases with different densities according to the following equation:

$$Q_1 = Q_2 \sqrt{\frac{\rho_2}{\rho_1}} \qquad (35)$$

where

Q_1 = volumetric flow rate of fluid 1 at a given meter reading, ft^3/min,

Q_2 = volumetric flow rate of fluid 2 at the same meter reading, ft^3/min,

ρ_1 = density of fluid 1, lb/ft^3, and

ρ_2 = density of fluid 2, lb/ft^3 .

Rotameter scale reading = 80. ft^3/min. The scale reading represents the calibration for 0.877 sp. gr. gas at 60°F and 14.7 psia. Call this gas 2.

The actual gas flowing through the rotameter (gas 1) is air containing a little water vapor. Its composition is the same as the inlet gas composition, y_o.

Average molecular weight of gas flowing through meter

$$= y_o M_{H_2O} + (1 - y_o) M_{air}$$

$$= (.0198)(18.) + (1 - .0198)(28.9) = 28.7$$

Temperature of fluid in meter = 533.7 °R

Pressure in meter = 31.29 in. Hg

Assuming the ideal gas laws and substituting in Eq. (35)

$$Q_1 = 80\sqrt{\frac{(.877)(28.9)(29.92)(533.7)}{(28.7)(31.29)(520.0)}} = 74.5 \text{ ft}^3/\text{min}$$

The flow rate may be converted to lb-moles per minute as follows:

$$V = \frac{(74.5)(29.92)(533.7)}{(359)(31.29)(592)} = 0.179 \text{ lb-moles/min}$$

This is the same as the inlet gas flow rate, V_o, since no moisture is gained or lost between the rotameter and the test column inlet. Therefore V_o = 0.179 lb-moles/min.

The flow rate of gas above the test plate, V_1, is then obtained as follows:

$$V_1 = V_o\left(\frac{1 - y_o}{1 - y_1}\right) = 0.179\left(\frac{1 - .01982}{1 - .04337}\right) = 0.183 \text{ lb moles/min}$$

The average gas flow rate through the froth on the test plate is taken as the arithmetic average of V_1 and V_o.

$$V_{avg} = \frac{(0.179 + 0.183)}{2} = 0.181 \text{ lb moles/min}$$

7. Average Gas Temperature

The temperature of the gas leaving the active plate was calculated with the following relation:

$$T_1 = T_o - E_{OG}(T_o - T_s)$$

where

T_1 = outlet temperature of gas, °F,

T_o = inlet temperature of gas, °F, and

T_s = adiabatic saturation temperature (temperature of liquid on the test plate), °F.

The inlet gas temperature, T_o, was 166°F

$T_1 = 166 - .908(166 - 90) = 97°F$ or 557°R

The average gas temperature = (166 + 97)/2 = 131°F or 591°R.

8. Superficial Velocity

If the active plate area is taken as the area between the splash baffle and the inlet downcomer (.615 ft^2) and the average pressure is taken as the pressure above the plate (30.89 in. Hg), V_{avg} can be converted to gas superficial velocity as follows:

$$\text{Superficial velocity, } v_s = \frac{(0.181)(359)(29.92)(591)}{(60)(.615)(30.89)(492)} = 2.05 \text{ ft/sec}$$

9. Average Gas Density, ρ_G

M_{avg} = 29.7 lbs/lb-mole

T_{avg} = 591°R

P_1 = 30.89 in. Hg

$$\rho_G = \frac{(28.7)(30.89)(492)}{(359)(29.92)(591)} = .0710 \text{ lbs/ft}^3$$

10. Gas F Factor

$$F = v_s\sqrt{\rho_G}$$

$$F = 2.05\sqrt{.0710} = 0.546$$

11. Slot Opening

The relation between gas flow rate per slot and slot opening, as derived by Rogers and Thiele (44), is given below:

$$Q_s = \frac{2}{3} CD_s \sqrt{\frac{2g(\rho_L - \rho_G)}{\rho_G}} h_s^{3/2} \qquad (36)$$

where

Q_s = flow rate per slot, ft^3/sec,

C = orifice coefficient, 0.61,

D_s = slot width, ft,

g = acceleration of gravity, ft/sec^2,

ρ_L = liquid density, lbs/ft^3

ρ_G = gas density, lbs/ft^3, and

h_s = slot opening, ft.

The ρ_G used in this equation was the inlet gas density.

$$\rho_G = \frac{(28.7)(492)(30.89)}{(359)(626)(29.92)} = 0.0649 \text{ lb/ft}^3$$

The gas flow rate at the inlet conditions is as follows:

$$Q_o = \frac{(0.179)(359)(60)(626)(29.92)}{(492)(30.89)} = 4750 \text{ ft}^3/\text{hr}$$

Since there are 9 caps on the plate with 18 slots each, the flow rate per slot is as follows:

$$Q_s = \frac{4750}{(9)(18)(3600)} = 0.00814 \text{ ft}^3/\text{sec}$$

$$\rho_L = 62.2 \text{ lbs/ft}^3$$

The slot opening is obtained by rearranging Equation (36):

$$h_s = \left[\frac{Q_s}{\frac{2}{3} CD_s \sqrt{\frac{2g(\rho L - \rho G)}{\rho G}}}\right]^{2/3}$$

$$h_s = \left[\frac{0.00814}{(.667)(.61)(.0104)\sqrt{\frac{(64.4)(62.2 - .06)}{(0.0649)}}}\right]^{2/3}$$

$$h_s = .0395 \text{ ft or } 0.47 \text{ in.}$$

12. Height of Liquid over the Weir

The height of liquid over the weir was calculated with the Francis weir formula given below:

$$q = 3.33(L - 0.2H) H^{3/2} \qquad (37)$$

where

q = liquid flow rate, ft^3/sec,

L = length of weir, ft, and

H = liquid height over the weir, ft.

$$q = 8.0 \text{ gal/min}$$

$$= \frac{(8.0)}{(7.48)(60)} = .0178 \text{ } ft^3/sec$$

$$L = 7.37 \text{ in. or } 0.615 \text{ ft.}$$

$$H = \left[\frac{0.0178}{3.33(.615 - 0.2H)}\right]^{2/3}$$

$$H = .0423 \text{ ft or } .51 \text{ in.}$$

13. Comparison of Experimental N_G with the Correlation Equation

The humidification data were correlated by Equation (32) given below:

$$N_G = 0.297 \left(\frac{\mu_G}{\rho_G D_V}\right)^{-0.23} \left(\frac{D_s v \rho_G}{\mu_G}\right)^{-0.33} \left(\frac{D_s \rho_G \sigma}{\mu_G^2}\right)^{0.16} \left(\frac{h_L}{D_s}\right)^{0.62} \left(\frac{\rho_L}{\rho_G}\right)^{-0.01} \left(\frac{\mu_L}{\mu_G}\right)^{-0.005}$$

The definitions of the symbols are given in the Nomenclature.

The fluid properties were evaluated at the average bulk conditions.

μ_G = .0472 lb/ft,hr (corrected for composition),

ρ_G = .0710 lb/ft^3,

D_V = 1.21 ft^2/hr,

D_s = 0.0104 ft,

v = (2.05)(3600) = 7400 ft/hr,

σ = 20.3 x 10^5 lb/hr^2,

h_L = 0.147 ft,

ρ_L = 61.5 lb/ft^3,

μ_L = 1.85 lb/ft,hr.

$$\left(\frac{\mu_G}{\rho_G D_V}\right)^{-0.23} = \left[\frac{.0472}{(.0710)(1.21)}\right]^{-0.23} = 1.15$$

$$\left(\frac{D_s v \rho_G}{\mu_G}\right)^{-0.33} = \left[\frac{(.0104)(7400)(.0710)}{(.0472)}\right]^{-0.334} = 0.200$$

$$\left(\frac{D_s \rho_G \sigma}{\mu_G{}^2}\right)^{0.16} = \left[\frac{(.0104)(.0710)(20.3 \times 10^5)}{(.0472)^2}\right]^{0.158} = 8.32$$

$$\left(\frac{h_L}{D_s}\right)^{0.62} = \left[\frac{0.147}{0.0104}\right]^{0.62} = 5.16$$

$$\left(\frac{\rho_L}{\rho_G}\right)^{-0.01} = \left[\frac{61.5}{.0710}\right]^{-0.01} = 0.935$$

$$\left(\frac{\mu_L}{\mu_G}\right)^{-0.005} = \left[\frac{1.85}{.0472}\right]^{-0.005} = 0.984$$

$$N_G = (0.297)(1.15)(0.200)(8.32)(5.16)(0.935)(0.984) = 2.62$$

(The experimental value of N_G was 2.47).

APPENDIX D

CALIBRATION DATA

The liquid rotameter was calibrated by collecting and weighing the water delivered at a constant meter reading in a measured length of time. The water calibration data were modified for the organic liquids according to the following equation:

$$\frac{Q_1}{Q_2} = \sqrt{\frac{\rho_2(\rho_F - \rho_1)}{\rho_1(\rho_F - \rho_2)}} \tag{38}$$

where

Q_1 = volumetric flow rate of fluid 1 at a given meter reading,

Q_2 = volumetric flow rate of fluid 2 for the same reading,

ρ_1 = density of fluid 1,

ρ_2 = density of fluid 2,

ρ_F = density of the rotameter float.

The scale reading of rotameter D8-1609 was checked by Warzel (65) and was found to be accurate within 3 to 5 per cent. The scale reading was corrected for gas density with Equation (38).

The thermometer used to measure the temperature of the liquid leaving the test plate was calibrated by comparison with a standard thermometer in a constant temperature bath. Several different thermometers were used in the course of the experiments, but all were checked against the same standard.

The wet test meters were calibrated by passing a known volume of saturated, room-temperature air through them. The air was displaced from a 3-gallon jug by slowly filling the jug with water. The volume of the

jug was measured by filling it with a volumetric flask, and checked by weighing the jug when empty and when filled with water.

TABLE 21

CALIBRATION OF ROTAMETER W70-4024/1
Water at 54°F
Float density = 7.85 gm/cc

Scale[1] Reading	Water, ft^3/sec
20	.01422
40	.02845
60	.04265
80	.05693

[1]Per cent of maximum flow (32.0 gal/min)

TABLE 22

CALIBRATION OF WET TEST METER B10SS
(Used to measure outlet gas samples)

Meter Reading, ft^3	Volume of Air, ft^3	Meter Correction Factor
.2399	.2411	1.005
.2410	.2411	1.001
.2411	.2409	.999
.2419	.2409	.996

TABLE 23

CALIBRATION OF WET TEST METER H9SS
(Used to measure inlet gas samples)

Meter Reading, ft^3	Volume of Air, ft^3	Meter Correction Factor
.2446	.2408	.985
.2454	.2409	.982

TABLE 24

THERMOMETER CALIBRATIONS

Temp. °C	Corrections to be Added to Thermometer Reading, °C			
	No. 271726	No. 55960	No. 50232	No. 55952
20	+.01	-.10	--	--
30	+.02	+.02	0	-.12
40	+.08	0	+.11	-.07
50	+.07	-.02	-.04	-.04

APPENDIX E

PROCEDURE FOR STARTING EQUIPMENT

PROCEDURE FOR STARTING EQUIPMENT

1. Connect fresh gas cylinder to make-up gas feed system and adjust pressure regulators and small flow control valve as required.
2. Force liquid by gas pressure from the liquid storage tank into both the test column circuit and the dehumidifier circuit, making sure sufficient liquid is in both circuits to keep the centrifugal pumps filled at all times after they are started. Liquid holdup in the lines and various pieces of equipment must be considered. The liquid level in the test column can be observed directly; the level in the dehumidifier is indicated by a manometer on the panel board.
3. Start the liquid pumps. Open the flow control valves wide momentarily to remove gas from the pumps and lines; then adjust valves to give the desired flow rates.
4. Turn on cooling water, which flows through the liquid heat exchanger and cools the liquid in the dehumidifier circuit.
5. Start the blower. Adjustment of the variable speed drive should be made in advance to give approximate desired speed. Fine adjustments of the gas flow rate are made by adjusting the gate valve in the blower by-pass line. Check to see that a slight pressure is maintained at the blower inlet and that excessive make-up gas is not required to do it.
6. Turn on steam to gas heater.
7. Plug in sample line heaters.

8. Adjust valve which bleeds liquid from dehumidifier circuit back into the test column circuit to maintain a constant level in the bottom of the test column.
9. Check to see that the de-entrained liquid is being withdrawn from the entrainment separator plate.

NOMENCLATURE

a - area available for mass transfer per unit volume of froth or packing, ft^2/ft^3.

c - concentration of diffusing component, lb mole/ft^3.

C_p - heat capacity of fluid at constant pressure, Btu/lb, °F.

C_o, C_1', C_2', C_1, C_2, C_3, C_4, C_5, C_6 - constants.

d - differential operator; or the diameter of a droplet or sphere, feet, in Equation (25); or the inside diameter of a wetted wall column, feet, in Equation (26).

D - diffusion coefficient, ft^2/hr.

D_L - diffusivity in the liquid phase, ft^2/hr.

D_V - diffusivity in the gas phase, ft^2/hr.

D_s - slot width, ft.

$\exp(x)$ - e^x.

E_{ML} - Murphree liquid plate efficiency.

E_{MV} - Murphree vapor plate efficiency.

E_o - overall column efficiency.

E_{OG} - point vapor efficiency.

f - arbitrary function in Equation (29); friction factor in Equations (23) and (24).

F - $v_s\sqrt{\rho}$, F factor, based on area between splash baffle and downcomer (0.615 ft^2).

G_M - molar mass gas velocity based on active cross-sectional area, lb mole/hr, ft^2.

h - effective froth height, ft, in Equations (29) through (32); heat transfer coefficient in Equation (23); vertical distance, inches, from middle of slots to top of liquid flowing over weir in Equation (5).

h_L - vertical distance between bottom of slot opening and top of liquid flowing over weir, ft.

H - Henry's law constant, ft^3-atm/lb mole.

H.T.U.$_G$ - height of a gas phase transfer unit as defined by Equation (27).

j_D - j-factor for mass transfer as defined by Equation (24).

j_H - j-factor for heat transfer as defined by Equation (23).

k_c - individual gas phase mass transfer coefficient, lb mole/hr, ft^2, lb mole/ft^3.

k_G - individual gas phase mass transfer coefficient, lb mole/hr, ft^2, atm.

k_L - individual liquid phase mass transfer coefficient, lb mole/hr, ft^2, lb mole/ft^3.

K_G - overall mass transfer coefficient based on gas phase, lb mole/hr, ft^2, atm.

K_L - overall mass transfer coefficient based on liquid phase, lb mole/hr, ft^2, lb mole/ft^3.

ln - natural logarithm (to the base e).

L_M - molar mass liquid velocity based on active cross-sectional area, lb mole/hr, ft^2.

m - slope of vapor-liquid equilibrium curve, dy/dx.

MIBK - methyl isobutyl ketone.

n - number of pools on plate as used in Equation (7).

N_A - diffusion rate of component A, lb mole/hr, ft^2.

N_G - number of individual gas phase transfer units per plate.

N_L - number of individual liquid phase transfer units per plate.

N_{OG} - number of overall gas phase transfer units per plate.

N_{Pr} - Prandtl number, $C_p\mu/k$.

N_{Re} - Reynolds number, $Dv\rho/\mu$.

N_{Sc} - Schmidt number, $\mu/\rho D_V$.

P - total pressure, atm.

p_{BM} - log mean partial pressure of non-diffusing component in film next to interface, atm.

s - term defined by Equation (5).

v - superficial gas velocity based on active bubbling area (0.615 ft^2), ft/hr.

v_s - superficial gas velocity based on active bubbling area (0.615 ft^2), ft/sec.

V_G - volume of pure gas added to system, ft^3.

V_S - volume of system, ft^3.

w - slot width in Equation (5), inches.

x - mole fraction solute in liquid.

x* - mole fraction solute in liquid at equilibrium with bulk of gas.

y - mole fraction diffusing component in gas.

y* - mole fraction diffusing component in gas at equilibrium with bulk of liquid.

y' - mole fraction diffusing component in gas at a given point on the bubble cap plate.

y'* - mole fraction diffusing component in gas at equilibrium with bulk of liquid at a given point on the bubble plate.

z - coordinate in direction of diffusion, ft.

ρ - fluid density, lb/ft^3.

ρ_G - gas density, lb/ft^3.

ρ_L - liquid density, lb/ft^3.

ρ_M - molar liquid density, lb mole/ft^3.

μ - fluid viscosity, lb/ft, hr; or liquid viscosity, cp, in Equation (5).

μ_G - gas viscosity, lb/ft, hr.

μ_L - liquid viscosity, lb/ft, hr.

σ - surface tension, lb/hr^2.

Subscripts

f - log mean value.

G - gas phase.

i - at the interface.

L - liquid phase.

M - mass units.

p - at constant pressure.

V - in the gas phase.

o - entering plate 1 from below (gas).

1 - on or leaving plate 1.

2 - entering plate 1 from above (liquid).

BIBLIOGRAPHY

1. Bakowski, S., Chem. Eng. Science, 1, 266 (1952).

2. Bridgman, P. W., Dimensional Analysis, New Haven, Yale University Press, 1922.

3. Bromley, L. A. and C. R. Wilke, Ind. Eng. Chem., 43, 1641-48 (1951).

4. Cairns, R. C. and G. H. Roper, Chem. Eng. Sci., 3, 37 (1954).

5. Carey, J. S., J. Griswold, W. K. Lewis, and W. H. McAdams, Trans. Am. Inst. Chem. Engrs., 30, 504 (1934).

6. Chilton, T. H. and A. P. Colburn, Ind. Eng. Chem., 27, 255 (1935).

7. Chilton, T. H. and A. P. Colburn, Ind. Eng. Chem., 26, 1183 (1934).

8. Colburn, A. P., Ind. Eng. Chem., 22, 967 (1930).

9. Danckwerts, P. V., Ind. Eng. Chem., 43, 1460 (1951).

10. Drickamer, H. G. and J. R. Bradford, Trans. Am. Inst. Chem. Engrs., 39, 319 (1943).

11. Duncan, W. J., Physical Similarity and Dimensional Analysis, London, Edward Arnold and Co., p. 44, 1953.

12. Dwyer, O. E. and B. J. Dodge, Ind. Eng. Chem., 33, 485 (1941).

13. Emmert, R. E. and R. L. Pigford, Chem. Eng. Progress, 50, 87 (1954).

14. Ezekiel, M., Methods of Correlation Analysis, New York, John Wiley and Sons, Inc., 1930.

15. Fellinger, L., Sc. D. Thesis, Massachusetts Institute of Technology, 1941.

16. Gautreaux, M. F. and H. E. O'Connell, Paper presented at Am. Inst. Chem. Engrs. Meeting, St. Louis, Mo., December 13-16, 1953.

17. Geddes, R. L., Trans. Am. Inst. Chem. Engrs., 42, 79 (1946).

18. Gerster, J. A., W. E. Bonnet, and Irwin Hess, Chem. Eng. Progress, 47, 523, 621 (1951).

19. Gerster, J. A., A. P. Colburn, W. E. Bonnet, and T. W. Carmody, Chem. Eng. Progress, 45, 716 (1949).

20. Gerster, J. A., J. H. Koffolt, and J. R. Withrow, Trans. Am. Inst. Chem. Engrs., 39, 37 (1943).

21. Gerster, J. A., J. H. Koffolt, and J. R. Withrow, Trans. Am. Inst. Chem. Engrs., 41, 393 (1945).

22. Gilliland, E. R. and T. K. Sherwood, Ind. Eng. Chem., 26, 416 (1934).

23. Goodgame, T. H. and T. K. Sherwood, Chem. Eng. Sci., 3, 37 (1954).

24. Gordon, K. F. and T. K. Sherwood, Chem. Eng. Progress, Symposium Series, No. 10, 15 (1954).

25. Higbie, R., Trans. Am. Inst. Chem. Engrs., 31, 365 (1935).

26. Hodgman, C. D., Handbook of Chemistry and Physics, 30th Edition, Cleveland, Chemical Rubber Publishing Co., 1947.

27. Houston, R. W. and C. A. Walker, Ind. Eng. Chem., 42, 1105 (1950).

28. Lee, C. Y. and C. R. Wilke, Ind. Eng. Chem., 46, 2381 (1954).

29. Lewis, W. K., Jr., Ind. Eng. Chem., 28, 399 (1936).

30. Lewis, W. K. and W. G. Whitman, Ind. Eng. Chem., 16, 1215 (1924).

31. Lynch, E. J. and C. R. Wilke, A.I.Ch.E. Journal, 1, 9 (1955).

32. Martin, J. J., Ind. Eng. Chem., 44, 920 (1952).

33. McAdams, W. H., Heat Transmission, 2nd Edition, New York, McGraw-Hill Book Company, Inc., 1942.

34. Mehta, J. J. and R. H. Parekh, S. M. Thesis, Massachusetts Institute of Technology, 1939.

35. Methyl Isobutyl Ketone, New York, Shell Chemical Corporation, 1948.

36. Murphree, E. V., Ind. Eng. Chem., 24, 726 (1932).

37. Murphree, E. V., Ind. Eng. Chem., 17, 747 (1925).

38. O'Connell, H. E., Trans. Am. Inst. Chem. Engrs., 42, 741 (1946).

39. Perry, J. H., Chemical Engineers' Handbook, 3rd Edition, New York, McGraw-Hill Book Company, Inc., 1950.

40. Polich, W. F., Ph. D. Thesis, Carnegie Institute of Technology, 1953.

41. Randall, M., B. Longtin, and H. Weber, J. Phys. Chem., 45, 343 (1941).

42. Ranz, W. E. and W. R. Marshall, Jr., Chem. Eng. Progress, 48, 141, 173 (1952).

43. Robinson, C. S. and E. R. Gilliland, Elements of Fractional Distillation, 4th Edition, Chapt. 17, New York, McGraw-Hill Book Company, Inc., 1950.

44. Rogers, M. C. and E. W. Thiele, Ind. Eng. Chem., 26, 524-28 (1934).

45. Scarborough, J. B., Numerical Mathematical Analysis, 2nd Edition, Baltimore, The Johns Hopkins Press, pp. 451-59, 1950.

46. Scheibel, E. G. and D. F. Othmer, Trans. Am. Inst. Chem. Engrs., 40, 611 (1944).

47. Schrage, R. W., A Theoretical Study of Interphase Mass Transfer, New York, Columbia University Press, pp. 72-76, 1953.

48. Sherwood, T. K., Trans. Am. Inst. Chem. Engrs., 36, 817, (1940).

49a. Sherwood, T. K. and K. F. Gordon, A.I.Ch.E. Journal, 1, 129 (1955).

49b. Sherwood, T. K. and F. A. L. Holloway, Trans. Am. Inst. Chem. Engrs., 36, 39 (1940).

50. Sherwood, T. K. and F. A. L. Holloway, Trans. Am. Inst. Chem. Engrs., 36, 21 (1940).

51. Sherwood, T. K. and R. L. Pigford, Absorption and Extraction, 2nd Edition, New York, McGraw-Hill Book Company, Inc., pp. 1-50, 1952.

52. Ibid., p. 58.

53. Ibid., pp. 63-69.

54. Ibid., p. 70.

55. Ibid., pp. 72-75.

56. Ibid., pp. 75-79.

57. Ibid., p. 281.

58. Shulman, H. L., C. F. Ullrich, and N. Wells, A.I.Ch.E. Journal, 1, 247 (1955).

59. Shulman, H. L., C. F. Ullrich, A. Z. Proulx, and J. O. Zimmerman, A.I.Ch.E. Journal, 1, 253 (1955).

60. Shulman, H. L., C. F. Ullrich, N. Wells, and A. Z. Proulx, A.I.Ch.E. Journal, 1, 259 (1955).

61. Stone, H. L., Sc. D. Thesis, Massachusetts Institute of Technology, 1953.

62. Surosky, A. E. and B. F. Dodge, Ind. Eng. Chem., 42, 1113 (1950).

63. Von Karman, Th., Trans. A.S.M.E., 61, 705 (1939).

64. Walter, J. F. and T. K. Sherwood, Ind. Eng. Chem., 33, 493 (1941).

65. Warzel, L. A., Ph. D. Thesis, University of Michigan, 1955.

66. West, F. B., W. D. Gilbert, and T. Shimizu, Ind. Eng. Chem., 44, 2470 (1952).

67. Whitman, W. G., Chem. Met. Engr., 29, 146 (1923).

68. Wilke, C. R. and C. Y. Lee, Ind. Eng. Chem., 47, 1253-57, (1955).

69. Zabban, W. and B. F. Dodge, Chem. Eng. Progress, Symposium Series, No. 10, 61 (1954).

70. Funk, G. L., Chemical and Physical Methods Laboratory, Carbide and Carbon Chemicals Company, South Charleston 3, West Virginia, personal communication, July 18, 1955.